

**A MORPHOLOGICAL AND DIAGNOSTIC IMAGING STUDY OF  
THE DISTAL PELVIC LIMB OF THE OSTRICH (*Struthio  
camelus*)**

**BY**

**DANNY LISWANISO**

Thesis submitted for the Degree of Master in Veterinary Medicine in the  
Faculty of Veterinary Medicine of the University of Glasgow.

**© Liswaniso D.**

Department of Veterinary Anatomy,

Glasgow Veterinary School,

February, 1996.

ProQuest Number: 11007784

All rights reserved

INFORMATION TO ALL USERS

The quality of this reproduction is dependent upon the quality of the copy submitted.

In the unlikely event that the author did not send a complete manuscript and there are missing pages, these will be noted. Also, if material had to be removed, a note will indicate the deletion.



ProQuest 11007784

Published by ProQuest LLC (2018). Copyright of the Dissertation is held by the Author.

All rights reserved.

This work is protected against unauthorized copying under Title 17, United States Code  
Microform Edition © ProQuest LLC.

ProQuest LLC.  
789 East Eisenhower Parkway  
P.O. Box 1346  
Ann Arbor, MI 48106 – 1346

Theris  
10453  
Copy 1

GLASGOW  
UNIVERSITY  
LIBRARY

## SUMMARY

The ostrich (*Struthio camelus*) farming industry is growing rapidly in many countries. Although the ostrich is now established as a commercial species, there are still some significant gaps in our knowledge of the structure and function of this unique species. One such area where there appears to be little information available is on the morphology of the distal region of the pelvic limb. Morphological knowledge of this area is important as distal limb deformities appear to present a significant problem in the husbandry and management of these birds.

The objectives of the present study in an attempt to fill this gap, were two fold:

- (i) To provide a detailed functional morphological account of the topographical anatomy of the distal region in the normal pelvic limb of the ostrich.
- (ii) To use two diagnostic imaging techniques, ultrasonography and radiography, in the identification and characterisation of the structures studied in the first part of this study, as a basis for the examination of the clinical leg deformities such as rolled toes.

Chapter 1 provides information about ostriches in general, and a brief history of ostrich farming, as well as summarising available research work carried out in relation to the pelvic limb of the ostrich. There are very few studies that have been done to evaluate the morphology of the pelvic limb in the ostrich. While many uses of diagnostic ultrasound imaging techniques have been cited in other species, there is very little information on the use of this technique in ostriches. Various types of common limb abnormalities in ostriches have been described and defined.

Chapter 2 provides information about ultrasonography, covering various aspects of this imaging technique. The areas covered include the development of the technique, its physical principles, types of image display modes and an explanation of image interpretation and common terminology used in ultrasonography. Ultrasonographic image artefacts, their identity, and, where possible, ways of minimising them have been explained. These artefacts include reverberations, acoustic shadows, distant enhancement, reflection and refraction, comet-tail and electronic noise.

In Chapter 3, a detailed explanation of the materials and methods used in this study is given. Fresh cadaverous limbs were carefully skinned and muscles separated by blunt dissection along their connective tissue planes, during which their origins, form, course and insertions were recorded. These were then boiled out to obtain bony specimens. Eight different pre-selected levels of the limb at which cross-sectional and ultrasonographical examinations were carried out are illustrated diagrammatically.

Chapter 4 presents the results of the present study. These results were classified in five categories namely: osteology, arthrology, myology, ultrasonographical and descriptive topographical anatomy, and rolled toe pathological aspects. Interesting osteological findings included the very marked cranially-projecting medial cnemial crest and a greatly reduced lateral cnemial crest of the tibiotarsus. The supratendinal groove is partially ossified while a large single hypotarsal ridge, devoid of flexor canals, is displaced slightly medially with concomitant loss of the intercotylar prominence. A unique pattern in the course of tendons and ligaments, and a special morphology of the joints, has been reviewed and illustrated diagrammatically. The former form the digital check apparatus, a structure that has not been described before in the ostrich, while the intertarsal joint was found to have only one meniscus, the lateral meniscus, and paired

medial and lateral collateral ligaments. A total of 15 muscles were identified and it was interesting to note that despite the absence of the hallux (digit I), *M. flexor hallucis longus* was amongst the muscles present in the ostrich. A description of the normal topographic anatomy and ultrasonographic appearance of the tendons and ligaments has also been given. Cross-sectional ultrasonographic scans of normal ostrich tendons appear hyperechoic and compact, with a stippled echopattern, while longitudinal scanning images present a multiple closely-aligned highly echogenic pattern (fibrillar sonographic texture). In adult birds with rolled toes, in this study regarded as long-standing cases of rolled toes, there was partial ossification of extensor tendons, distal rotation of the tarsometatarsal bone, (as much as 35 degrees), distal rotation the first phalanx of digit III (as much as 30 degrees), and the formation of osteophytes. Most of these features in this study confirm the advanced morphological placement of the monophyletic origin of the superfamily *Struthionoidea* over the more primitive ratites.

The overall findings of these studies are interpreted and discussed in detail in Chapter 5. There is need for more of future work to explore the usefulness of ultrasound and causal factors of musculoskeletal disorders in ostriches. There is also need for study on the normal vasculature and innervation of the ostrich hind limb in order to ascertain whether or not any injuries or damage occurs to these structures as a result of conditions such as slipped tendon, or rolled toes in these birds.

# LIST OF CONTENTS

	<b>Page</b>
<b>LIST OF FIGURES</b>	<b>vii</b>
<b>ACKNOWLEDGEMENT</b>	<b>xi</b>
<b>DEDICATION</b>	<b>xii</b>
<b>DECLARATION</b>	<b>xiii</b>
<b>CHAPTER 1. INTRODUCTION AND REVIEW OF LITERATURE</b>	<b>1</b>
1.1 General introduction	1
1.2 Historical review of ostrich farming	4
1.3 Scientific review	5
<b>CHAPTER 2. ULTRASONOGRAPHY</b>	<b>9</b>
2.1 Development of ultrasound technology	9
2.2 Ultrasonographic imaging	10
2.2.1 Physical principles of ultrasound	10
2.2.2 Tissue interactions with ultrasound	11
2.2.3 Emission and reception of ultrasound	13
2.3 Image display modes	14
2.3.1 A-mode (Amplitude mode)	14
2.3.2 B-mode (Brightness modulation)	15
2.3.3 M-mode (Time motion)	15
2.4 Real-time ultrasonography	16
2.4.1 Real-time transducers	16
2.5 Image interpretation and terminology	17
2.6 Ultrasound image artefacts and interpretation	19
2.6.1 Reverberations	21
2.6.2 Acoustic shadows	22
2.6.3 Distant enhancement	24

2.6.4 Reflection and refraction	24
2.6.5 Comet-tail	24
2.6.6 Electronic noise	24
2.7 Summary of terms used in ultrasonography	24
<b>CHAPTER 3. MATERIALS AND METHODS</b>	<b>27</b>
3.1 Gross dissections	27
3.2 Sonographic anatomy and cross-sections	27
3.2.1 Equipment selection	29
3.2.2 Ultrasonographic examination of ostrich limb	32
<b>CHAPTER 4. RESULTS</b>	<b>34</b>
4.1 Osteology	34
4.1.1 Tibiotarsus	34
4.1.2 Fibula	35
4.1.3 Tarsometatarsus	36
4.1.4 Phalanges	37
4.2 Arthrology	44
4.2.1 Tarsometatarsal (intertarsal) joint	44
4.2.2 Tarsometatarsophalangeal joint	52
4.2.3 Interphalangeal joints	53
4.3 Musculature	55
4.3.1 Superficial layer	55
4.3.2 Deep layer	58
4.3.1 Deepest layer	63
4.4 Normal ultrasonographic and descriptive topographic anatomy of the distal pelvic limb of the ostrich	72
4.5 Pathological study results	101
<b>CHAPTER 5. DISCUSSION</b>	<b>112</b>

5.1 Osteology	112
5.2 Distal pelvic musculature	114
5.3 Functional morphology	116
5.3.1 Joint stability	116
5.3.2 Tendons and ligaments as functional units.	118
5.4 Ultrasonography in the examination of the ostrich limb.	121
5.5 Gross pathological observations on rolled toes in the ostrich.	122
5.6 Future work and conclusion	132
<b>APPENDICES</b>	<b>135</b>
<b>REFERENCES</b>	<b>137</b>

## LIST OF FIGURES

	<b>Page</b>
<b>Fig. 1.</b> Longitudinal linear scan of the hind limb flexor tendons of the ostrich demonstrating accoustic shadows.	23
<b>Fig. 2.</b> A diagram of the distal region of the pelvic limb in <i>Struthio camelus</i> , denoting the eight levels at which cross-sections were made.	28
<b>Fig. 3.</b> The ultrasound diagnostic scanner, (Toshiba, CAPASEE), Tokyo, JAPAN.	31
<b>Fig. 4.</b> Cranial (1) and caudal aspects (2) of the tibiotarsus and tarsometatarsus of <i>Struthio camelus</i> .	38
<b>Fig. 5.</b> Proximal articular facets of tibiotarsus (1) and tarsometatarsus (2) of <i>Struthio camelus</i> .	40
<b>Fig. 6.</b> Lateroventral (A) and dorsal (B) aspects of of the phalanges of the third (a) and fourth (b) digits of <i>Struthio camelus</i> .	42
<b>Fig. 7.</b> Basic classification of joints.	44
<b>Fig. 8.</b> Diagrammatic presentation of the medial (A) and lateral (B) aspectsof the intertarsal joint of <i>Struthio camelus</i> with accompanying cross-sections around this joint.	48
<b>Fig. 9.</b> Paraxial section (1) and the cranial aspect (2) of the intertarsal joint of <i>Struthio camelus</i> .	50

<b>Fig. 10.</b> Paraxial section showing the metatarsophalangeal and interphalangeal joints of the third digit of <i>Struthio camelus</i>	54
<b>Fig. 11.</b> Lateral view of the superficial muscle layer of the distal pelvic limb of <i>Struthio camelus</i> .	57
<b>Fig. 12.</b> Lateral view of the deeper muscle layer of the distal pelvic limb of <i>Struthio camelus</i> .	62
<b>Fig. 13.</b> Lateral aspect of the tarsometatarsal region showing various tendons.	68
<b>Fig. 14.</b> Dorsoabaxial view of <i>Struthio camelus</i> foot (1) and crural region (2) showing deepest muscles, tendons and ligaments.	69
<b>Fig. 15.</b> Plantar aspect of <i>Struthio camelus</i> with the digital cushions removed to show the pattern of insertion of flexor tendons and the digital check apparatus.	71
<b>Fig. 16.</b> Normal ultrasonographic appearance of ostrich tendons. Transverse (1) and longitudinal scans (2).	75
<b>Fig. 17.</b> Frozen transverse section of the distal pelvic limb of <i>Struthio camelus</i> . The section corresponds to Level 1 in Fig. 2	77
<b>Fig. 18.</b> Frozen transverse section of the distal pelvic limb of <i>Struthio camelus</i> . The section corresponds to Level 2 in Fig. 2.	80

- Fig. 19.** Frozen transverse section (A) and a corresponding transverse ultrasound scan (B) of the distal pelvic limb of *Struthio camelus* at Level 3 in Fig. 2. 83
- Fig. 20.** Frozen transverse section of the distal pelvic limb of *Struthio camelus* corresponding to Level 4 in Fig. 2. 87
- Fig. 21.** Transverse (A) and longitudinal (B) ultrasound scans of the distal pelvic limb of *Struthio camelus* corresponding to Level 4 in Fig. 2. 88
- Fig. 22.** Frozen transverse section of the distal pelvic limb of *Struthio camelus* corresponding to Level 5 in Fig. 2. 92
- Fig. 23.** Transverse (A) and longitudinal (B) ultrasound scans of the distal pelvic limb of *Struthio camelus* corresponding to Level 5 in Fig. 2. 93
- Fig. 24.** Frozen transverse section (A) and a corresponding transverse ultrasound scan (B) of the distal pelvic limb of *Struthio camelus*. The point corresponds to Level 6 in Fig. 2. 96
- Fig. 25.** Frozen transverse sections of the distal pelvic limb (digits) of *Struthio camelus*. (A) represents Level 7 whilst (B) represents Level 8 in Fig. 2. 99

<b>Fig. 26.</b> Lateral radiograph of the distal left pelvic limbs of 48 day-old ostrich chicks. Rolled (A) and normal (B) digit.	103
<b>Fig. 27.</b> Frozen cross-section of the distal pelvic limb of an adult <i>Struthio camelus</i> with a rotated toe, corresponding to Level 5 in Fig. 2.	106
<b>Fig. 28.</b> Frozen cross-section of the distal pelvic limb of an adult <i>Struthio camelus</i> with a rotated toe, corresponding to Level 7 in Fig. 2.	107
<b>Fig. 29.</b> Tarsometatarsus and phalanges from an adult ostrich with a rotated tarsometatarsus and rolled toes.	108
<b>Fig. 30.</b> Normal (A) and rotated (B) tarsometatarsus and digiti III first phalanx of adult <i>Struthio camelus</i> .	110
<b>Fig. 31.</b> Dorsoplantar radiograph of rotated (A) and normal toe (B) of adult <i>Struthio camelus</i> .	111

## ACKNOWLEDGEMENTS

I wish to accord my appreciation to my two supervisors, Professor J. S. Boyd and Dr. M. D. Purton for their constructive criticism, help and encouragement during my studies.

I owe thanks also to members of staff and technicians in the Department of Veterinary Anatomy, in particular to Mr. A. Reid, the chief technician who was always offering me a help whenever I needed it. I also extend my thanks to Susan , David, Sheena Frances and Pat for their invaluable assistance in the sectioning of my ostrich limbs. Special thanks are due to Mr. C. Paterson who taught me so much on ultrasound, and to Mr. A. May who took excellent photographs of all my specimens.

I would also wish to express my sincere gratitude to Dr. D. C. Deeming of Hangland Ostrich Farm in Oxford, the largest ostrich farm in Britain, for sharing with me some of his practical ostrich farming experiences and providing me with all the specimens used in this study.

I am very grateful to British Council (O.D.A) for sponsoring me during my studies in Glasgow.

I wish to name Lina Audicana, Zuki Abu Bakar, Careen Hankanga and Mary-Catherine Madekurozwa for their invaluable assistance, refreshing jokes and friendship.

Finally, and most importantly, I want to express my deepest gratitude to my father, Sailas Liswaniso, my mother, Matilda Liswaniso, and my brothers and sisters for their constant love and support.

## **DEDICATION**

This work is dedicated to my father, Mr. Sailas Liswaniso, and mother, Matilda Liswaniso, to whom I owe so much.

## **DECLARATION**

I, Danny Liswaniso, do hereby declare that the work presented in this thesis is original and was carried out by me personally.

Signature:

# CHAPTER 1

## INTRODUCTION AND REVIEW OF LITERATURE

### 1.1 GENERAL INTRODUCTION

Although ostriches (*Struthio camelus*) have been raised domestically in South Africa since the 1850s, it is only in recent years that ostrich farming has began to show a marked expansion in various countries around the world simply because the world demand for ostrich meat, leather, and feathers far exceeds current production levels (Odle, 1994). The resultant growth of the ostrich industry has, as might be expected, resulted in a demand for veterinary services including management programmes, and diagnostic, clinical and preventive medical programmes. As a result, veterinarians offering such services to ostrich producers need to have a basic understanding of ostrich anatomy and physiology.

**General anatomy.** The ostrich (*Struthio camelus*) belongs to the super order of flightless or running birds known scientifically as Ratitae which secondarily descended from flighted ancestors (Beddard, 1898; Sanft, 1972 ). There are five families of living ratites (Webb *et al.*, 1979).

- (a) Ostrich (*Struthionidae*)
- (b) Emu (*Dromaiidae*)
- (c) Rheas (*Rheidae*)
- (d) Cassawaries (*Cassawaridae*)
- (e) Kiwis (*Apterygidae*)

Ostriches belong to:

Family: *Struthionidae*,

Genus: *Struthio*,

Species: *camelus*

The major anatomical differences between ostriches (as representative of ratites) and carinate birds include rudimentary wings, a digestive system modified for grazing, and the loss of selected digits as an adaptation for running (Marshall, 1960, Webb *et al.*, 1979). Mature ostriches may stand 2.4 to 2.8 m tall and can weigh up to 160 kg (Sanft, 1972). Males are basically black and white, females are brown. There are three recognised subspecies in the world, although some authors recognise four subspecies (Deeming, 1994) : the "red neck", the "blue neck", and a hybrid "African black". The "red neck" is the largest of the subspecies, originating in the northern regions of Africa. The male has a red neck, red legs, and a bald spot on the top of his head. The male also has a white ring of feathers on the neck where the long feather line ends (Cho *et al.*, 1984). The "blue neck" originated from the middle of the southern part of the African continent, and the male exhibits blue pigmentation of the neck and legs. However, the beak and shins are red. It is intermediate in size, and its head is feathered on top. The "African black" is a term that has been assigned to the hybrid that is domestically raised in South Africa. It is the shortest of the subspecies and its body type is distinguished by shorter legs and a "boat-shaped" body compared to the "rounded" bodies of the other two subspecies. The male "African black" has a very dark blue to black pigmentation to the skin on the neck and legs, and again, a red beak and shin scales making it difficult to differentiate it from the blue subspecies by colour alone. The hens of all subspecies are brown and can only be differentiated by size and shape of the body.

All ostriches have a large flattened keelless sternum or breast bone, which resembles a raft (hence the name, ratites from the Latin word *ratia*, a raft). They also have several anatomical adaptations of the gastrointestinal tract that allows grazing with other ungulates in their native habitat. The ostrich

has a large sac-like proventriculus with a defined area of secretory glands. The ventriculus (gizzard) is a large structure lying within the body cavity just caudal to the breast bone in the standing bird. Ostriches are hindgut fermenters and rely on microflora for digestion of their highly fibrous diet. The colon comprises 60 % of the length of the intestinal tract compared to 6 % in the domestic chicken. The microflora of the intestinal tract is similar to that of the tract of grazing ruminants. Other important anatomical features include the location of the cutaneous ulnar veins on the ventral aspect of the wings and the medial metatarsal veins which are good venipuncture and catheterization sites in all ages. The ostrich may become sexually mature at 2 years of age although males often mature later than females. Indeed, while it is not uncommon for hens to begin laying at 2-3 years of age, males may take as long as 4-5 years to be functionally mature. In captivity, females may lay as many as 100 eggs in a season, although 20-40 are more common. Eggs are whitish in colour, weigh about 3 pounds (1000-1500 grams) and are generally laid every other day. Although mating may occur many times during the day, it is believed that a single mating may be effective for up to a week.

Ostriches are equipped with many advantageous features for their survival in the wild including excellent eye sight, large external ear canals, and heavily muscled legs. The principal muscles of the shank (gastrocnemius and digital flexors ) have almost three times the mass of corresponding muscles in the antelope (Alexander *et al.*, 1979). As might be expected, kicking, which in the ostrich is forward, is the major means of defence although some birds have been reported to peck and bite when threatened.

## 1.2 HISTORICAL REVIEW OF OSTRICH FARMING

Ratites are the oldest living birds on earth. Regarded with other birds as reptilian in origin, they are believed to have been separated from the main line of avian evolution since at least the Middle Cretaceous period, 80-90 million years ago. Twenty to sixty million years ago, ostriches ranged the Mediterranean Sea area in the west, China in the east, and Mongolia in the north, migrating across Africa about a million years ago. Large ostrich herds roamed the Western Cape of Africa when the Dutch landed in the 17th century. Egyptian cave art and other records trace the hunting, and perhaps farming, of ostriches to antiquity. The Arabs and Bushmen hunted the birds for sport, the Bushmen with poison arrows. Ostriches have traditionally been hunted in Namibia for sport, for diamonds (sometimes found in their gizzards), and because sheep and cattle farmers regard them as vermin for tearing down fences (Sanft, 1972).

Greek and Roman generals decorated their helmets with ostrich feathers. Egyptian pharaohs and their families bedecked themselves with Ostrich head-dresses and fans. The great liking of Elizabeth I of England and Marie Antoinette of France for ostrich feathers as fashion items created an international feather trade out of North Africa and Arabia, and later South Africa, that lasted until World War I. By the mid-19th century, the fashion industry had so devastated wild ostrich herds that ostrich farming was established, helped by the introduction into South Africa of wire fencing, the farming of alfalfa to feed the bird, and mechanical ostrich incubators. The industry boomed between 1900 and 1914. In 1913, ostrich plumes were the fourth largest South African export after gold, diamond, and wool (Smit, 1963). Ostrich plumes went out of style during World War I, partly as a result of the international campaign against the cruel trade. Ostrich farming lagged until 1945, when the government-supported Klein Karoo

Agricultural Co-operative was formed in South Africa (Deeming and Ayres, 1994). It added trade in meat and skin to that in feathers, building the world's first ostrich slaughterhouse in 1963-64. A leather tannery followed in 1969-70, and, in 1980-81, a new slaughterhouse was built to supply the demand for ostrich meat abroad. The South African government banned the exportation of fertile ostriches or eggs in 1988 in order to maintain their monopoly on the industry. This move prompted an effort by many countries to establish their own ostrich farms. However, with the fall of apartheid, South Africa is likely to open its market for ostrich exportation.

Although now well established as a commercial species in South Africa, Australia, USA, Canada and Israel, the ostrich has also recently begun to be farmed in the UK, with the first flock being established by Hangland Farm in 1990. There are now about three hundred ostrich farmers in the UK.

### **1.3 SCIENTIFIC REVIEW**

The vast amount of anatomical detail and variety of form to be found in avian species has led to considerable diversity in avian anatomy. To date, although many descriptions of avian anatomy and nomenclature are readily available (Baumel, 1979; King and McLelland, 1984; McKittrick, 1991) specific information on the ostrich is noticeably lacking. Most of this available information in the literature dealing with the anatomy of the ostrich was produced during the past two centuries. Indeed, one of the first presentations given to the Zoological Society of London was on the anatomy of the ostrich (*Struthio camelus*) and subsequent volumes of the Proceedings of the Society contain numerous anatomical and disease-related articles about ratites (Macalister, 1864; Haughton and Norman, 1865). The latter described the musculature of the ostrich leg, a paper of

direct relevance to this thesis. However, interpretation of these early references is often difficult, owing to the many variations and changes in nomenclature and interpretations that have occurred in the intervening years, a situation the International Committee on Avian Anatomical Nomenclature has made great progress in reviewing and stabilising recently (Baumel, 1979).

More recent studies on ratite anatomy include those of Cho *et al.*, (1984) and Cracraft (1974). The latter described a number of osteological features of the pelvic limb of the ostrich and his work, therefore, of particular relevance to the present study. Other studies relevant to the present investigation include Fowler (1991) who has provided a brief account of the ostrich foot, and Pavaux and Lignereux (1995) who identified a tendinous-like *M. fibularis brevis* in their dissection of a pair of ostrich legs. Furthermore, descriptions of the muscles of the proximal part of the ostrich limb have been given in which two major muscle peculiarities were observed (Mallet, 1994), the presence of *M. pectineus* in the position occupied by *M. ambiens* in other birds, and the origin of *M. ambiens* from the lateral surface of the ilium.

Alexander *et al.*, (1979) in their study of the mechanics of running of the ostrich noted that the principal muscles of the crural region of the ostrich are some three times the mass of the corresponding muscles of the antelope, although the comparatively smaller total fibre area of the longer individual muscle fibres in the ostrich exert slightly less force than in the antelope. On the mechanical aspects of the magnitude of the stresses which act in the bones, tendons and muscles of the leg an adult ostrich when running have been quantified (Alexander, 1985).

Although the use of diagnostic ultrasound imaging technique in most

examinations of mammalian soft tissue structures is well established, its use in the field of avian studies has been surprisingly slow. In horses, diagnostic ultrasound has been shown to be an effective imaging modality to assess the morphology of tendons and ligaments (Hauser and Rantanen, 1983; Spaulding, 1984; Rantanen and Gaines, 1983; Rantanen, 1982). Ultrasonographic imaging has proved highly popular because it is an easy, safe, and non-invasive method of musculoskeletal morphological evaluation (Cuesta *et al.*, 1994). As a technique that has therefore excelled in the examination of the distal extremities of other species, it was thought that its use in the study of tendons and ligaments in ostriches would warrant investigation, in the hope that such a technique could play an important role in avian anatomical, pathological and clinical studies by helping to elucidate soft tissue structures and relationships in a non-invasive manner. The ability to perform and interpret an ultrasonographic examination requires a basic understanding of ultrasonography, an accurate knowledge of the involved topographical anatomy of the relevant region, and the development of the practical ability to perform a diagnostic examination.

The accumulation of such knowledge and experience in relation to the normal anatomical structures is imperative for the development of a basis for the examination and understanding of the musculoskeletal disorders of this region, such as clinical cases of rolled toes, deviated toes, turned or crooked legs, slipped tendons, and rotated tibiotarsus or tarsometatarsus (Gandini *et al.*, 1986 ; Bezuidenhout *et al.*, 1994; Kocan and Crawford, 1994; Benzuidenhout and Burger, 1993; Guittin, 1986; Deeming and Ayres, 1994; Vorster, 1984; Van Heerden *et al.*, 1983). Although there are no specific studies documenting the actual causes of most of these musculoskeletal disorders in ostriches (these pathological disorders are discussed later in Chapter 5), there are a number of aetiologies that have

been attributed to as primary causes. These include improper incubation temperature (Hallam, 1992; Jensen *et al.*, 1992; Anon, 1993), excessive incubator humidity (Anon, 1993), allowing chicks too much room to move around in the hatcher tray (Hallam, 1992; Anon, 1993), and a deficiency of riboflavin (vitamin B2) (Foggin and Honywill, 1992; Anon, 1993).

However, it is regrettable that most of the information about ratites is not collected in a single or readily available source. Such compilation would be useful for veterinarians who, when dealing with medical and surgical problems or propagation management of ratites, need to have a basic understanding of ratite anatomy to safely handle these birds and to understand how best to collect blood samples, administer medications, evaluate radiographs, perform surgery, and indeed distinguish between normal and abnormal tissue at necropsy (Fowler, 1991).

In this thesis an anatomical and diagnostic imaging study (ultrasonography), with accompanying pictures, radiographs and graphical presentations, of the normal distal pelvic limb of the ostrich (*Struthio camelus*) is defined and described. A gross anatomical study of pathologic specimens of one of the common distal hind limb disorders in ostriches, rolled toes, was also carried out.

# CHAPTER 2

## ULTRASONOGRAPHY

### 2.1 DEVELOPMENT OF ULTRASOUND TECHNOLOGY

The first practical application of the pulse-echo production of ultrasound was patented in 1912 when Richardson devised apparatuses to detect submerged objects and potential hazards for fog-bound ships. Further development of this concept led to the invention of a device for the detection of submarines (during the second world war) (Winsberg and Cooperberg, 1982), a system which was further improved and named SONAR (Sound Navigation and Ranging). The application of this newly developed technology, over the next few years, then slowly extended into the medical field. In 1942, the use of ultrasound as a diagnostic aid was proposed (Cameron and Skofronick, 1979; Athey and McClendon, 1983) and, in 1947, "hyperphonograms" of the head were produced. Later, ultrasound was used to identify gallstones and foreign bodies by the acoustic shadows which they produced (Ludwig and Struthers, 1949) , and throughout the 1950's reports of the identification of intracranial masses were published (Ballantine *et al.*, 1950; Wild *et al.*, 1950; Miyajima *et al.*, 1952). The use of ultrasonography to image the heart was proposed in 1955 (Edler, 1955), and the structure of the eye in 1956. From then on, the use of ultrasound became an established technique in the clinician's armoury. In animals, the first application of ultrasound was as a technique for assessing carcass quality in pigs by the measurement of the back fat (Shirley *et al.*, 1978)

These early techniques utilised a system now known as A-mode. A single beam of sound was interrogated along one dimension to give a one

dimensional image. The location and amplitude of the returning echoes was displayed as a graph of amplitude against location relative to the origin. The first compound water bath scanner which produced two dimensional images was first described in 1958 (Howry, 1958). This system was based on the sequential analysis of an area with multiple sound beams. The location of each interface producing an echo was calculated and displayed on a visual display unit as a series of dots to describe a two-dimensional area of the body. This system was limited to experimental situations because it required total submersion of the subject in water (Shirley *et al.*, 1978). In order to avoid water immersion of the subject, in 1960, the first contact scanner, which used coupling gel, was developed in Glasgow (Brown, 1960). This apparatus was mainly used by gynaecologists to distinguish between cystic and solid lesions within the female reproductive tract (Donald and Brown, 1961). Since then, ultrasound has been a major diagnostic tool in medical studies.

## **2.2 ULTRASONOGRAPHIC IMAGING**

**2.2.1 Physical principles of ultrasound.** Ultrasound is the term applied to mechanical pressure waves transmitted as compressions and rarefactions through a medium (Ziskin, 1975; Herring and Bjornton, 1989; Thaler and Manor, 1990). These vibrations are not random, but orderly oscillatory pressure waves generated by an ultrasound transducer. The term ultrasound is applied when the frequency of the oscillations is higher than the upper range of human hearing, approximately 20,000 cycles per second (20 KHz). Frequency is defined as the number of times a wave is repeated (cycles) per second. One cycle per second is 1 hertz; 1000 and 1 million cycles per second are 1 kilohertz (KHz) and 1 megahertz (MHz), respectively (Nyland and Mattoon, 1995). Frequencies in the range of 2 to 10 MHz are commonly employed in diagnostic examinations. An

ultrasound wave can be compared to a longitudinal wave having a wavelength, frequency and velocity. The wavelength (m) is the distance from two similar points on the given wave i.e. the distance that a wave travels during one cycle. The shorter the wavelength, the better the resolution. Frequency and wavelength are inversely related if the sound velocity within a medium remains constant. Since sound velocity is independent of frequency and nearly constant (1540 m/sec) in the body's soft tissues (Wells, 1969), selecting a higher frequency transducer will result in decreased wavelength of the emitted sound, providing better resolution. The relationship between velocity, frequency and wavelength can be summarised in the following equation:

$$\text{Velocity (m/sec)} = \text{Frequency (cycles/sec)} \times \text{Wavelength (m)}$$

**2.2.2 Tissue interactions with ultrasound.** Ultrasound imaging is based on the pulse-echo principle. This means that sound is produced by the transducer in pulses rather than continuously (Nyland and Mattoon, 1995). Short bursts of ultrasound are emitted into the animal's body from the transducer element. These short bursts travel through the tissues at a constant speed until they meet a reflecting surface or tissue interface. At the tissue interface, a small proportion of the sound beam is reflected back, producing a returning pulse or echo to the transducer. The image is formed from the echoes returning to the transducer from the tissues after each pulse. Therefore, adequate time must be allowed for all echoes to return before the transducer is pulsed again. In fact, sound is transmitted less than 1% of the time while the transducer waits for the returning echoes more than 99% of the time (Miles, 1989). The strength of the reflected ultrasound beam depends on a number of factors but of primary importance are the abrupt change in sound velocity and density of the

media (acoustic impedance), the angle at which it meets the tissue boundaries, and the distance travelled

The product of the tissue's density and the sound velocity within the tissue is known as the tissue's acoustic impedance. Acoustic impedance is used to refer to the reflection or transmission characteristics of a tissue. Acoustic impedance can be defined by the following equation:

$$\text{Acoustic impedance (z)} = \text{Velocity (v)} \times \text{Tissue density (p)}$$

Thus, the acoustic impedance is determined by the density of the medium and the velocity of sound in that medium. The size of the echo (or intensity) is proportional to the difference between the acoustic impedance of the two tissues forming the reflecting interface. There are only small differences in acoustic impedance among a body's soft tissues (Wells, 1969). This is ideal for imaging purposes because only a small percentage of the sound beam is reflected at such interfaces, the majority of the beam being transmitted further into the tissues to provide for imaging of deeper structures.

However, bone and gas have a very high and low acoustic impedance respectively. Air is less dense and more compressible than soft tissue and transmits sound at a lower velocity. Bone, on the other hand, is more dense and less compressible than soft tissues and transmits sound at a higher velocity. Therefore, when a sound beam encounters a soft tissue-bone or soft tissue-gas interface, nearly all sound is reflected and little is available for imaging deeper structures. This effect represents a high acoustic impedance mismatch. Distal acoustic shadowing is produced deep to the bone or gas because little sound penetrates. Increasing output intensity will not improve penetration but merely increase artifacts such as

reverberation echoes (Nyland and Mattoon, 1995). A higher-frequency transducer emits shorter wavelengths, and therefore correspondingly shorter pulses, than a lower frequency transducer. The relevance of this difference is explained below.

The rest of the sound beam continues through the deeper tissues generating an echo whenever a pulse reaches an interface between two tissues with different acoustic properties. The depth to which sound penetrates into soft tissues is directly related to the frequency employed. Higher-frequency sound waves are attenuated more than lower-frequency waves. This means that any attempt to improve resolution by increasing the frequency will invariably decrease penetration. The velocity of sound within each tissue and the tissue's density determine the percentage of the beam reflected or transmitted as it passes from one tissue to another.

**2.2.3 Emission and reception of ultrasound.** The production of ultrasonic frequencies is by the electrical stimulation of piezoelectric crystals housed within a transducer. The term piezo refers to the transformation of pressure to electricity (piezo, Greek for pressure). A material such as lead zirconate-titanate (PZT) which has piezoelectric properties can both transform sound energy to electricity and vice-versa (Goddard, 1995). An electrical current passing through a piezoelectric material deforms the internal structure of that material in such a way that a pressure change can be transmitted across the medium by causing the molecules composing the material to vibrate and thus propagate a sound wave. Similarly, a distortion and production of pressure changes in a piezoelectric material, by bombarding it with returning sound waves, will result in a change in electrical potential difference. Further, the amplitude of the sound produced by a piezoelectric material is directly proportional to the voltage applied to stimulate the material and conversely, the voltage

produced is directly proportional to the amplitude of the sound which stimulates it. Consequently, piezoelectric materials have the ability to distinguish and describe different voltages and amplitudes (Shirley *et al.*, 1978; Bartrum and Crow, 1983; Powis and Powis, 1984). Because of the unique properties of these crystals, the transducer can emit and receive sound (Cartee, 1980; Rantanen and Ewing, 1981). The transducer acts as a receiver 99% of the time (registering returning echoes between pulses of transmitted sound) and as a transmitter only 1% of the time (Miles, 1989). These principles are the basics of the use of ultrasound for diagnostic medical imaging.

## **2.3 IMAGE DISPLAY MODES**

There are three visual modes of echo display in diagnostic ultrasound, two of which are used more frequently in clinical application in veterinary medicine. They are A-mode, B-mode, and M-mode.

**2.3.1 A-mode (amplitude mode).** This is the least frequently used and the simplest of the three modes, but still has special use for ophthalmic examinations and other applications requiring precise length or depth measurements (Nyland and Mattoon, 1995). Echosounding or sonar is the principle behind A (Amplitude) scanning. The returning ultrasound echoes are displayed as vertical spikes either on an oscilloscope or video monitor. The height or amplitude of each spike varies (is modulated) in proportion to the strength of the returning echo received by the system. All A-mode displays are standardised such that time, or distance, from the transducer is represented on the horizontal axis and amplitude, or echo strength, is shown on the vertical axis. The display is oriented as if the transducer is at the left edge of the horizontal axis. Therefore, the distance from the left margin of the display to an individual spike is directly proportional to the

depth within the body of the corresponding tissue interface. Absence of returning signal from within a tissue infers the presence of fluid within that tissue. This form of ultrasound scanning was previously used in echoencephalography, but it has now been largely replaced by CT scanning (Herring and Bjornton, 1989).

**2.3.2 B-mode (Brightness modulation).** This is a method of displaying echo information, not as vertical spikes, but on a display screen as dots whose brightness or grey scale is proportional to the amplitude of the returning echo and whose position corresponds to the depth at which the echo originated along a single line (representing the beam axis) from the transducer. B-mode is usually displayed with the transducer position located at the top of the screen and depth increasing to the bottom of the screen. The B-mode display is used in all two-dimensional ultrasound images, static or real. All modern ultrasound scans are produced with grey scale B-mode technique. In fact, "real time" scans (see below) are B-mode scans.

**2.3.3 M-mode (Time motion).** This method is used along with B-mode for echocardiographic evaluation of the heart. It is a method of tracing the movement of reflecting structures and relating such movement to time. M-mode tracings usually record depth on the vertical axis and time on the horizontal axis, and the image is oriented with the transducer at the top. The M-mode display is akin to B-mode in that echoes are registered as bright dots but only a single transducer line of sight is displayed. This line of sight is held stationary while the time base is moved to trace oscillations of the echo-producing structures. Because only one single line of sight is shown, only one dimension, distance, is indicated in M-mode displays. Hence, M-mode displays are one-dimensional.

## 2.4 REAL-TIME ULTRASONOGRAPHY

Real-time refers to the ability to see motion on the displayed ultrasound image. The image is electronically or mechanically renewed at a regular interval which is fast enough to continuously image moving structures or to provide a clear, uninterrupted view as the transducer is moved over the surface of the body (Zwiebel, 1983; Herring and Bjornton, 1989). The older static B-mode scanners, which displayed a simple frozen image, have been largely replaced by real-time scanners. Real-time images are in fact made up of successive static scans or frames, which are rapidly produced (written) and erased to exceed flicker fusion of the human eye. Real-time B-mode scanners display a moving grey-scale image of cross-sectional anatomy. This is accomplished by sweeping a thin, focused ultrasound beam across a triangular or rectangular field of view in an animal many times per second. Sound pulses are sent out and echoes received back sequentially along each B-mode line of the field until a complete sector or rectangular image is formed. Each line persists on the display monitor until it is renewed by a subsequent sweep of the beam. The beam may be steered mechanically or electronically through the field, with the frame rate (image renewal time) dependent on the depth displayed. The frame rate is slower for displaying deeper depths because more time is needed for the echoes to return to the transducer. Two basic types of real-time B-mode transducers are available: sector and linear-array.

### 2.4.1 Real-time transducers

*Sector transducer.* This real-time transducer is so named because the beam shape and resulting screen image are sector-shaped or triangular. This image may also be described as pie-, wedge-, or fan-shaped. The

sector angles vary for different purposes. Sector scanners may be classified as either mechanical or electronic depending on the method used to sweep the beam through the sector field.

*Linear-array transducer.* The linear-array transducer is an electric scanner with multiple crystals arranged in a line within a bar-shaped scan head. The narrow beam is swept through a rectangular field by firing the transducer's crystals in order sequentially. There are no moving parts and therefore this type of transducer is very reliable, and also cheaper than a sector transducer.

## **2.5 IMAGE INTERPRETATION AND TERMINOLOGY**

Ultrasound is a technique that images anatomy in any desired topographic plane. Therefore, a knowledge of the normal three-dimensional anatomy of the region to be scanned is important to recognise artifacts, interpret normal variations, and detect pathological changes (Nyland and Mattoon, 1995). In general terms, any soft tissue in the body can be imaged provided that the sound wave can reach it unimpeded. Tissues which produce echoes are described as *echogenic or echoic*. The echoes are described as hyperechoic (increased), isoechoic (normal), hypoechoic (decreased), or anechoic (absent or dark) compared with the normal echo amplitude for the surrounding tissues (Park *et al.*, 1981).

The ultrasonographic image is determined by the number and strength of the sound waves reflected by the body tissues. The amount of beam reflected back to the transducer is directly proportional to the change in acoustic impedance as the sound passes from one tissue to another. Acoustic impedance is the product of the material density and the velocity of sound propagation through the material. The absolute value of the acoustic impedance of any tissue is relatively unimportant because it is the

magnitude of the difference in acoustic impedance at a tissue interface that determines the amount of beam reflection (Rantanen and Ewing, 1981; Herring and Bjorton, 1989; Thaler and Manor, 1990).

Although reflected sound is necessary to permit imaging, sound transmission beyond a particular interface is necessary to permit the deeper structures to reflect still-available sound for further imaging (Miles, 1989). A large change in acoustic impedance, such as occurs at a soft tissue- air interface or soft tissue - bone interface, results in reflection of nearly all of the sound and leaves little sound available for imaging deeper structures. Bone and gas, therefore, severely compromise ultrasonographic examinations because they are nearly perfect reflectors (Wortman and Rantanen, 1986). The inability to penetrate gas or bone is a primary disadvantage of ultrasonography (Miles, 1989).

As an ultrasound wave travels through the body, its energy is progressively lost or attenuated. This attenuation is due to absorption, reflection and scattering of the sound energy (Shirley *et al.*, 1978; Rantanen and Ewing, 1981; Herring and Bjorton, 1989). The attenuation rate is directly proportional to the frequency of the sound wave. The depth of penetration of an ultrasound beam is frequently dependent on an attenuation rate of approximately 1 db/cm/MHz (Miles, 1989). For example, a 3.0 MHz sound beam would be attenuated at a rate of 3 db/cm, whereas a 7.5 MHz beam is attenuated at a rate of 7.5 db/cm. Thus , lower-frequency sound beams provide greater tissue penetration than higher- frequency beams (Wortman and Rantanen, 1986).

In order to overcome the progressive decrease in the intensity of the sound wave due to attenuation, ultrasonographic units are fitted with amplification systems so that tissues at varying depths could be compared. The depth or

time-gain compensation function was developed whereby echoes from interfaces near the transducer are electronically suppressed, whereas the strength of echoes from more distance tissue interfaces is amplified in proportion to the degree of attenuation. This maintains a uniform echo intensity throughout the image (Powis and Powis, 1984; Bartrum and Crow, 1983).

Although frequency and depth of penetration are inversely related, frequency and resolution of the sound beam are directly proportional. Two types of resolution are particularly important in ultrasonography. Axial resolution of any ultrasonographic unit is the ability of the sound beam to differentiate two objects along the path of the beam. If the pulse width or wavelength of the sound beam is large, structures less than one pulse width apart are visualised as a single object. Therefore, the smaller the pulse width, the better the axial resolution. It therefore follows that equipment which utilises ultrasound with higher frequencies has inherently superior axial resolution (Bartrum and Crow, 1983; Powis and Powis, 1984)

The ability of the pulsed sound wave to delineate two objects that are side by side is called lateral (Azimuthal) resolution. Lateral resolution is principally determined by the size of transducer crystal. Smaller, higher-frequency crystals have better lateral resolution and are recommended for use in examining superficial tissues like tendons. On the other hand, low-frequency beams which provide greater tissue penetration, are necessary to visualise deeper structures adequately. Lateral resolution is dependent on the width of the beam, as two structures which are less than one beam width will be perceived as one.

## **2.6 ULTRASOUND IMAGE INTERPRETATION AND ARTIFACTS**

The image created during diagnostic ultrasonography is sometimes less than precise. This is essentially due to the sub-optimal interrelationship between operator, equipment and animal, and the physics involved in image production. However, the non-invasiveness, moderate cost, safety, and ability to evaluate tissue and organ structure far outweigh any possible disadvantage and have resulted in diagnostic ultrasound becoming a primary technique in veterinary medicine (Kirberger, 1995). However, ultrasonographic imaging artifacts are commonly encountered during routine ultrasonographic examinations and contribute to image inaccuracies. The International Dictionary of Medicine and Biology (Becker and Landau, 1986) defines an artifact as " any record or image obtained in the course of applying a medical diagnostic technique which is not representative of the structures under study but is adventitious". An artifact may be defined as any alteration in the ultrasound image which does not portray a true presentation of actual structures. Bartrum and Crow (1983) define an artifact on a B- mode, grey- scale ultrasound image as any dot appearing in the ultrasound image that does not correspond to a real echo in the animal's body. When evaluating the distal hind limbs of ostriches, acoustic artifacts result in added (not real), missing, improperly located, brightness, shape or size alterations. Artifact production results from the following equipment computer software assumptions: sound only travels in straight lines: echoes only originate from reflectors located along the transducer axis; the intensity of the returning echoes is directly related to the scattering strength of the imaged objects; distance is proportional to the round trip travel time of 1540 m/sec or 13 microseconds per centimetre depth (Kirberger, 1995). A working knowledge of acoustic artifacts is required to correctly interpret ultrasonograms. This optimises available

information when evaluating tissue or organ structure and prevents incorrect diagnosis. Artifacts may be produced by electronic noise or interference, echo distortions caused by ultrasound-matter interactions, and technical imaging errors. Echo distortion caused by ultrasound-matter interactions occur more frequently than other artifacts. These consist of reverberations, shadowing, refractive and reflective zones and enhancement or through-transmission. All but reverberations also serve as diagnostic ultrasound signs.

**2.6.1 Reverberations.** Reverberating echoes are the most frequent and troublesome artifacts produced on ultrasound images. These are produced by a sound pulse bouncing back and forth between two interfaces with a large difference in acoustic impedance. They may also be produced between the transducer and the tissue interface such as the skin surface. Echoes returning to the transducer are reflected at its surface back into the body where they continue until they reach an interface and are again reflected back towards the transducer. The time lapses that occur between the second, third or fourth returning echoes places them at a greater depth in tissue on the recorded image. Only the initial recorded echoes are real: other reverberation echoes that appear deep in the tissue will be multiples of the original transducer interface echo and succeeding reverberation echoes will be smaller because of attenuation. Reverberation produces a series of parallel echoes. A similar process can also occur internally between two large interfaces in the body, thereby producing mirror images. Reverberation artifacts have been reported to be associated with muscular aponeuroses and with the interface between the stand-off pad and the skin. Not all reverberation is undesirable or possible to eliminate. It provides information about the acoustic impedance of an image surface. Reverberation can be avoided by reducing the power (voltage) and undertaking proper preparation of the area to be scanned, along with only

light pressure of the scan head.

**2.6.2 Acoustic shadows** (Fig. 1.). Acoustic shadowing is the reduction in amplitude of reflected sound caused by reflectors that lie behind a strongly reflecting or attenuating structure (Kremkau, and Taylor, 1986; Kirberger, 1995). The zone deep to the reflecting or attenuating structure is anechoic. Shadowing may be produced by bone, gas or calculi. It is a diagnostic sign used to identify calculi. Bone and other mineralised structures cast an acoustic shadow because they reflect 20-30% and absorb most of the remaining sound beam (Sommer and Taylor, 1983). The acoustic shadow caused at a soft tissue-gas interface is often filled in by multiple small echoes due to reverberations, whilst that caused by a soft tissue-bone interface is relatively echo-free. Acoustic shadows may also be caused by refraction of the sound beam at the edge of rounded structures such as urinary bladder or liver edges. In the scanning of ostrich limbs, acoustic shadows due to reflection of the sound beam by heavily keratinised skin scales were common. In some areas with very thick keratinised skin, such as the intertarsal joint and those areas distal to the tarsometatarsus, it was not possible practically to scan them because there was complete reflection of the ultrasound beam.

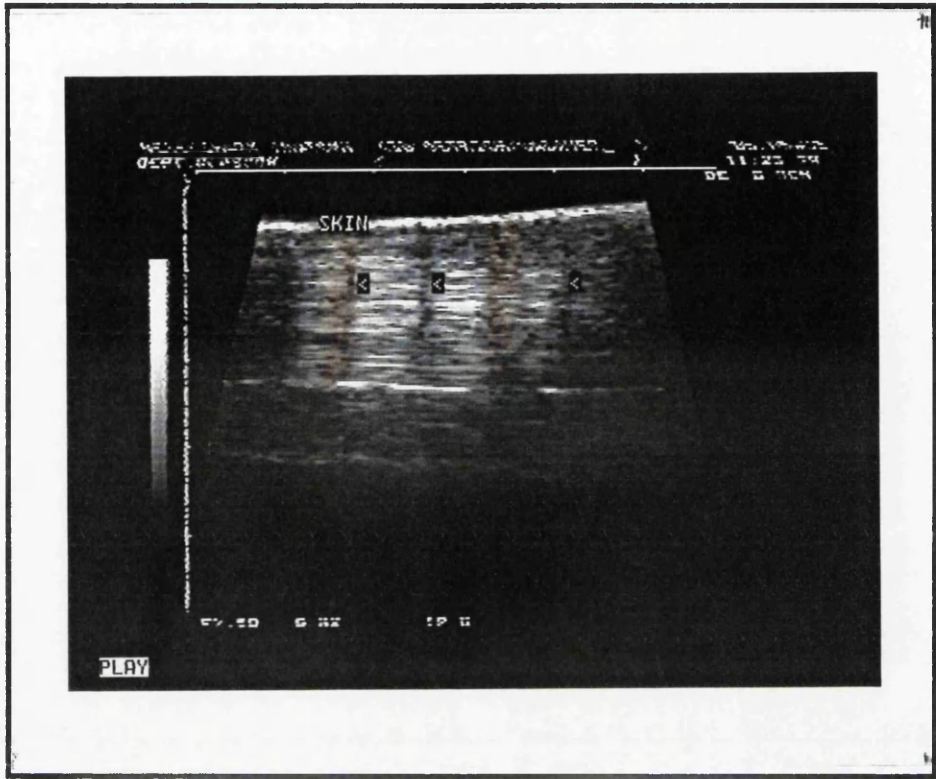


**Figure 1.** Longitudinal linear scan of the hind limb flexor tendons of the ostrich, demonstrating acoustic shadows (arrow heads) caused by heavily keratinised skin scales.

**2.6.3 Distant enhancement or through-transmission.** As the sound beam passes through a relatively homogeneous medium, such as urine or bile, less attenuation takes place than in surrounding echogenic areas. When the sound beam strikes the far end of the medium, the echoes appear to be brighter than the surrounding structures. This is the confirmation of the presence of an anechoic structure such as the urinary bladder, gall bladder or a fluid-filled cyst.

**2.6.4 Reflection and refraction.** Acoustic shadowing zones may occur distal to the margins of a rounded structure containing material of lower acoustic velocity, such as fluid-filled cystic structures. The sound penetrating the edge of such a structure may be slightly reflected or refracted producing a linear anechoic zone deep to the cystic structure. Such zones are evidence of a cystic, fluid-filled structure and should not be mistaken for shadows produced by calculi, gas or bone.

**2.6.5 Comet-tail.** These are the least common artifacts. They are caused by a highly refractive interface, most commonly an air-fluid interface. A highly echogenic stream of reverberations trailing the original interface.

**2.6.6 Electronic noise or interference.** This is caused by random electron movements within the ultrasonographic unit and any surrounding electrical equipment which may produce electronic noise. These are superimposed on the image as low level echoes.

## **2.7 A SUMMARY OF SOME TERMS USED IN ULTRASONOGRAPHY**

*Acoustic impedance:* The resistance to passage of sound waves.

*Anechoic, anechogenic:* Adjectives which describe an area on an ultrasonogram in which there are no echoes, producing a black region.

*Attenuation:* The progressive loss of energy which occurs as a sound wave or microwave travels further away from its source.

*Echoes:* The reflections of sound energy which are produced when a sound wave passes from a medium of one acoustic impedance to a medium of another acoustic impedance.

*Echogenicity:* The level of brightness of echoes on an ultrasonogram.

*Echoic, echogenic:* Adjectives which describe an area which produces echoes on an ultrasonogram producing a white or grey area.

*Echolucent:* An adjective which describes a material which contains no acoustic interfaces and consequently does not produce any echoes on an ultrasonogram.

*Grey scale:* An adjective which describes the form of ultrasonographic imaging which utilises a range of shades of brightness of white dots to denote the amplitude of the returning echoes.

*Hyperechoic, hyperechogenic:* Adjectives which describe an area on an ultrasonogram in which there is a high level of echo production, producing a white region.

*Hypoechoic, hypoechogenic:* Adjectives which describe an area on an ultrasonogram in which there is a low level of echoes, producing a grey area.

*Interface:* A boundary between a tissue of one acoustic impedance and a tissue of another acoustic impedance, at which an echo is produced.

*Piezoelectric:* An adjective which describes a material which can convert pressure to electrical energy, and vice versa.

*Real-time image:* A continuously updated, moving image.

*Reverberation:* Used to describe both the situation where, and the artifacts which result from, ultrasound bouncing repeatedly between two structures.

*Specular echoes:* The form of echoes which are produced by an

ultrasound beam which is not perpendicular to the tissue interface.

*Time-gain compensation:* A control on the ultrasonographic unit which determines the amount of amplification which is applied to overcome the attenuating effects of distance.

*Transducer:* That part of an ultrasonographic unit which emits and receives ultrasound.

*Ultrasonogram:* An image produced by ultrasonographic means.

# CHAPTER 3

## MATERIALS AND METHODS

### 3.1 GROSS DISSECTIONS

In the first part of this study, gross dissections were carried out on 14 (seven pairs) cadaverous pelvic limbs of commercially-raised clinically normal ostriches (young and adult birds). The limbs were carefully skinned and muscles separated by blunt dissections along the connective tissue planes. Their origins, form, course and insertions were examined and recorded. Tendons, ligaments and joints were also examined. Finally, the bony specimens were thoroughly cleaned of any soft tissue remnants, before being wrapped in a stockinet and cooked (100 °C) in a water boiler until such a time that all the cartilage, tendons and other soft tissues were completely detached. Washing of the bones was then carried out under running water over a sieve to avoid losing tiny bony elements. Slow drying (2-3 days) at room temperature concluded the process before the actual examination of individual bones.

### 3.2 ULTRASONOGRAPHIC ANATOMY AND CROSS-SECTIONS

The second part of this study involved an ultrasonographic examination correlated with a cross-sectional study of two fresh cadaverous limbs from a normal adult ostrich. Eight 5 cm. wide transverse bands, located just proximal to the intertarsal joint down to the level of the metatarsophalangeal joint, were identified on each limb for use as standardised sites for the examination of the cross-sectional anatomy of limb structures (Fig. 2)

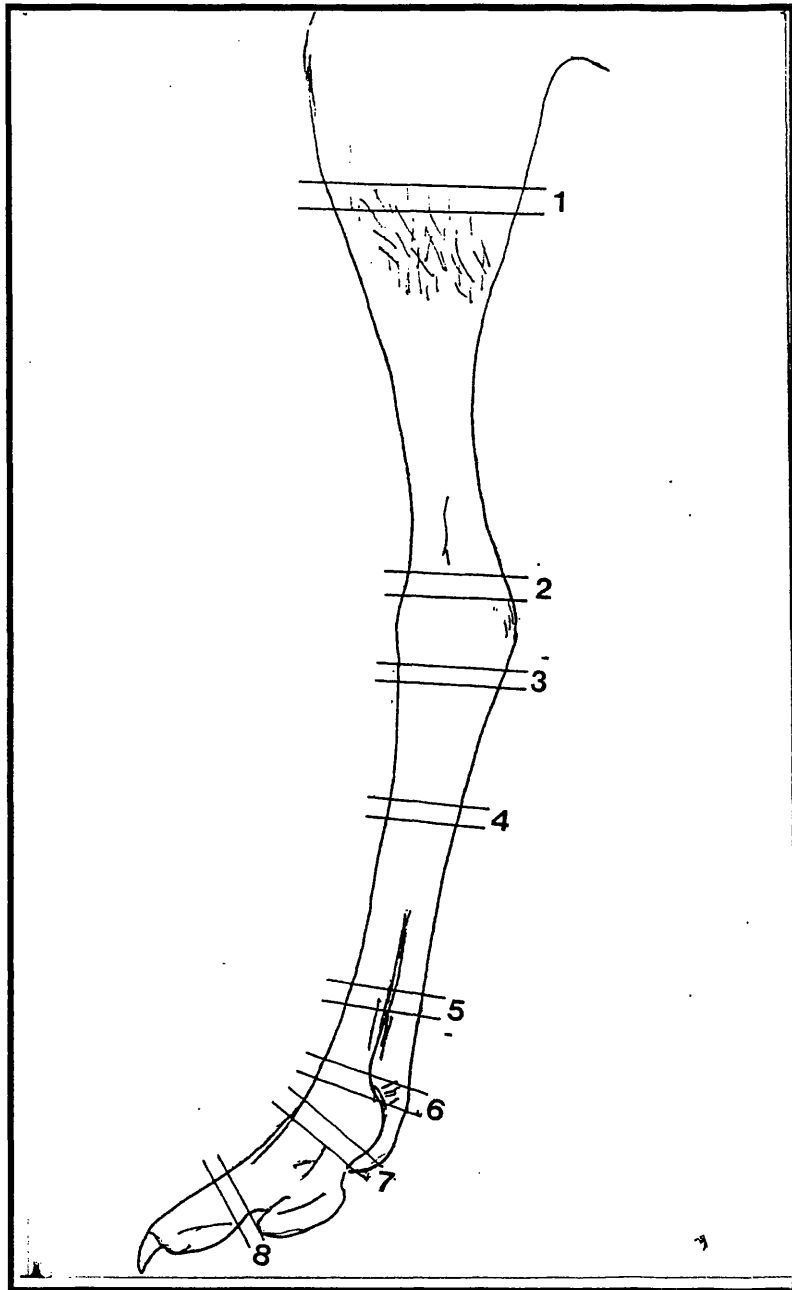


**Figure 2.** A diagram of the distal region of the pelvic limb in *Struthio camelus*, denoting the eight levels at which cross sections were made.

### 3.2.1 Equipment selection

*Scanner and Transducer selection:* High resolution real-time ultrasonographic machines were preferred for evaluation of soft tissue structures in the distal pelvic limb of the ostrich. These allow rapid identification of the structures of interest and accurate determination of the optimal scanning planes. High frequency transducers are recommended because the imaging involves superficially situated tendons and ligaments. Generally, a 7.5 MHz transducer is used in evaluation of structures of up to 4 cm in depth and the ostrich's tendons and ligaments fall within this range. In order to permit maximal resolution of these target tissues, the use of a 7.5 MHz or higher frequency transducer was necessary. High-frequency transducers are associated with spatial and contrast resolution; however, one of the disadvantages of high-frequency probes lies in their limited depth of penetration (increased attenuation) and narrow field of view (Fornage, 1986).

The linear-array transducer is advantageous for imaging superficial structures such as tendons and ligaments because it gives less near-field artifact (less distorted image in the very near field i.e. depths of less than 2 cm), and produces a clearer tendon and ligament fibre pattern. Linear-array probes also have beams perpendicular to the superficial structures making it possible to have an increased field of view. In comparison, sector scanners have a smaller field of view in the near field, and the beam is oriented obliquely in relation to the skin and longitudinally oriented tendons (Fornage and Rifkin, 1988; Harcke *et al.*, 1988).

*Stand-off system:* The convex shape of the plantar tarsometatarsal region made it extremely difficult to achieve adequate contact between the face of the ultrasonographic transducer and the skin surface. Poor contact with the

skin leads to unsatisfactory visualisation of the superficial tendons and ligaments. The use of the stand-off pad provides good acoustic coupling between a linear-array ultrasonographic transducer and the ostrich's skin. Furthermore, by increasing the distance between the probe and the region of interest, the stand-off places the tendons and ligaments in the optimal focal zone of the transducer. Stand-off pads have similar acoustic properties to those of animal tissues, and are made of a gelatinous mixture of oil and viscoelastic synthetic polymer (Fyke *et al.*, 1979; Fornage, 1989). They are flexible and adequately contour to irregular scanning surfaces. One common artifact produced by a stand-off pad is the production of linear artifacts within the regions of the image resulting from the fixed nature of the piezoelectric crystals in the transducer, sending sound beams onto the stand-off housing or stand-off margins (Pharr and Nyland, 1984). This artifact was noted, but did not interfere with image interpretation as the tissues of interest were located superficial to the artifactual echo.

In this study, diagnostic ultrasonography was carried out using a Toshiba, CAPASEE, diagnostic scanner and a 7.5 MHz linear-array transducer (Fig. 3). All images were recorded on a SONY super VHS video cassette for later printing and analysis. Attempts to scan the dorsal (i.e. "extensor") surface of the distal pelvic limb, and the plantar region distal to the metatarsophalangeal joint (sites 7 and 8), were unsuccessful due to high contours and/or thick, heavily keratinised epithelial skin covering these surfaces. Therefore, only four out of the eight levels could be successfully scanned.



**Figure 3.** The ultrasound diagnostic scanner, (Toshiba, CAPASEE), Tokyo, Japan.

### **3.2.2 Ultrasonographic examination of the ostrich distal pelvic limb.**

*Preparation:* Adequate preparation of the bird was essential for imaging tendinous and ligamentous structures with diagnostic ultrasound. Image quality is mainly affected by the quantity of the scales and the air trapped between the scales. Both attenuate the ultrasound beam. The plantar tarsometatarsal region between the intertarsal joint and the metatarsophalangeal joint was thoroughly cleaned using a soft brush, and then scanned using an echolucent stand-off pad and aqueous contact gel to improve contact between the scanning transducer and the skin. The best image was obtained by scanning the areas with minimal amounts of thick scales. The maintenance of adequate amounts of gel is essential for good image quality, and frequent reapplications may be necessary to provide an air-free interface between the skin and the transducer.

*Orientation of the beam :* Two ultrasonographic examinations were performed within each 5 cm. zone; one paraxial (longitudinal), to observe the normal alignment of the ligament fibres, and the other transverse, (in the middle of each zone) to obtain transverse morphological relationships and dimensions. When scanning the distal pelvic limb of the ostrich, the orientation of the ultrasound beam is important for reliable and comparative examination of anatomic structures. Tendons and ligaments are very sensitive to angulation in ultrasonographic imaging; they are more echogenic where fibres are perpendicular to the ultrasound beam.

*Tension/relaxation:* Hypoechoic artifacts can be obtained when the tendon or ligaments being examined are not under traction. Their relaxation induces bending of fibres at the insertion sites and the collagen fibre bundles producing artefactual sound waves in the intervening regions. This induces

typical hypoechoic artifacts that impede correct imaging. A study done by Nicoll *et al.*, (1993), demonstrated that significant reduction in mean grey-scale was obtained when the flexor tendons were relaxed. This phenomenon can be observed in the flexor tendons in ostriches if the examination is performed in a non-weight bearing position of the limb. To avoid this artifact in cadaverous specimens, weights were tied to each limb to ensure that tendons and ligaments were tensed at imaging. After scanning, each stretched limb was then frozen and sectioned transversely at all the previously marked and scanned levels. Cut-surface photographs of the frozen sections were taken to compare with the scanning prints from the same sites, in order to identify and characterise the ultrasonographic appearance of the various anatomical structures in these regions of the pelvic limb.

# CHAPTER 4

## RESULTS

### 4.1 OSTEOLOGY

Bone carries out several important functions. It provides a mechanical support for the body and is involved in the maintenance of mineral balance. It also has a protective function, reducing the potential for mechanical harm to delicate systems within it (bone marrow in long bones) and to internal organs. But it is also a dynamic structure, being jointed and providing a framework on which muscles can act to allow motion. Forces are applied to bone at the sites of attachment of ligaments and tendons, or through the joints. Bone is a living tissue and its post-natal development and growth-modelling process represents extensions of force interactions. As bone increases in length and size, its shape must be continually remodelled to maintain a form appropriate to its biomechanical function. Therefore, bone deformity is dependent upon the degree of the stress and the number of loading cycles a bone may undergo during this growing period.

**4.1.1 Tibiotarsus** (Fig. 4). The tibiotarsus articulates proximally with the femur and distally with the tarsometatarsus. In cross-section, the shaft is three-sided in the proximal third, and oval in the middle and distal thirds of its length. The lateral part bears a well-defined ridge, the fibula crest, to which the fibula is strongly attached by fibrous connective tissue. Smooth areas above and below the crest form, with the fibula, the proximal and distal interosseus spaces. The distal interosseus space is less prominent in older birds where the spine of the fibula is closely attached to the body of the tibiotarsus by strong connective tissue. Examination of an additional

museum specimen showed that, in very old birds, the two bones fuse completely in this area. Also lying on the lateral aspect of this bone is a nutrient foramen with a vascular groove leading into it.

The proximal extremity is large and roughly three sided. The articular surface (Fig. 5) consists of a medial part, *Facies articularis medialis*, hemispherical in outline, and a much smaller, oval lateral part, *Facies articularis lateralis*, situated on the caudal margin of the extremity. Cranial to, and between, these articular surfaces is a depression, the *Fossa retrocrustales*. A deep popliteal notch (on the caudal margin of the extremity) separates the lateral and medial parts of the articular surface. A very prominent tibial eminence projects cranially between these articular surfaces, curving slightly lateral and subsiding rapidly as it travels distally (Fig. 4). It carries two cnemial crests, *Crista cnemialis medialis* and *Crista cnemialis lateralis*.; the latter is greatly reduced and knob-like compared with its enormously developed counterpart. The articular surface of the distal extremity presents the large ridge-like *Condylus medialis* and *Condylus lateralis*, the bulk of these condyles lying cranial to the shaft. The *Epicondylus medialis* (medial epicondyle) is enlarged and plate-like with both deep *Depressio epicondylaris lateralis* and *medialis* (ligamental pits). The *Epicondylus lateralis* is absent. Cranially, the two condyles are separated by a deep *Incisura intercondylaris* which strongly undercuts the proximal portions of the condyles, making them more nearly horizontal and less V-shaped. In the ostrich, a vestigial supratendinal bridge (Pons supratendinous) is represented by a reduced bony spicule.

**4.1.2 Fibula** (Fig. 4). The fibula is a reduced long bone located along the lateral border of the tibiotarsus. The large, flat proximal extremity, *Caput fibularis*, rises slightly above the level of the articular surface of the tibiotarsus, continuing distally into the shaft, which is generally flattened

except for a small oval area over the proximal interosseous space. Below the level of the proximal interosseous space lies a prominent *Tuberculum m. iliofibularis* followed by a long *Spina fibulae*. The distal extremity is pointed and usually located at the distal part of the tibiotarsus.

**4.1.3 Tarsometatarsus** (Fig. 4). Proximally, the shaft is triangular in cross-sectional outline with a deep dorsal concave groove on its dorsal surface and a convex plantar surface. The concave groove gradually fades out towards the distal third of the shaft. Generally the shaft has muscular impressions in this region. The proximal articular surface (Fig. 5) consists of two concave areas, the *Cotyla lateralis* and *Cotyla medialis*, poorly separated due to a reduced *Eminentia intercondylaris*. A broad centrally located prominence, the hypotarsus, is found extending distally along the shaft on the plantar aspect, its plantar surface being marked by two vertical grooves, the *Fossae parahypotarsalis lateralis* and *medialis*. These grooves are occupied by tendons of the digital flexor muscles. Two large interosseous foramina pierce the proximal region of the shaft on either side of the hypotarsus, clearly separating the more distally fused metatarsal bones II, III (lying centrally) and IV.

At the distal extremity, the reduction in the number of digits from the typical avian condition of four to two is indicated by the presence of two trochleae. *Trochlea metatarsi III* is the larger and has two very deep *Foveae ligamenta collateralia* on each side of the condyles. The medial condyle of this trochlea extends a short distance proximally onto the dorsal surface of the shaft. The condyles are separated by a shallow *Sulcus intercondylaris*. *Trochlea metatarsi IV* is smaller and slightly oblique to the digital axis, with condyles of unequal size and extent, and relatively shallow *Foveae ligamenta collateralis* on either side. The two trochleae are separated by an *Incisura intertrochlearis*. A vestigial process representing *Trochlea*

*metatarsi II* is found on the medial extremity of the tarsometatarsus. Fusion lines can be seen running proximally up the shaft of the tarsometatarsal bone, back to the early identifiable proximal section of metatarsal bone II (Fig. 4).

**4.1.4 Phalanges** (Fig. 6). The ostrich has two cranially-directed digits, *Digiti III* and *IV*. As in other birds, the larger *Digitus III* has four phalanges and *Digitus IV* has five. The terminal (ungual ) phalanx of *Digitus IV* is the least-developed phalanx and is seen as a minute, round bone. Therefore the descriptions that follow will not apply to this phalanx unless otherwise stated. The proximal phalanx of each toe is the longest. The succeeding phalanges of each digit become progressively shorter. Each phalanx is a long bone with a shaft and two extremities of which the proximal is larger. The dorsal surface is smooth and strongly convex transversely. The plantar surface is flattened and slightly concave along its longitudinal axis. Each phalanx has a concave proximal articular surface (facet) and a convex distal articular facet devoid of any ridge. Axial and abaxial tubercles are present adjacent to these articular facets. Distal tubercles of the succeeding phalanges, after phalanx I of each digit, are seen as well-developed, laterally-flattened extensions above which are the *Foveae ligamenta collateralia*. The terminal or unguual phalanx on *Digitus III* has special characteristics. It has a proximal base and a claw-like distal projection. The base represents a rather extensive articular surface with two tubercles, one below and one above. The dorsal tubercle (*Tuberculum extensorium*) is the site for the attachment of the digital extensor muscles, whilst the ventral tubercle (*Tuberculum flexorium*) acts as the site for the attachment of the digital flexor muscles. The cranially-projecting unguual process is conical in shape, narrow in width with a dorsal convexity and two lateral grooves. The surface is rough and porous and in the fresh state covered by the corium for the strong claw.

**Figure 4.** Cranial (1) and caudal aspects (2) of the tibiotarsus and tarsometatarsus of *Struthio camelus*. The fibula is shown in (1).

1. Spina fibulae
2. Tuberculum m. iliofibularis
3. Caput fibularis
4. Crista cnemialis medialis
5. Nutrient foramen
6. Condylus lateralis
7. Condylus medialis
8. Incisura intercondylaris
9. Dorsal anterior groove
10. Trochlea tarsometatarsi IV
11. Trochlea tarsometatarsi III
12. Incisura intertrochlearis
13. Depressio epicondylaris medialis
14. Popliteal notch
15. Epicondylus medialis
16. Fusion lines
17. Hypotarsus

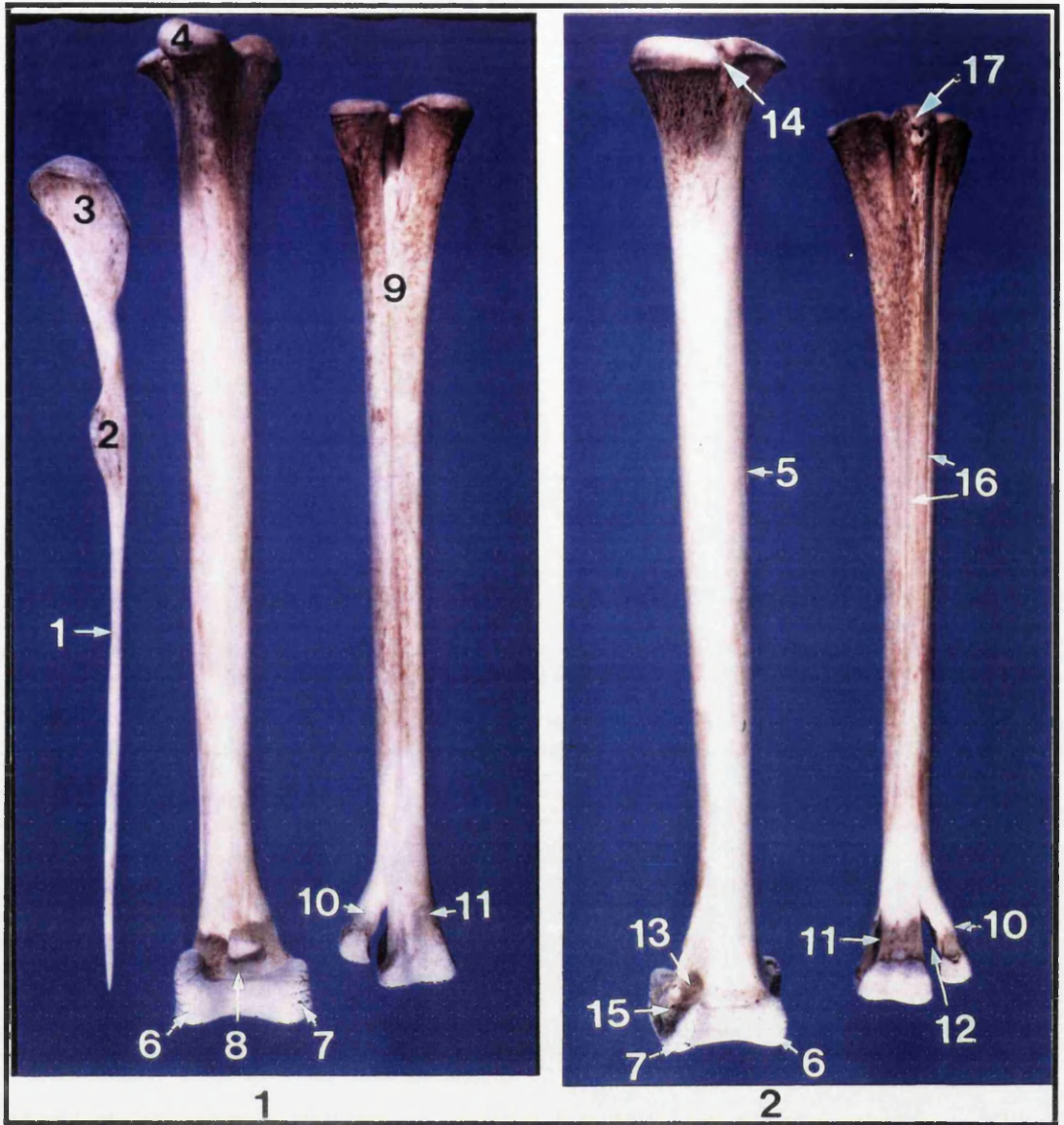
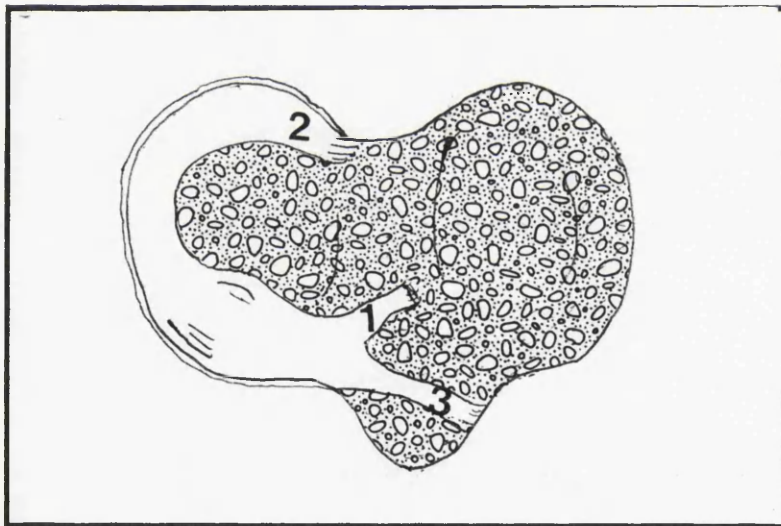


**Figure 5.** Proximal articular surfaces of tibiotalus (1) and tarsometatarsus (2) of *Struthio camelus*.

1. Facies articularis lateralis
2. Fossa retrocristales
3. Facies articularis medialis
4. Eminentia intercondylaris
5. Cotyla lateralis
6. Fossa parahypotarsalis lateralis
7. Fossa parahypotarsalis medialis
8. Cotyla medialis



Insert figure of proximal articular surface of the tarsometatarsus to show the portions and connections of lateral meniscal cartilage.

1. Ligamentum meniscotibiale
2. Ligamentum meniscotarsometatarsale, pars cranialis
3. Ligamentum meniscotarsometatarsale, pars caudalis

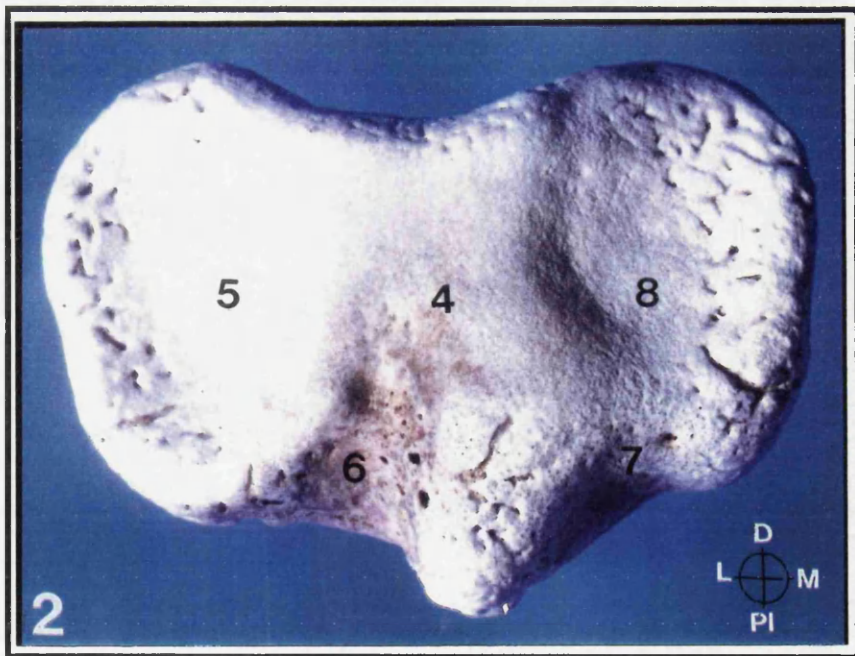
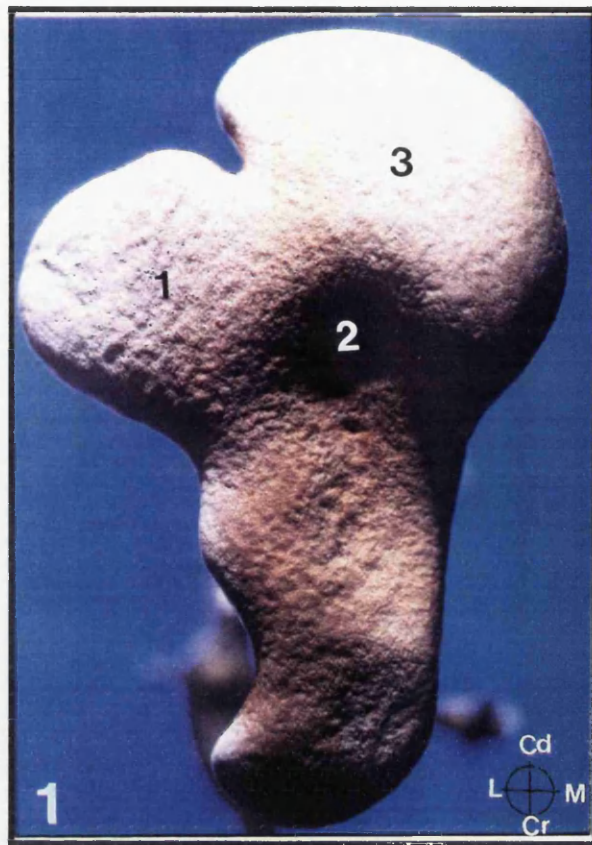
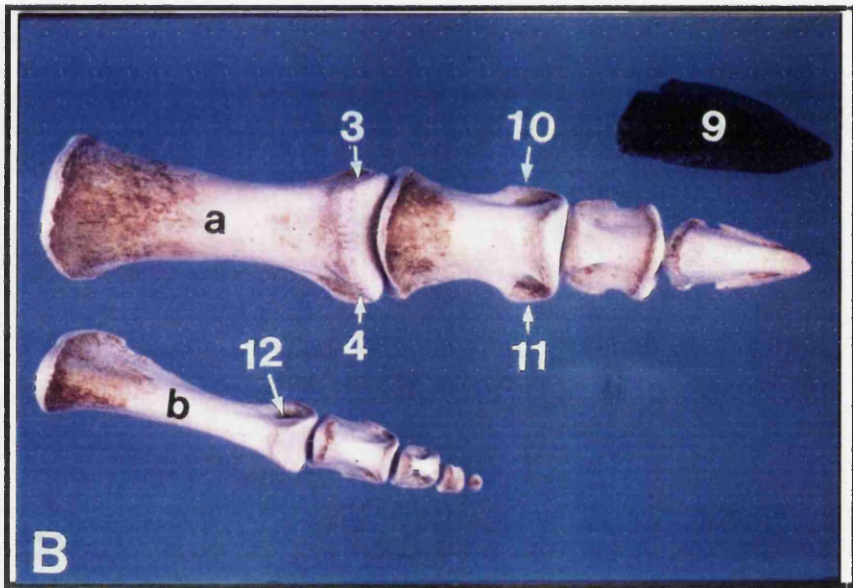
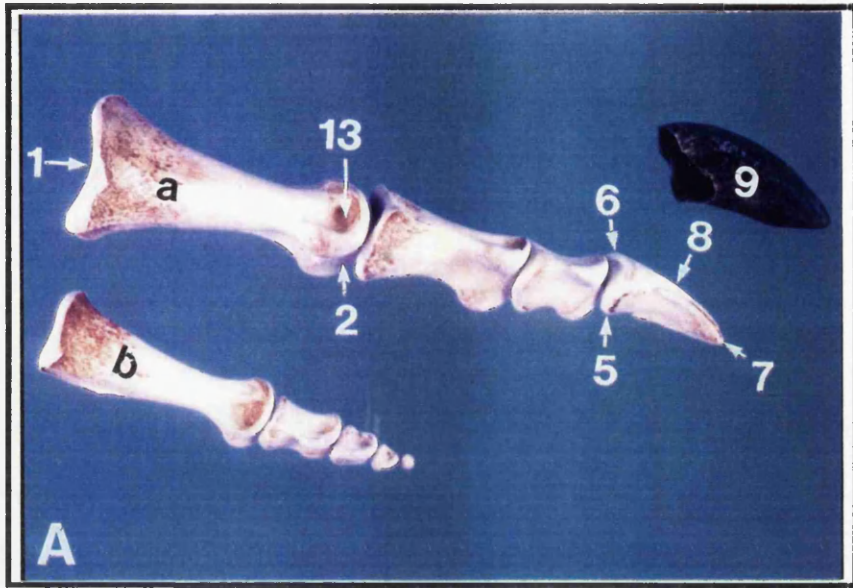


**Figure 6.** Axioplantar (A) and dorsal aspects (B) of the phalanges of the third (a) and fourth (b) digits of *Struthio camelus*.

1. Proximal articular surface
2. Distal articular surface
3. Condylus abaxialis
4. Condylus axialis
5. Tuberculum flexorium
6. Tuberculum extensorium
7. Apex phalangis
8. Ungual process
9. Claw
10. Tuberculum abaxialis
11. Tuberculum axialis
12. Fovea ligamentum collateralium axialis digiti IV
13. Fovea ligamentum collateralium axialis digiti III



## 4.2 ARTHROLOGY

The skeleton is made up of many individual bones and the sites where these bones meet are called joints (arthroses) or articulations. Joints are concerned with differential growth, transmission of forces and movement. The basic classification of joints, as laid out by Dyce *et al.*, (1987) is indicated in Fig. 7, showing both classes and naming systems.

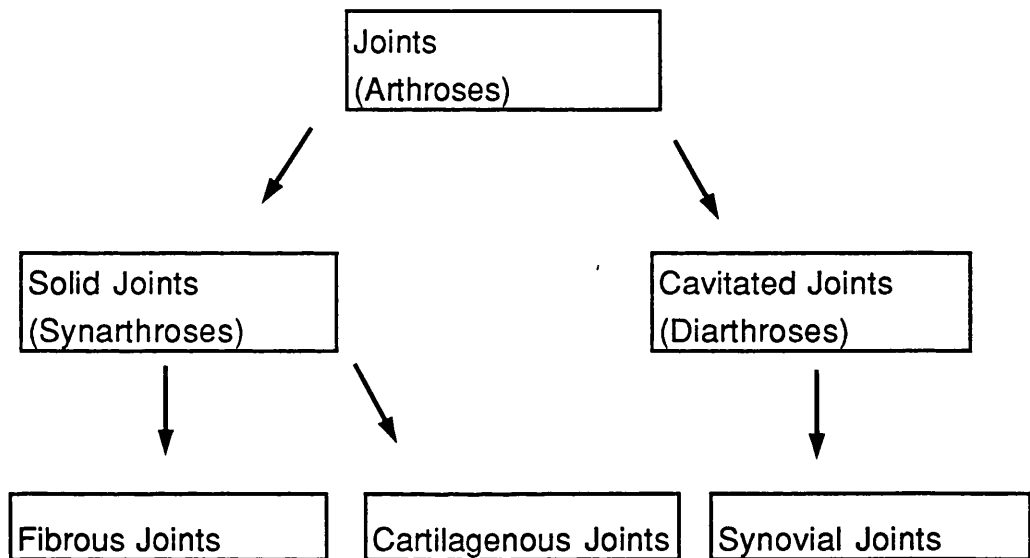


**Figure 7.** Basic classification of joints.

### 4.2.1 Tibiotarso-tarsometatarsal (Intertarsal) joint (Figs. 8, and 9).

This diarthrodial joint is equivalent to the hock joint of mammals since the tarsal bones fuse with the adjacent tibia and the metatarsus. The gross anatomy of this joint consists of opposing, congruent articular cartilage between which lies a relatively small laterally-situated cartilaginous meniscus. It is enclosed by a loose joint capsule which pouches cranially. A prominent *Cartilago tibialis* is located on the plantar surface. The

tendons of the digital flexor muscles occupy canals in this cartilage. Medial and lateral collateral ligaments secure the stability of this joint medially and laterally respectively. The insertion tendon of *M. tibialis cranialis* passes over the cranial part of this joint before inserting on the dorsal proximal tarsometatarsus, while the tendon of *M. extensor digitorum longus* also passes over the cranial aspect of this joint on its distal course down to the digits. As well as flexing it, these tendons support the cranial aspect of this joint.

The meniscus is a relatively small C-shaped cartilaginous disc located laterally in the intertarsal joint space. It is wedge-shaped in transverse section and its thick convex peripheral border is connected to the joint capsule by a fibrous attachment. It is held in position by a number of ligaments that have not been described or named before. Such connections are to the tibiotarsus by a relatively small, centrally situated *Ligamentum meniscotibiale*, and to the tarsometatarsus by a wide, substantial cranial part (*pars cranialis*), and a slightly narrower caudal part (*pars caudalis*) of the *Ligamentum meniscotarsometatarsale* (Insert, Fig. 5)

The *Ligamentum collaterale laterale* can be divided into long (*pars longa*) and short (*pars brevis*.) pars The *Ligamentum collaterale laterale pars longa* is the longer, smaller and more centrally located of the two parts, and originates from the *Depressio epicondylaris lateralis* of the tibiotarsus. From this discrete origin, this ligament passes superficial to the tendon of *M. fibularis longus* tendon that can be found transversing this joint. It extends distally as a fibrous band before inserting on the proximal lateral tarsometatarsal area. The fibres of this ligament are oriented longitudinally and maintain a relatively constant width. Loose connective tissue joins the ligament to the joint capsule; attachments were not noticed between the *Ligamentum collaterale laterale, pars longa* and the lateral meniscus. By

moving the joint it can be seen that the *Ligamentum collaterale laterale, pars longa* gets tensed during flexion and relaxes slightly during extension, of the joint.

The *Ligamentum collaterale laterale, pars brevis* is shorter, cranially located and bigger in size. It originates from a depressed roughened area, *Depressio epicondylaris lateralis*, of the tibiotarsus just distal to the point of origin of the *Ligamentum collaterale laterale, pars longa*. This ligament runs distally to insert on the proximal lateral surface of the tarsometatarsus. The fibres of this ligament are oriented longitudinally with a slightly wider distal end. It is also attached to the joint capsule by loose connective tissue. The *Ligamentum collaterale laterale, pars brevis* was seen to get tensed during extension of the joint, relaxing slightly during flexion.

Another fibrous band, thinner and longer than either of the collateral ligaments and having its origin from the proximal part of the lateral tibiotarsal condyle, crosses the joint with the superficial part of the lateral collateral ligament to insert on the plantar surface of the tarsometatarsus. It has been suggested that this band is a remnant of *M. fibularis brevis* (Pavaux and Lignereux, 1995). It is tensed when the joint is extended and relaxed when flexed.

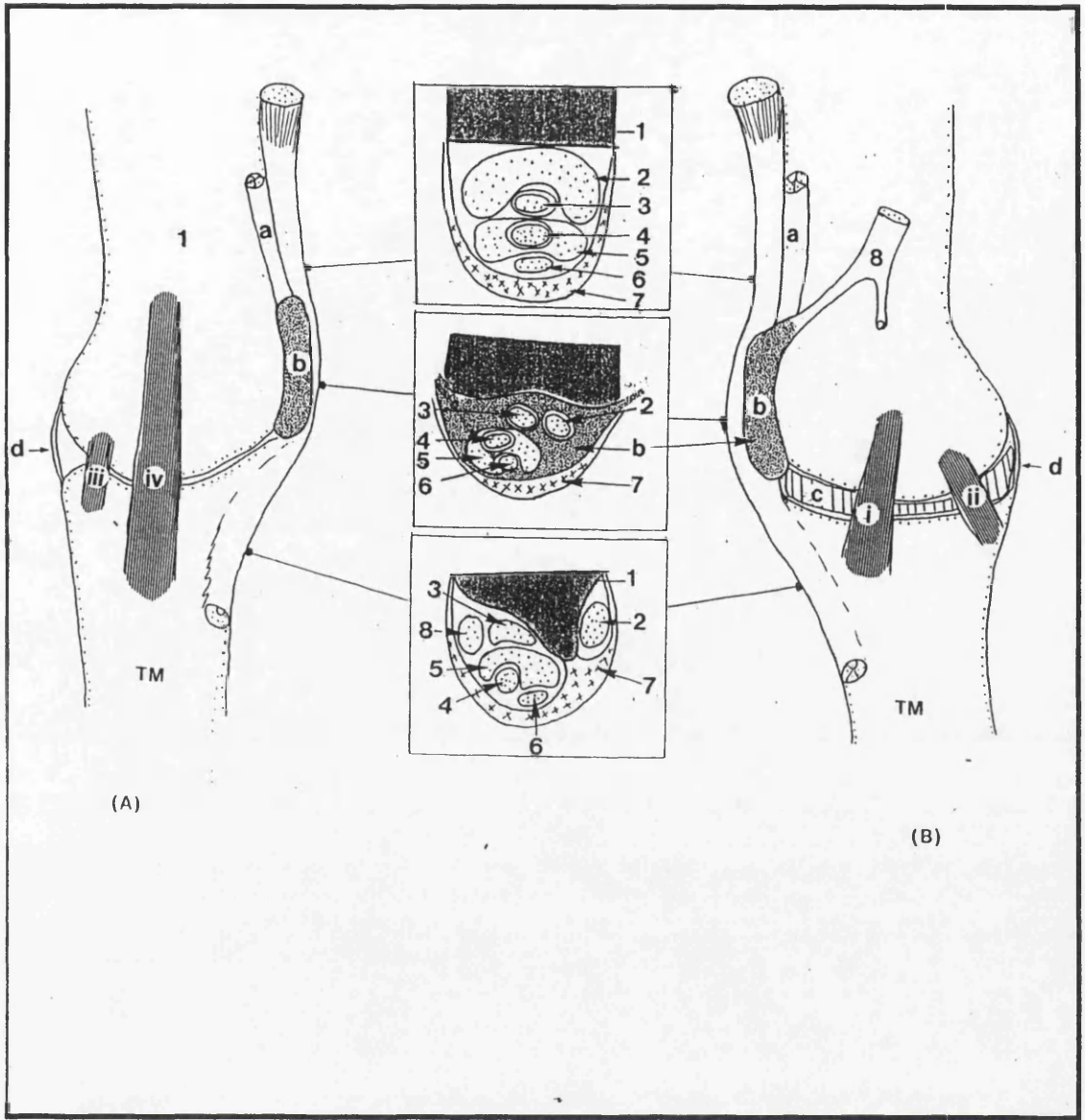
The *Ligamentum collaterale mediale* is also divided into *Ligamentum collaterale mediale, pars longa* and *brevis*. Unlike the *Ligamentum collaterale laterale*, this ligament has a wider and thicker *pars longa*, while *pars brevis* is narrower and thinner. The *Ligamentum collaterale mediale, pars longa*, is the largest of all the collateral ligaments, arising from the medial tibiotarsal condyle and crossing the intertarsal joint to insert on an extensive rectangular area of the medial proximal surface of the tarsometatarsus. As it passes distally, it is attached to the joint capsule by

loose connective tissue. The fibres of the ligament are longitudinally oriented and maintain a relatively uniform width. It is tense intermittently between full extension and flexion of the intertarsal joint.

The *Ligamentum collaterale mediale, pars brevis* is shorter and narrower. It originates from the enlarged *Epicondylaris medialis* of the tibiotarsus and runs distally to insert on the medial proximal part of the tarsometatarsus. It is tensed when the joint is extended. The *Ligamentum collaterale mediale* is better developed compared to the *Ligamentum collaterale laterale*.

**Figure 8.** Diagrammatic presentation of the medial (A) and lateral (B) aspects of the intertarsal joint of *Struthio camelus*, with accompanying cross-sections around this joint.

1. Tibiotarsus
  2. Tendon of M. flexor digitorum longus
  3. Tendon of M. flexor hallucis longus
  4. Tendon of M. flexor perforatus digiti IV
  5. Tendon of M. flexor perforatus digiti III
  6. Tendon of M. flexor perforans et perforatus digiti III
  7. Tendon of M. gastrocnemius
  8. Tendon of M. fibularis longus
- 
- a. Flexor tendon bundle comprising 2, 3, 4, 5 and 6
  - b. Cartilago tibialis
  - c. Lateral meniscus
  - d. Joint capsule
- 
- (i) Ligamentum collaterale laterale, pars longa
  - (ii) Ligamentum collaterale laterale, pars brevis
  - (iii) Ligamentum collaterale mediale, pars brevis
  - (iv) Ligamentum collaterale mediale, pars longa

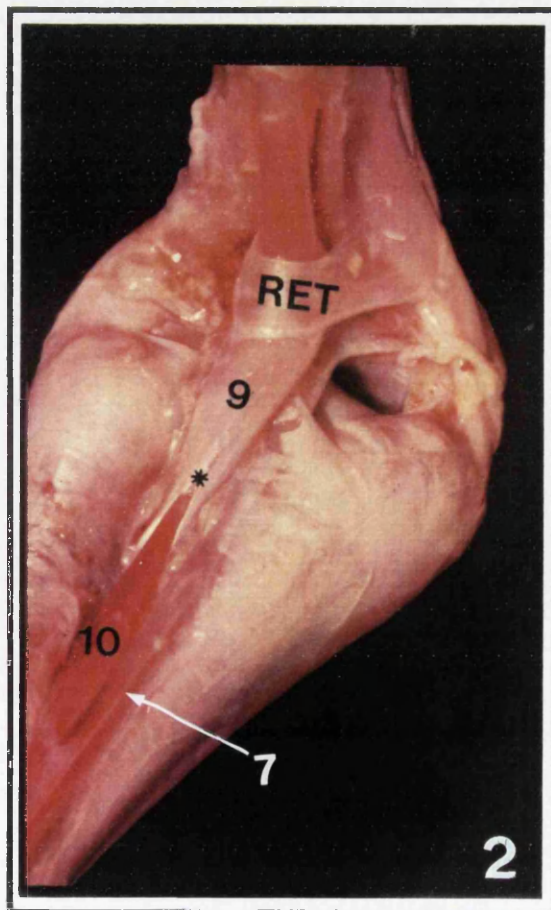
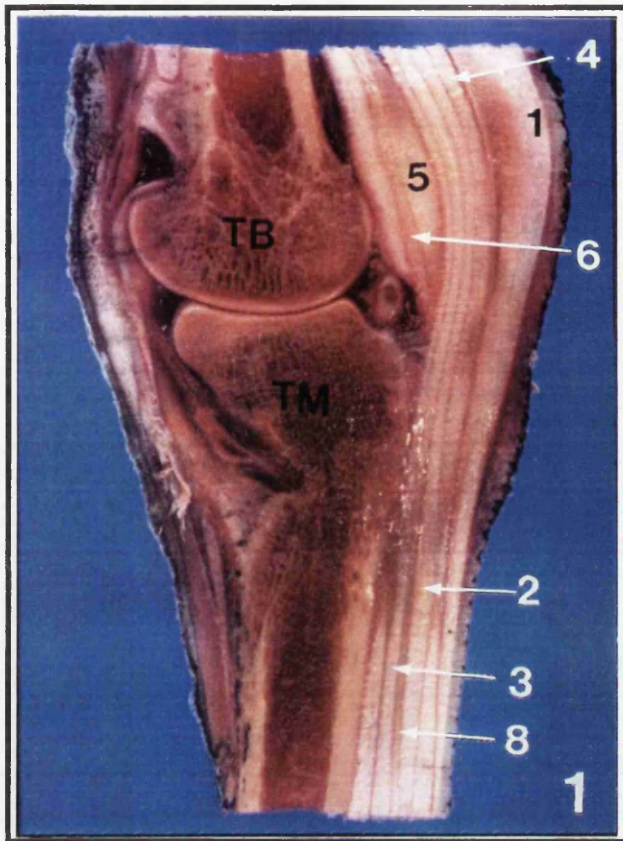


(A)

(B)

**Figure 9.** Paraxial section (1) and cranial aspect (2) of the intertarsal joint of *Struthio camelus*

1. Tendon of *M. gastrocnemius*
  2. Tendon of *M. flexor perforatus digiti III*
  3. Tendon of *M. flexor perforatus digiti IV*
  4. Tendon of *M. flexor perforans et perforatus digiti III*
  5. *Cartilago tibialis*
  6. Tendon of *M. flexor hallucis longus*
  7. Tendon of *M. extensor digitorum longus*
  8. Tendon of *M. fibularis longus*
  9. Tendon of *M. cranialis tibialis*
  10. *M. extensor proprius digiti III*
- TB= Tibiotarsus  
TM= Tarsometatarsus  
RET= Retinaculum extensorium tibiotarsi
- Note:* Canals in the tibial cartilage and the splitting (\*) of the tendon of *M. cranialis tibialis* before its insertion.



**4.2.2 Metatarsophalangeal joints** (Fig. 10). The two diarthrodial metatarsophalangeal joints, located between the tarsometatarsal trochlear surface and the proximal phalanx of each digit, exhibit a number of characteristic features. A lateral and medial supporting collateral ligament is associated with each joint. The joint capsule is continuous on its plantar surface with a very substantial *Ligamentum plantaris*, whilst the thin, relatively insubstantial dorsal part of the joint capsule is loosely connected to the digital extensor tendons.

A thick, dense fibrocartilaginous *Ligamentum plantaris* forms the plantar wall across each metatarsophalangeal joint. It is firmly attached to the base of the proximal phalanx and the laterally-placed collateral ligaments. Its plantar surface exhibits a deep sulcus through which the digital flexor tendons run, these tendons being restrained within the sulcus by a fibrous sheath (*Vaginae fibrosae*), arising as a continuation of the *Ligamentum plantaris*, that stretches across the sulcus. Its deep surface, forming part of the plantar wall of each metatarsophalangeal joint, is adapted in a general way to the plantar surface of each trochlea. A rounded vertical ridge divides the articular surface of the *Ligamentum plantare* into two parts, to fit into the corresponding groove on the trochlea; this deepens the socket of reception for the head of the trochlea. The *Ligamentum plantaris* over the metatarsophalangeal joint of digit III differs from that of digit IV in that it is significantly more developed and detaches single axial and abaxial ligamentous bands which are attached to the base of the distal end of the proximal phalanx. The *Ligamenta plantare* are connected loosely to the underlying flexor tendon bundles by a small muscle, *M. lumbricalis*. At the interphalangeal joints these ligaments originate from the distal plantar aspect of a proximal phalanx and cross the interphalangeal joint to insert on the proximal plantar aspect of the following distal phalanx.

**4.2.3 Interphalangeal joints** (Fig. 10). There are three diarthrodial joints within digit III and four for digit IV although, on digit IV, only three joints are distinguishable because of the minute nature of the last phalanx. The first interphalangeal joint on each digit is the largest and best developed with succeeding joints becoming progressively smaller and less developed. Each joint consists of a joint capsule, two collateral ligaments, and a *Ligamentum plantaris*. *Ligamenta plantare* are located at all interphalangeal joints, with the exception of the terminal interphalangeal joint of the fourth digit. The joint capsule is connected on its plantar surface with the substantial *Ligamentum plantaris*. The dorsal part of the joint capsule is thin and connected to the digital extensor tendons. The presence of *Ligamentum plantaris*, joint capsules and collateral ligaments coupled with very narrow articular surfaces on the heads of the adjacent phalanges, gives the interphalangeal joints a limited range of motion.

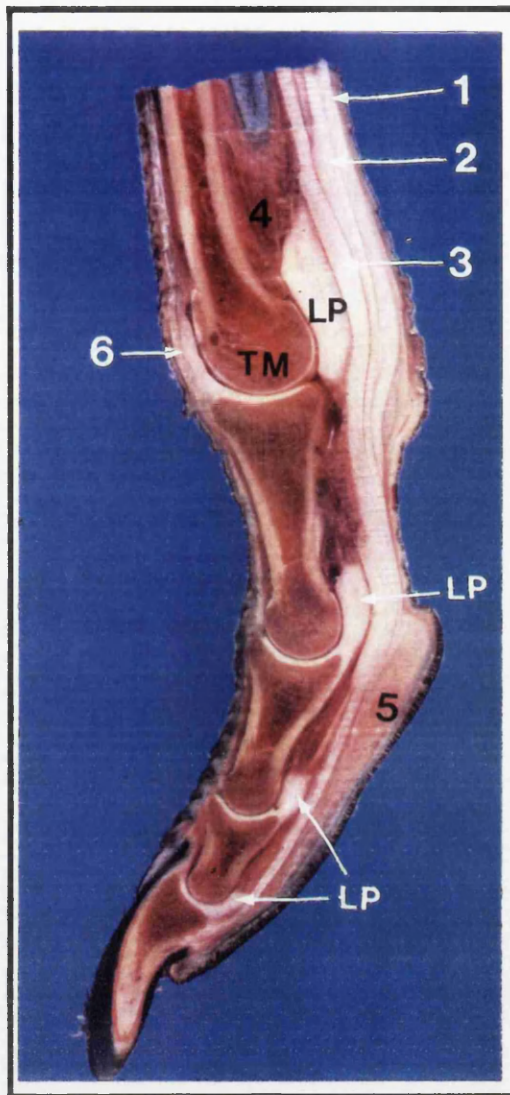


**Figure 10.** Paraxial section showing the metatarsophalangeal and interphalangeal joints of the third digit of *Struthio camelus*.

1. Tendon of M. flexor perforatus digiti III
2. Tendon of M. flexor perforans et perforatus digiti III
3. Tendon of M. flexor digitorum longus
4. M. lumbricalis
5. Digital cushion
6. Joint capsule

TM= Tarsometatarsus

LP= Ligamentum plantaris

## 4.3 MUSCULATURE

### 4.3.1 Superficial layer (Fig. 11)

***M. gastrocnemius***. This is the largest and most superficial muscle on the caudal aspect of the crus and consists of three distinct parts, *pars externa*, *pars intermedia* and *pars interna*. *Pars externa* lies on the lateral surface of the crus, arises by a thick tendon from the lateral surface of the lateral condyle of the femur, and is in contact cranially with the belly of *M. fibularis longus*. *Pars intermedia*, the smallest of the three parts, lies deeper in the caudoproximal crural musculature, arising by fleshy fibres from the medial condyle of the femur. *Pars interna*, the largest of the three parts, lies on the medial surface of the crural region and has a broad fleshy and tendinous attachment from the medial surface of *Crista cnemialis* of the tibiotarsus. The inserting tendons of these three parts fuse near the distal end of the crural region to form a common tendon of insertion, the *Tendo Achilles*. This tendon passes over the caudal surface of the *Cartilago tibialis* where the two become tightly bound together. It then broadens before inserting onto the hypotarsus and the medioplantar and lateroplantar surfaces of the proximal tarsometatarsus, where it forms a sheath covering the digital flexor tendon bundles.

***M. fibularis longus***. This is a superficial broad flat muscle which lies on the cranio-lateral surface of the crural region. The belly is large, extending along the proximal three quarters of the tibiotarsus before tapering distally into its tendon of insertion. It almost conceals from view the deeper muscles on the cranio-lateral surface of the crural region. The muscle has a broad tendinous superficial origin from the tibiotarsus, originating along the cranial border of *Crista cnemialis medialis*, and then curves distally, onto the belly of *M. flexor perforans et perforatus digiti III*. As in most birds, the long flat tendon of insertion passes distally and bifurcates near the distal

end of the tibiotarsus. A long thin branch passes distally across the lateral surface of the intertarsal joint (*Articulatio intertarsalis*) to insert upon the insertion tendon of *M. flexor perforatus digiti III* in the proximal half of the tarsometatarsal region. The shorter branch inserts on the proximal end of the *Cartilago tibialis*.

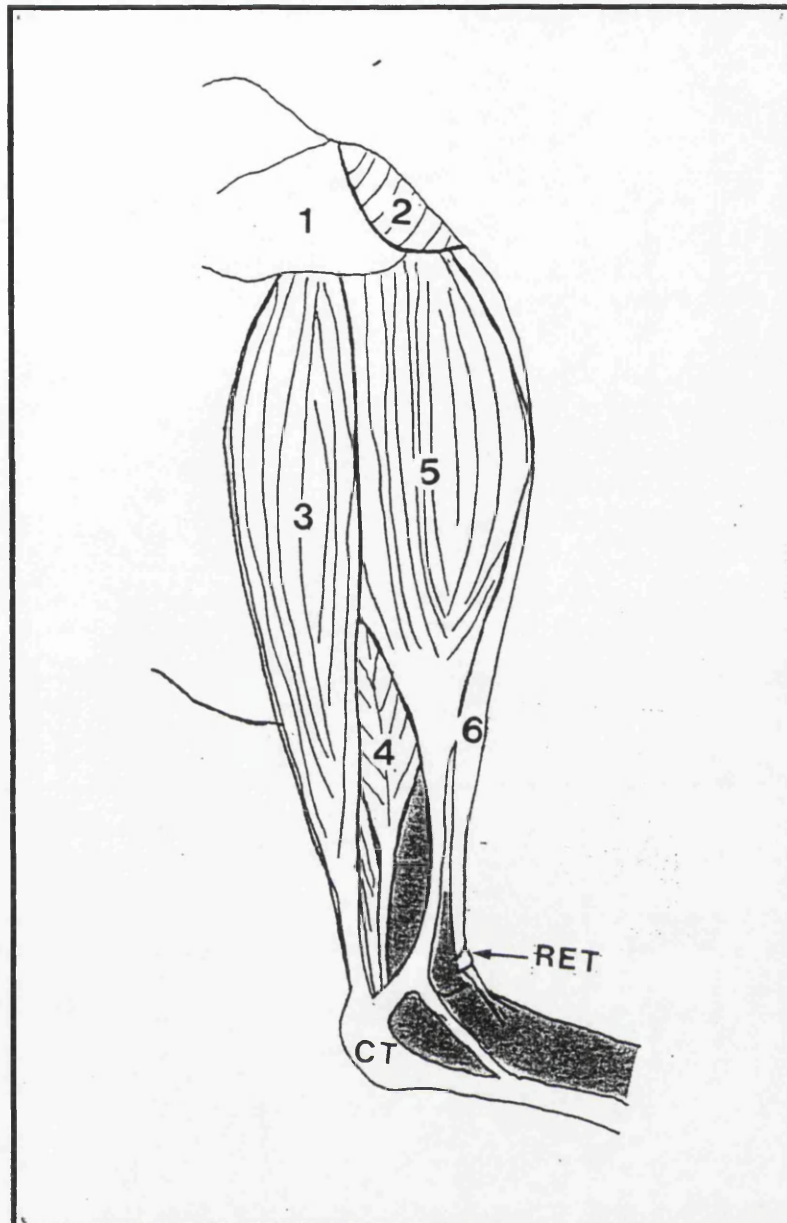


**Figure 11.** Lateral view of the superficial muscle layer of the distal pelvic limb of *Struthio camelus*.

- 1. Fascia of M. iliotibialis lateralis
- 2. M. femorotibialis medius
- 3. M. gastrocnemius (pars externa)
- 4. M. flexor perforans et perforatus digiti III
- 5. M. fibularis longus
- 6. M. tibialis cranialis
- RET=Retinaculum extensorium tibiotarsi
- CT= Cartilago tibialis

#### 4.3.2 Deep layer (Fig. 12)

***M. flexor perforans et perforatus digiti III***. The belly of this bipinnate muscle lies within the proximal half of the lateral crus, cranial to *Mm. flexor perforatus digiti IV* and *flexor perforatus digiti III*. The muscle arises by fleshy fibres from *Crista cnemialis lateralis* and from the ligamentous material covering the head of the fibula. There is also a tendinous connection with the proximocranial edge of *M. flexor perforatus digiti IV*, and a fine aponeurotic connection to the inserting tendon of *M. ambiens*. The tendon of *M. flexor perforans et perforatus digiti III* travels distally along the lateral surface of the tibiotarsus, superficial to the tendons of insertion of *Mm. flexor perforatus digiti III* and *flexor perforatus digiti IV*, to continue across the distocaudal surface of the tibiotarsus, down through a common canal in the *Cartilago tibialis* (this canal also carries inserting tendons of *Mm. flexor perforatus digiti III* and *flexor perforatus digiti IV*), and through the *Fossa parahypotarsalis lateralis* before descending down the plantar surface of the tarsometatarsus.

When nearing the distal end of the tarsometatarsus the inserting tendon becomes connected by a short vinculum (*Vinculum tendinum flexorum*) to the tendon of insertion of *M. flexor perforatus digiti III*. Like other flexor tendons in this area, it increases in size and travels through a deep sulcus in the plantar ligament located on the plantar aspect of the metatarsophalangeal joint of the third digit. While running through this sulcus it is topographically deep to the tendon of insertion of *M. flexor perforatus digiti III* and superficial to the tendon of insertion of *M. flexor digitorum longus*; here all three superficial flexor tendons are ensheathed by the fibrous sheath (*Vaginae fibrosae*) that stretches across the sulcus. The combined tendon bundle runs on the plantar aspect of the third digit, inserting in a systematic manner as shown in Fig. 15.

The inserting tendon perforates the inserting tendon of *M. flexor perforatus*

*digiti III* near the proximoplantar end of phalanx I of digit III, then bifurcates and is itself perforated by the inserting tendon of *M. flexor digitorum longus* in the proximoplantar half of phalanx II. The axial and abaxial branches insert upon the axioplantar and abaxioplantar surfaces, respectively, of the *Ligamentum plantaris* which lies on the plantar aspect of the second interphalangeal joint.

***M. tibialis cranialis.*** This large muscle of the craniolateral crus lies deep to *M. fibularis longus*, and consists of two closely apposed heads of origin, a small caudolateral *Caput femorale* and a larger craniomedial *Caput tibiale*. *Caput femorale* arises by a long thick tendon from *Fovea tendinis m. tibialis cranialis* on the distal craniolateral aspect of the femur whilst *Caput tibiale* arises by fleshy fibres from the craniolateral edge of *Crista cnemialis medialis*. At a point approximately two-thirds the way distally down the tibiotarsus, the two heads fuse and give rise to a tendon of insertion. This stout tendon of insertion passes distally under an oblique fibrous loop, *Retinaculum extensorium tibiotarsi*, to broaden over the *Incisura intercondylaris*, and cross over the cranial surface of the intertarsal joint to insert on *Tuberositas m. tibialis cranialis* on the proximodorsal surface of the tarsometatarsus, with two short tendons, one slightly cranial to the other. *Retinaculum extensorium tibiotarsi* (Fig. 9) is a stout ligamentous loop that extends between the distal craniolateral and craniomedial surfaces of the tibiotarsus, just proximal to and roughly parallel with the smaller *Pons supratendineus*.

***M. flexor perforatus digiti IV.*** This small muscle is located in the crural region between the muscle bellies of *Mm. flexor perforans et perforatus digiti III* and *flexor perforatus digiti III*. It originates from medial and lateral heads, which are separated by the insertion tendon of *M. iliofibularis*. The caudodistal surface of each head consists of a tendinous

sheet. These sheets fuse near the midpoint of the tibiotarsus, and taper distally to form a flat tendon of insertion which immediately becomes ensheathed by the tendon of insertion of *M. flexor perforatus digiti III*.

The medial head arises by fleshy fibres from the popliteal notch and the lateral head by tendinous fibres from *Condylus lateralis femoris* and an additional small fleshy slip from the inserting tendon of *M. ambiens*. The tendon of insertion remains ensheathed through the common canal in *Cartilago tibialis*, and through the *Fossa parahypotarsalis lateralis*, before separating again in the proximal tarsometatarsal region. It then descends as a free tendon along the plantar surface of the tarsometatarsus, along with other flexor tendons, down to the digits. After this separation, the tendon of *M. flexor perforatus digiti III* is joined by a branch of the tendon of insertion of *M. fibularis longus*.

At the level of the metatarsophalangeal joint of digit IV, this tendon, like other flexor tendons in this area, increases in size to ensheath the small tendon of insertion of *M. flexor digitorum longus* (branch to the fourth digit). The two tendons run through a deep sulcus in the *Ligamentum plantaris* located across this joint, ensheathed by a fibrous sheath stretching across the sulcus in a similar manner to that of digit III. The inserting tendon continues its plantar course before giving off axial and abaxial branches over the proximoplantar end of phalanges I and II of digit four, before bifurcating and being perforated by the inserting tendon of *M. flexor digitorum longus*

***M. flexor perforatus digiti III***. This large muscle of the caudal crural region consists of two widely separated bellies, femoral and distal. The femoral belly arises by a short tendon from the proximocaudal intercondylar region of the femur, distal to the origin of the medial head of

*M. flexor perforatus digiti IV*. The distal belly arises by a fleshy attachment from the inserting tendon of *M. ambiens*, and by a long tendon from the ligamentous material covering the head of the fibula. The bulky femoral belly extends distally along the proximal three quarters of the mediocaudal crus. The smaller distal belly lies deep in the laterocaudal crus, medial to the lateral head of *M. flexor perforatus digiti IV*. The laterocaudal surface of the distal belly is indented by the inserting tendon of *M. flexor perforatus digiti IV*.

Distally, each belly continues as a short tendon; these join to form the large tendon of insertion. This inserting tendon passes distally, ensheathing the inserting tendon of *M. flexor perforatus digiti IV*, through the common canal in *Cartilago tibialis* (Fig. 18) and through the *Fossa parahypotarsalis lateralis*, before separating from the inserting tendon of *M. flexor perforatus digiti IV*. After this separation, the tendon of *M. flexor perforatus digiti III* is joined by a branch of the tendon of insertion of *M. fibularis longus* in the proximal tarsometatarsal region (Fig. 13), after which it continues distally along the plantar surface of the tarsometatarsus before getting connected by a short vinculum to the tendon of *M. flexor perforans et perforatus digiti III* in the distoplantar third of the tarsometatarsus. It increases in size, and together with the other flexor tendons to the third digit, runs through a deep sulcus in the *Ligamentum plantaris* located across the metatarsophalangeal joint, where it is ensheathed by the fibrous flexor sheaths that stretch across the sulcus. The insertion tendon then bifurcates and is perforated by the inserting tendons of *M. flexor perforans et perforatus digiti III* and *M. flexor digitorum longus* near the proximoplantar end of phalanx I of digit III, the lateral and medial branches of the tendon then attaching to the lateroplantar and medioplantar surfaces respectively of the *Ligamentum plantaris* lying plantar to the first interphalangeal joint of digit III.

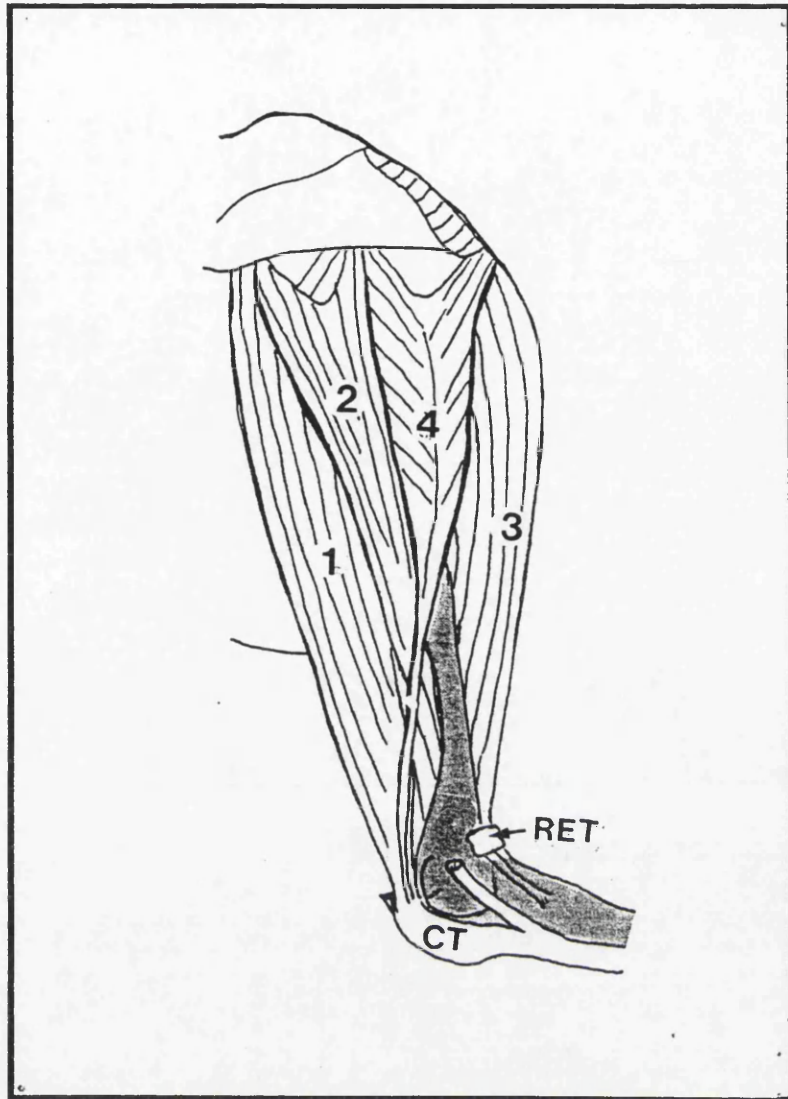


**Figure 12.** Lateral view of the deeper muscle layer of the distal pelvic limb of *Struthio camelus*. *Mm. gastrocnemius* and *fibularis longus* have been removed.

- |  |
|--|
| <p>1. M. flexor perforatus digiti III<br/>         2. M. flexor perforatus digiti IV<br/>         3. M. tibialis cranialis<br/>         4. M. flexor perforans et perforatus digiti III</p> <p>CT= Cartilago tibialis<br/>         RET= Retinaculum extensorium tibiotarsi</p> |
|--|

#### 4.3.3 Deepest layer (Fig. 14)

***M. extensor digitorum longus.*** The bipinnate elongated belly of this muscle lies deep to *M. tibialis cranialis* and is the deepest muscle on the cranial surface of the crus. This muscle has an extensive fleshy origin, deep to the belly and origin of *M. tibialis cranialis*, from the lateral surface of *Crista cnemialis medialis* and the distal end of *Crista cnemialis lateralis*. The tendon of insertion takes a distal course, deep to the tendon of *M. tibialis cranialis*, under the *Retinaculum extensorium tibiotarsi* and *Pons supratendineus*. It continues through the *Incisura intercondylaris* and crosses the intertarsal joint cranially, to continue distally along the cranial surface of the tarsometatarsus. In the distal tarsometatarsal region the tendon of *M. extensor digitorum longus* bifurcates. The bigger branch runs distally over the dorsal surface of digit III to insert via laxial, abaxial and dorsal bands onto the first phalanx.

The smaller branch continues in the direction of the fourth digit but bifurcates again before passing over the first phalanx; one resultant branch continues distally to insert on all the phalanges of the fourth digit, while the other branch crosses over to the third digit where it has strong attachments dorsally to the second, third and fourth phalanges, but has a primary insertion on the fourth phalanx of the third digit.

***M. flexor digitorum longus.*** The flat bipinnate belly of this deep muscle lies on the proximal three-quarters of the caudal surface of the tibiotarsus, deep to *M. flexor perforatus digiti III* and at the same level as the small fusiform belly of *M. flexor hallucis longus*. Proximally the belly consists of two closely apposed small heads, a lateral head arising by fleshy fibres from the caudal surface of the head and proximal shaft of the fibula, and a smaller medial head arising by fleshy fibres from the proximocaudal region

of the shaft of the tibiotarsus. The fleshy origin of the muscle extends distally to the midpoint of the caudal surface of the tibiotarsus.

The tendon of insertion that arises from the tapering muscle belly passes distally, along the crus, deep to tendon of insertion of *M. flexor hallucis longus*, through a separate medial canal in the *Cartilago tibialis*. It continues distally as the only tendon that runs through the *Fossa parahypotarsalis medialis*, where it remains covered by the broad sheath of the inserting tendon of *M. gastrocnemius*. It continues along the plantar aspect of the tarsometatarsus, to fuse with the inserting tendon of *M. flexor hallucis longus* in the proximal tarsometatarsal region. The resulting common tendon continues its plantar course distally, along with other flexor tendons, towards the two digits.

Near the distal end of the tarsometatarsus, this common tendon of insertion bifurcates to send a branch to each digit. The branches to these digits perforate the appropriate long digital flexor tendons, as previously described, and then each branch continues distally along the plantar surface of the appropriate digit. A short fibro-elastic slip passes from the branch to digit III to attach to the proximoplantar surface of the *Ligamentum plantaris* of the second interphalangeal joint. Each main branch continues distally and bifurcates before inserting upon the proximoplantar surface of the ungual phalanx (*phalanx distalis*).

***M. flexor hallucis longus.*** This is one of the muscles that lie on the caudal surface of the crus. It is a relatively small-bellied fusiform muscle lying caudal to *M. flexor digitorum longus* and having a fleshy origin from the intercondyloid area of the femur. The small belly tapers into a flat tendon of insertion which runs distally along the distal half of the large muscle belly of *M. flexor digitorum longus*. Its tendon of insertion passes

distally through a separate lateral canal in *Cartilago tibialis* (Fig.18) and then through the *Fossa parahypotarsalis lateralis*. After passing through this groove, the tendon takes a diagonal course from lateral to medial, to fuse with the tendon of *M. flexor digitorum longus* in the proximal tarsometatarsal region.

***M. extensor proprius digiti III*** (Fig. 9 and 14). This tiny muscle arises from the dorsal surface of the proximal quarter of the tarsometatarsus. Its fleshy fibres originate from between the two short tendons of insertion of *M. tibialis cranialis*, with additional small tendinous fibres originating from the fibrous joint capsule of the intertarsal joint. The small muscle belly is restricted to the proximal quarter of the tarsometatarsus. The slender tendon of insertion runs distally alongside the tendon of *M. extensor digitorum longus*, before following the latter's branch to the third digit. It passes dorsally over the first phalanx, sends minor fibrous attachments to the dorsal surfaces of the first three phalanges, then fans out dorsally to its main point of insertion on the proximal end of the fourth phalanx.

***M. adductor digiti IV*** (Fig. 14). This very small muscle is composed of two muscle bellies situated on the plantolateral surface of the tarsometatarsus. The proximal belly is located deep to the flexor tendon bundle, just distal to the intertarsal joint; the distal belly is located in the distal third of the tarsometatarsus. It has fleshy points of origin and insertion within this region of the tarsometatarsus with both muscle bellies being connected by a fibrous aponeurotic sheet.

***M. extensor brevis digiti IV*** (Fig.14). This very small muscle has a fleshy origin from the distal third of the dorsolateral surface of the tarsometatarsus. The tendon of insertion passes through a bony canal (*Canalis interosseus tendineus*) between the *Trochleae metatarsi III* and

IV to insert on the axial surface of the base of the proximal phalanx of digiti IV.

***M. extensor brevis digiti III.*** This is a tiny, poorly-developed fan-shaped muscle located on the distal quarter of the dorsal surface of the tarsometatarsus, deep to the tendon of insertion of *M. extensor digitorum longus*. It originates from tendinous fibres arising from the distodorsal quarter of the tarsometatarsus, near the *Trochlea metatarsi III*. A broad flat tendon of insertion is incorporated into the *Capsula articularis* of the metatarsophalangeal joint of digit III, whilst a few other tendinous fibres can be seen to insert upon the proximal dorsal surface of the first phalanx of digit III.

***M. lumbricalis*** (Fig. 10). This muscle is situated dorsal (deep) to the bifurcation of the inserting tendon of *M. flexor digitorum longus*. The muscle originates over a short distance by means of fleshy fibres arising directly from the dorsal surface of the inserting tendon of *M. flexor digitorum longus*. These fibres run distally towards digits III and IV, to insert directly upon the proximal region of the *Ligamentum plantaris* across the metatarsophalangeal joints of both digits.

***M. popliteus.*** This is a very small, deep-lying muscle situated on the proximal end of the caudal surface of the tibiotarsus, deep to the proximal portion of the belly of *M. flexor hallucis longus*. It is represented primarily by an aponeurotic sheet carrying only a few grossly visible muscle fibres running between the proximal tip of the fibula and the tibiotarsus. Given its small size, it can easily be missed in dissection.

***Digital check apparatus.*** A special, apparently previously undescribed group of ligaments is located on the plantar aspect of the foot. These

ligaments form a network originating from the *Pulvinus metatarsalis* and spreading out in a radiating pattern as shown in Fig. 15. This network is composed of the *Ligamentum abaxiale digiti III* and *Ligamentum axiale digiti III*, *Ligamentum axiale digiti IV*, a reduced *Ligamentum abaxiale digiti IV*, and *Ligamentum interdigitale digiti III et IV* in the *Tela interdigitalis* connection between the two digits. Because such a network of ligaments does not appear to have been described before, it seemed appropriate to refer to it as the digital check apparatus and assign names to its component parts, as noted above.

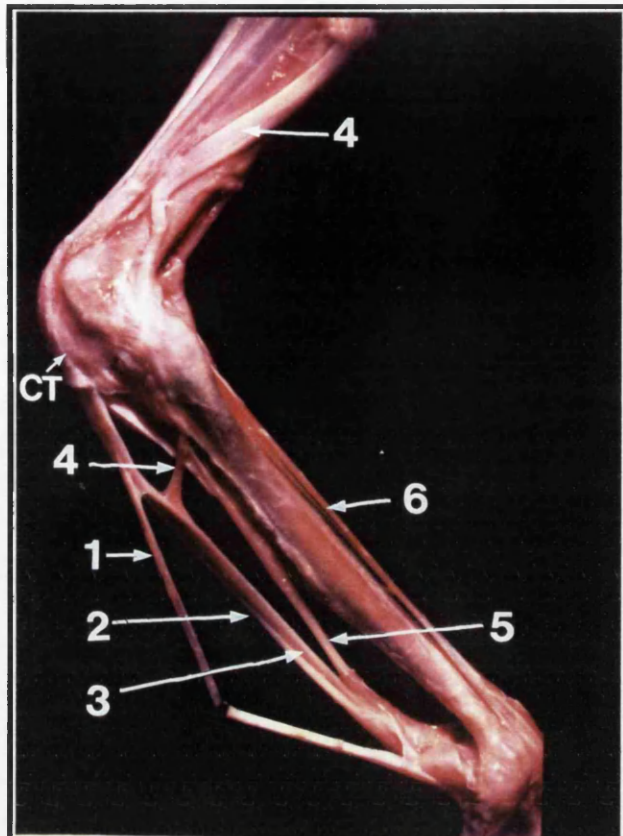


**Figure 13.** Lateral aspect of the tarsometatarsal region of *Struthio camelus* showing various tendons.

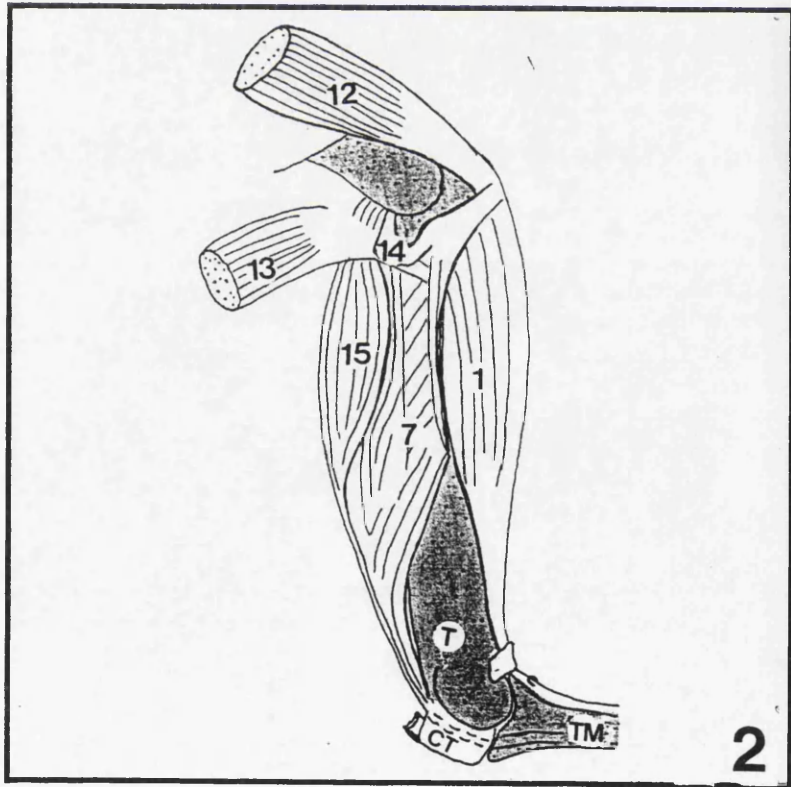
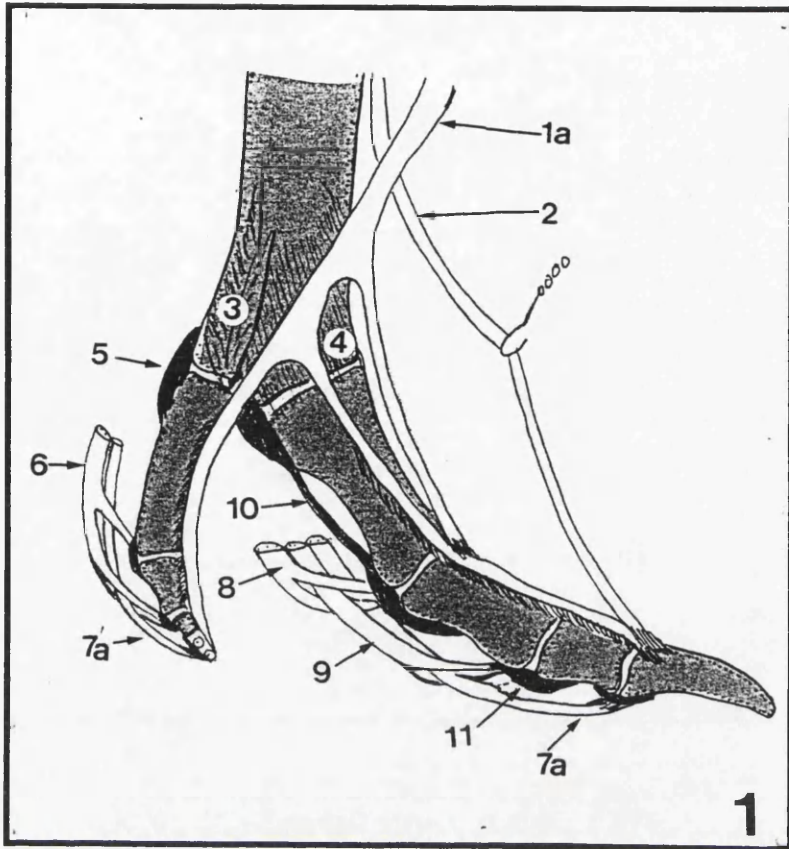
1. Tendon of M. flexor perforans et perforatus digiti III
2. Tendon of M. flexor perforatus digiti IV
3. Tendon of M. flexor perforatus digiti III
4. Tendon of M. fibularis longus
5. Co-joined tendons of Mm. flexor hallucis longus and M. flexor digitorum longus.
6. Tendons of Mm. extensor digitorum longus and extensor proprius digiti III.

CT= Cartilago tibialis

Note: The joining of 3 and 4.

**Figure 14.** Dorsoabaxial view of *Struthio camelus* foot (1) and crural region (2) showing deepest muscles, tendons and ligaments.

1. M. extensor digitorum longus
  - 1a. Tendon of M. extensor digitorum longus
  2. M. extensor proprius digiti III
  3. M. extensor brevis digiti IV
  4. M. extensor brevis digiti III
  - 5 Plantar ligament of metatarsophalangeal joint
  6. Tendon of M. flexor perforatus digiti IV
  7. M. flexor digitorum longus
  - 7a. Tendon of M. flexor digitorum longus
  8. Tendon of M. flexor perforatus digiti III
  9. Tendon of M. flexor perforans et perforatus digiti III
  - 10 Ligamentous band from plantar ligament of metatarsophalangeal joint
  11. Interphalangeal plantar ligaments
  12. M. femorotibialis
  13. M. iliofibularis
  14. Loop of M. biceps femoris
  15. M. flexor hallucis longus
- T= Tibiotarsus  
TM= Tarsometatarsus  
CT= Cartilago tibialis  
RET= Retinaculum extensorium tibiotarsi



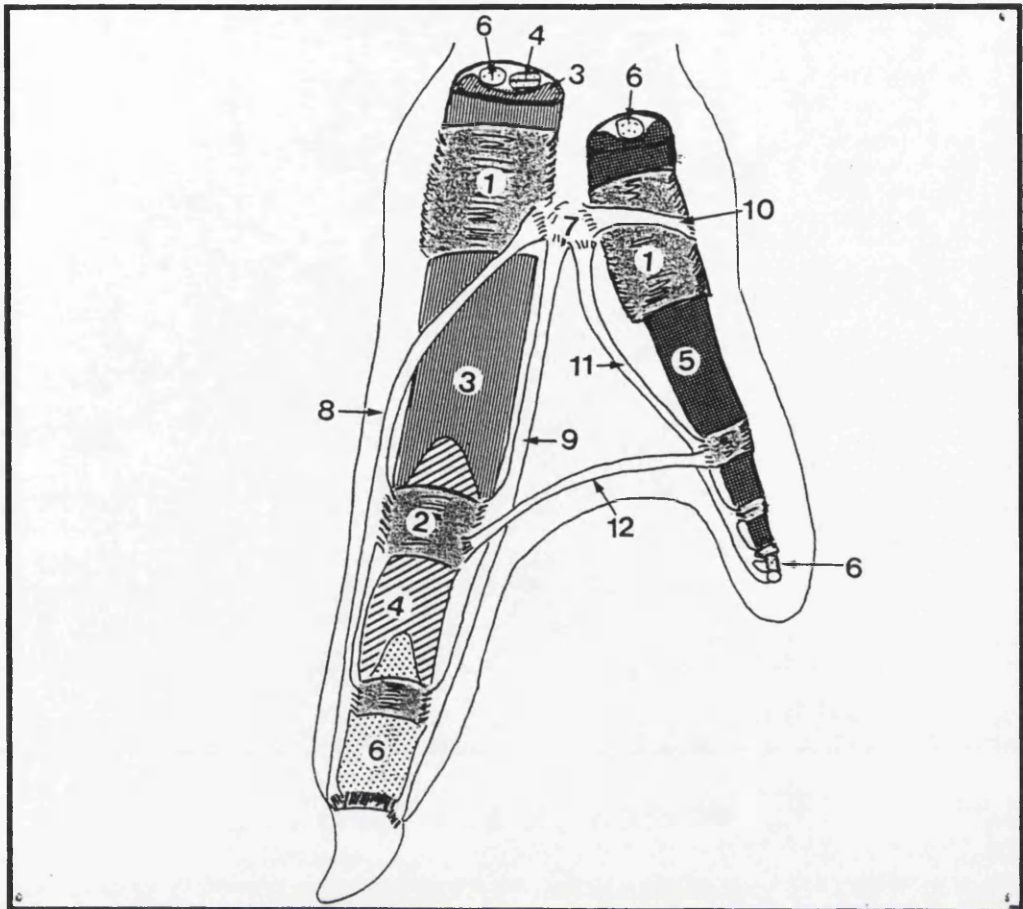


**Figure 15.** Plantar aspect of *Struthio camelus* foot with the digital cushions removed to show the pattern of insertion of flexor tendons and the digital check apparatus.

1. Plantar ligament of metatarsophalangeal joint
  2. Plantar ligament of interphalangeal joint
  3. Tendon of M. flexor perforatus digiti III
  4. Tendon of M. flexor perforans et perforatus digiti III
  5. Tendon of M. flexor perforatus digiti IV
  6. Tendon of M. flexor digitorum longus
  7. Pulvinus metatarsalis\*
  8. Ligamentum abaxiale digiti III\*
  9. Ligamentum axiale digiti III\*
  10. Ligamentum abaxiale digiti IV\*
  11. Ligamentum axiale digiti IV\*
  12. Ligamentum interdigitale digiti III et IV\*
- \* These structures comprise the digital check apparatus.

#### **4.4 NORMAL ULTRASONOGRAPHIC AND DESCRIPTIVE TOPOGRAPHIC ANATOMY OF THE DISTAL PELVIC LIMB OF THE OSTRICH**

A thorough knowledge of the normal gross topographical anatomy of the muscular, tendinous and ligamentous structures of the distal pelvic limb of the ostrich is essential for the interpretation of ultrasonographs of this region. In the ostrich each tendinous or ligamentous structure being observed had its own characteristic appearance which changed from origin to insertion. In this study, such structures were identified and described at each of the eight referral sites noted in Chapter 3.

The ultrasonographic anatomy of normal tendon is reviewed first because tendons constitute the bulk of the soft tissues in the distal pelvic limb of the ostrich and their echogenicity is based on their histologic structure. Furthermore, the common problems of ostrich legs appear to be tendon-related. Reference is also made to mammalian tendon studies, as these have received considerably more attention than their ostrich counterparts, and there appears to be a basic similarity in the structure and function of most vertebrate tendons.

Generally, tendons are composed of thick, closely packed parallel bundles of longitudinally-oriented submicroscopic collagen fibrils (Evans and Barbenel, 1975; Dyson, 1994). Fibroblasts (tenoblasts) are arranged in long parallel rows in the spaces between the collagenous bundles. The aggregation of collagen fibrils within a tendon or ligament is variable, but it is reasonable to consider the principal unit of tendon structure to be the coherent bundle of collagen fibrils lying between the fibroblasts (Elliot, 1965; Evans and Barbenel, 1975). These primary bundles group into

secondary bundles or fascicles, and these, in turn, are aggregated into larger tertiary tendon bundles. Tendon fibroblasts do not contribute clinically to tendon strength, but their viability is of paramount importance to the maintenance of this strength. Tendon, being a dynamic structure, is capable of renewing its collagen; as fibrils are broken down, the fibroblasts replace them.

There are a number of physical factors that affect the ultrasonographic appearance of tendons. The amount of sound wave reflected back to a transducer is an individual characteristic of each type of tissue, and is related not only to its acoustic impedance but also to the physical organisation of the tissue. The acoustic impedance of a tissue is determined in part by the density of the tissue. In tendon, tissue density is directly related to collagen content. The ultrasonographic effect of the small percentage of glycosaminoglycans present in tendon and ligament has yet to be evaluated. Studies carried out on bovine flexor tendons show that the quantity and type of glycoprotein present varies according to tendon site, with slightly higher concentrations being found in regions of increased pressure (for example at joints) and slightly lower concentrations being found in regions undergoing increased tensional stresses (Vogel and Heinegard, 1985). It is to be expected, therefore, that the ultrasonographic appearance of any particular tendon will be affected by the tissue density (i.e collagen concentration) of that particular tendon.

Tendon echogenicity will also vary markedly with the settings of the various image parameters on the ultrasound machine and it is therefore important to establish a relatively stable or constant set of image acquisition settings in order to reduce the amount of image variability originating from fluctuating machine settings.

Tendon echogenicity will also vary slightly in normal conditions based on the individual characteristics of the tendon. These include the size, its depth, the type of tissue surrounding the tendon normally, and any pathological conditions in the surrounding tissues. Ultrasonographic appearance of tendon varies markedly with the angle of image acquisition, i.e. the echogenicity of tendon is very angle-dependent, a characteristic known as anisotropy (Crass *et al.*, 1988). An accurate cross-sectional image of normal tendon can only be obtained with the transducer held perpendicular to the longitudinal axis of the tendon fibres. Similarly, a longitudinal scan will only produce an accurate image when the transducer is oriented in parallel with the longitudinal axis of the tendon fibres. When imaged at oblique angles, the ultrasound image of tendon will have a variable degree of artifactually-decreased echogenicity, ranging from near normal to an image that is anechoic (Fornage, 1987; Crass *et al.*, 1988).

In cross-section, the ultrasonographic image of ostrich tendon is normally composed of a highly echogenic, compact, stippled echopattern (Fig. 16). This sonographic appearance reflects the compact longitudinal orientation of the collagen fibre bundles. A longitudinal evaluation shows an image of the linear organisation of the tendon fibres. Multiple closely-aligned, highly echogenic lines, parallel to the longitudinal axis of the tendon, are seen. This appearance is typically described as a "fibrillar" ultrasonographic texture (Fornage and Rifkin, 1988; Kaplan *et al.*, 1990). The peritendinous sheath appears as a thin highly echogenic line surrounding the tendon.

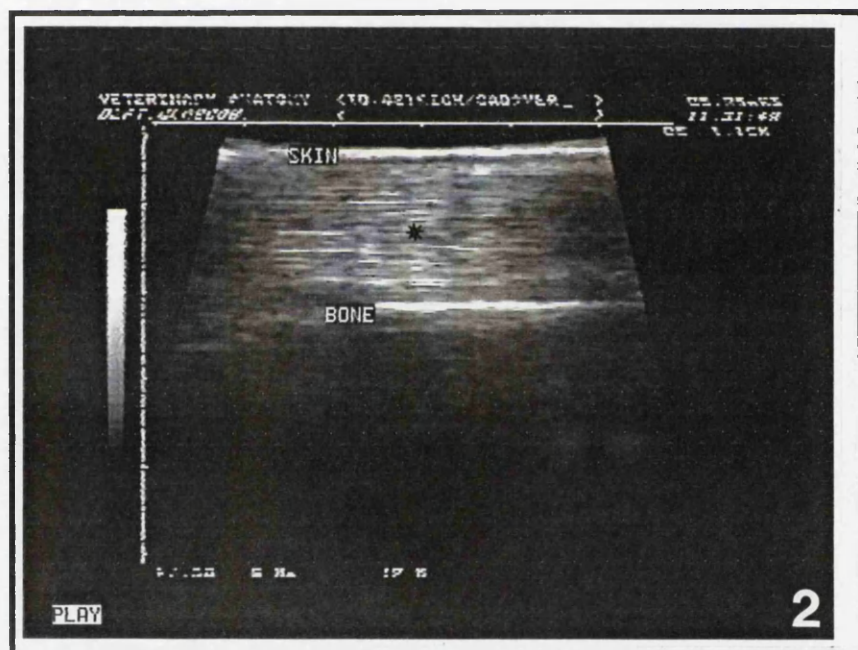
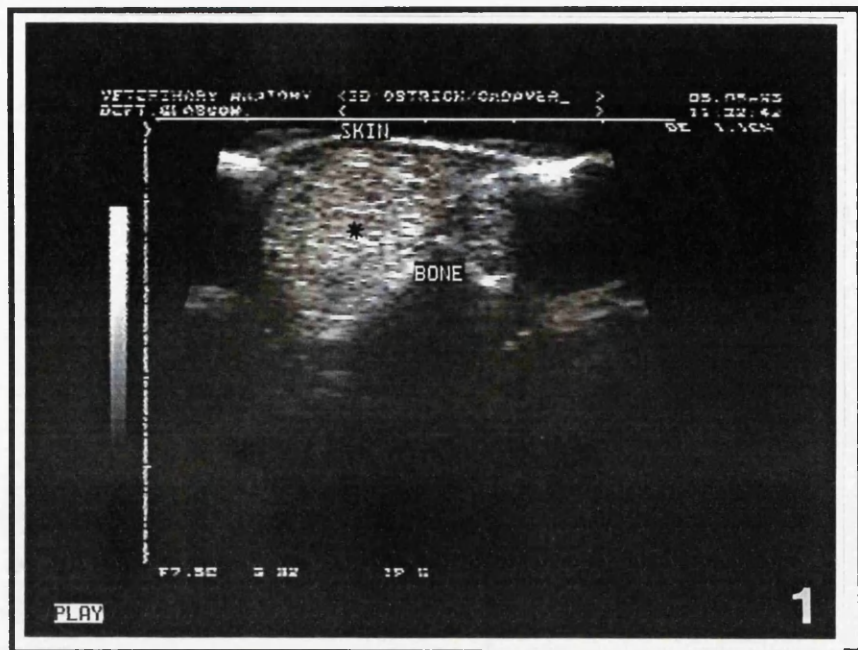


**Figure 16.** Normal ultrasonographic appearance of ostrich tendons. Transverse (1) and longitudinal (2) scans. Note the highly echogenic, compact, stippled echopattern, and fibrillar appearance, of the tendons (\*) in transverse and longitudinal scans respectively.

## Level 1 (Fig. 17)

**Cross-sectional anatomy.** The distal hindlimb muscles and their topographical relationships were identified as shown in Fig. 7. The muscles identified included the three heads of *M. gastrocnemius*, *M. extensor digitorum longus*, the two heads of *M. tibialis cranialis*, *M. fibularis longus*, *M. flexor perforans et perforatus digiti III*, *M. flexor perforatus digiti IV*, *M. flexor perforatus digiti III*, *M. flexor hallucis longus* and *M. flexor digitorum longus*.

**Ultrasonographic appearance.** Due to the presence of feathers in this region, ultrasonographic scanning was unsuccessful at this level.

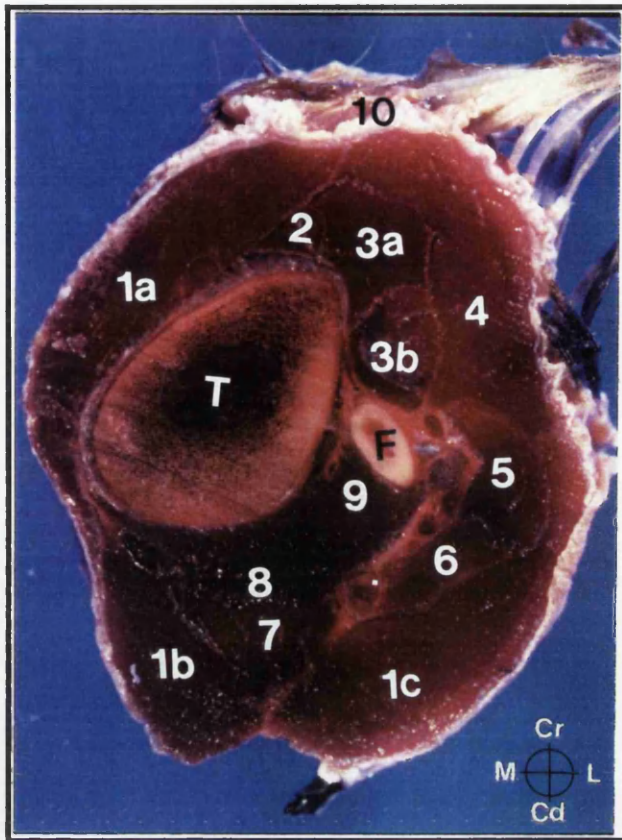


**Figure 17.** Frozen transverse section of the distal pelvic limb of *Struthio camelus*. This section corresponds to Level 1 in Fig. 2.

- 1a. M. gastrocnemius (pars interna)
- 1b. M. gastrocnemius (pars intermedia)
- 1c. M. gastrocnemius (pars externa)
- 2. M. extensor digitorum longus
- 3a. M. tibialis cranialis (caput tibiale)
- 3b. M. tibialis cranialis (caput femorale)
- 4. M. fibularis longus
- 5. M. flexor perforans et perforatus digiti III
- 6. M. Flexor perforatus digiti IV
- 7. M. flexor perforatus digiti III
- 8. M. flexor hallucis longus
- 9. M. flexor digitorum longus
- 10. Feathered skin

T= Tibiotarsus

F= Fibula

## Level 2

**Cross-sectional anatomy** (Fig. 18). The tibial cartilage is pierced by three flexor tendon canals. In adult birds, the largest and measures approximately 2 cm in a medial-to-lateral direction and 1 cm in a plantar-to-dorsal direction and contains the tendons of insertion of *Mm. flexor perforatus digiti III*, *flexor perforatus digiti IV* and *flexor perforans et perforatus digiti III*. The crescent-shaped tendon of *flexor perforatus digiti III* is the largest and surrounds the tendons of *Mm. flexor perforatus digiti IV* (totally) and *flexor perforans et perforatus digiti III* (partially). The inserting tendon of *M. flexor digitorum longus* passes through the more medially-located canal which measures, in adult birds, approximately 0.6 cm and 0.4 cm across its long and short axes respectively. It is the second largest flexor canal in the tibial cartilage. The third and the smallest of the three canals is located more centrally. It carries the small tendon of *M. flexor hallucis longus* and measures approximately 0.4 cm and 0.2 cm in its long and short axes. *Tendo Achilles* is seen on the plantar aspect of the intertarsal joint as a thick, half moon-shaped collagenous structure. There is a very strong fibrous connection between the *Tendo Achilles* and the tibial cartilage, formed by a homogenous intermingling of the fibres of the two anatomical structures. This connection is so strong that the two can be considered to act as a single functional unit. Laterally and medially, the two collateral ligaments can be seen. The medial collateral ligament is better developed (bigger) and deeply undercuts the proximal tarsometatarsus at its insertion. The small muscle belly of *M. extensor proprius digiti III* is located between the two cranially-placed insertion tendons of *M. tibialis cranialis* themselves located deep to the tendon of *M. extensor digitorum longus*.

**Ultrasonographic appearance.** Due to the curved surface contour of

the limb and the highly keratinised callosities in this region, it was impossible to get adequate contact or penetration to permit the limb to be successfully examined ultrasonographically at this level.

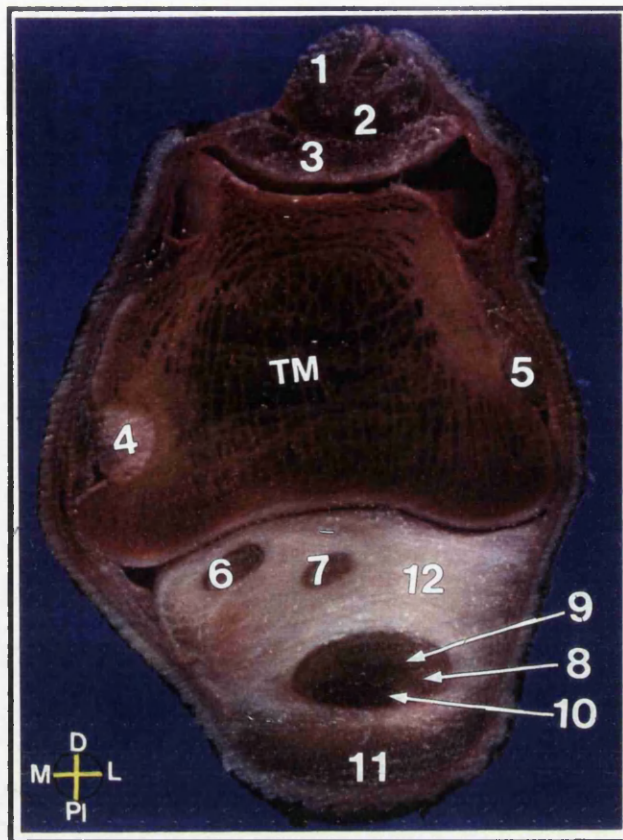


**Figure 18.** Frozen transverse section of the distal pelvic limb of *Struthio camelus* . The section corresponds to Level 2 in Fig.2

1. Tendon of M. tibialis cranialis
2. M. extensor proprius digiti III
3. Tendon of M. extensor digitorum longus
4. Ligamentum collaterale mediale, pars longa
5. Ligamentum collaterale laterale, pars longa
6. Tendon of M. flexor digitorum longus
7. Tendon of M. flexor hallucis longus
8. Tendon of M. flexor perforatus digiti III
9. Tendon of M. flexor perforatus digiti IV
10. Tendon of M. flexor perforans et perforatus digiti III
11. Tendo Achilles
12. Cartilago tibialis

TM= Tarsometatarsus

*Note the strong fibrous connection between the tendon of M. gastrocnemius and the Cartilago tibialis*

### Level 3

**Cross-sectional anatomy** (Fig. 19A). Here the hypotarsus separates the flexor tendons into a medial and a lateral group, with only the tendon of *M. flexor digitorum longus* taking a medial course while the rest of the flexor tendons run lateral to the hypotarsus. The tendon of *M. flexor perforatus digiti III* still completely surrounds the tendon of *M. perforatus digiti IV* while the tendon of *M. flexor perforans et perforatus digiti III* now lies superficial to the tendon of *M. flexor perforatus digiti III*. The sizes and shapes of these three tendons remain relatively constant as in the previous level.

The long and slender branch of the tendon of *M. peroneus longus* joins the flexor group of tendons in this region. Transversely, this tendon is ovoid, with an average diameter of 0.4 cm in adult birds, and it is the most laterally situated tendon here. The tendon of *M. flexor hallucis longus* narrows to become a narrow comma-shaped tendon situated deep to the rest of the flexor tendons lying lateral to the hypotarsus. Medially only the tendon of *M. flexor digitorum longus*, in close proximity with the medial metatarsal vein, is found and its overall size does not increase much, although its shape now becomes more ovoid when compared to level 2. The *Ligamentum collaterale mediale* can still be seen at this level attaching medially on the tarsometatarsus.

At this level the *Tendo Achilles* plays an important role as a flexor sheath. As well as inserting onto the hypotarsus, it sends two strong collagenous sheaths, lateral and medial to the hypotarsus, to envelope and hold down the flexor tendon bundles, before attaching also onto the medial and lateral surfaces of the tarsometatarsus.

Dorsally, the tendon of *M. extensor digitorum longus* is seen lying close to the small muscle belly of *M. extensor proprius digiti III*. Its shape changes from a flat tendon (Level 2) to a more ovoid tendon with the longer diameter averaging 0.5 cm in adult birds. The dorsal metatarsal vein is also seen lying on the dorsal surface close to *M. extensor proprius digiti III*.

**Ultrasonographic appearance** (Fig. 19B). Although plantar longitudinal scans at this level were unsuccessful due to the scattering effects of the ultrasound waves by the highly reflective surface of the hypotarsus in this region, transverse scans could be carried out successfully. These plantar transverse ultrasonographic scans correlated well with the gross cross-sectional specimen. The tendons appeared as structures exhibiting a markedly echogenic, compact, stippled echopattern. The interfaces of the densely packed collagen fibre bundles were difficult to differentiate as there was a homogenous echogenicity within the tendon bundle. However, partly due to its position, the tendon of *M. flexor digitorum longus* could be easily identified as a separate echogenic structure on the medial aspect of the hypotarsus.

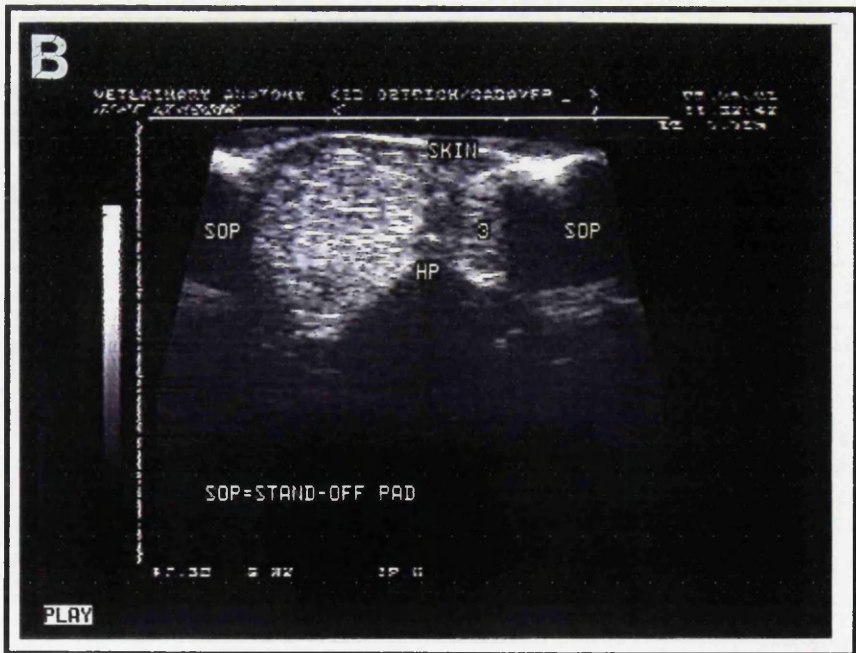
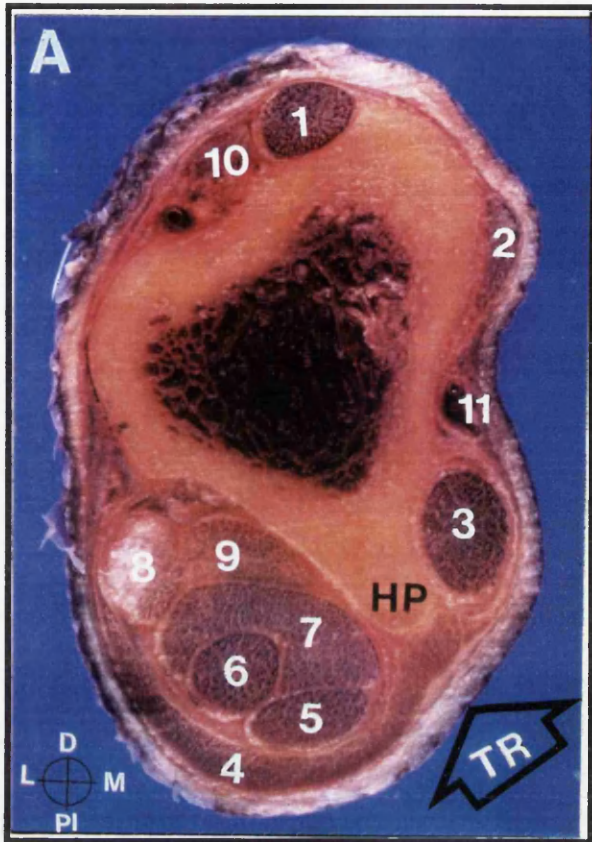
**Figure 19.** A frozen transverse section (A) and a corresponding transverse ultrasound scan (B) of the distal pelvic limb of *Struthio camelus* at Level 3 in Fig. 2

- 1 Tendon of M. extensor digitorum longus
2. Ligamentum collaterale mediale, pars longa
3. Tendon of M. flexor digitorum longus
4. Flexor sheath of flexor tendon bundle
5. Tendon of M. flexor perforans et perforatus digiti III
6. Tendon of M. flexor perforatus digiti IV
7. Tendon of M. flexor perforatus digiti III
8. Tendon of M. fibularis longus
9. Tendon of M. hallucis longus
10. M. extensor proprius digiti III
11. Medial metatarsal vein

HP = Hypotarsus

SOP= Stand-off pad

TR =Transducer position



#### Level 4

**Cross-sectional anatomy** (Fig. 20). A number of topographic changes take place at this level. Firstly, the tendon of *M. flexor digitorum longus* joins the rest of the flexor tendons to form one flexor tendon bundle surrounded by a very strong flexor sheath attaching to the medial and lateral tarsometatarsal surfaces. The size and shape of the tendon of *M. flexor digitorum longus* remains fairly constant and it is the most deeply situated tendon medially. Secondly, the tendon of *M. flexor hallucis longus* changes shape from being comma-shaped (level 3) to ovoid with an average long diameter of 0.3 cm in adult birds. It is the most deeply and more centrally located tendon in the bundle. Furthermore, the tendon of *M. flexor perforatus digiti III* no longer surrounds the tendon of *M. flexor perforatus digiti IV*, but instead fuses with the tendon of *M. fibularis longus* to form a somewhat rectangular-shaped tendon measuring 0.4 cm to 0.7 cm along its long axis and 0.2 to 0.4 cm in its short axis. The superficial layer at this level consists of two ovoid tendons of *Mm. flexor perforatus digiti IV* (more on the lateral side) and *flexor perforans et perforatus digiti III* (more on the medial side). These two tendons are approximately of the same size (0.3 cm in long diameter) and are tightly apposed to the deeper-lying tendon of *M. flexor perforatus digiti III*. Medially, the medial metatarsal vein and artery can be seen while dorsally the tendon of *M. extensor digitorum longus* and the small muscle belly of *M. extensor proprius digiti III* still remain as the main anatomical features.

**Ultrasonographic appearance.** Both transverse (Fig. 21A) and longitudinal (Fig. 21B) scans were successful at this level. In transverse scans, all the normal tendons appeared homogenous and highly echogenic. However, due to the tight apposition of the tendons of *Mm.*

*flexor perforatus digiti III*, *flexor perforatus digiti IV*, *flexor perforans et perforatus digiti III*, and *flexor digitorum longus*, individual tendon margins for these four tendons were indistinctly defined. On the other hand, the tendon margins of the deeply located *M. flexor hallucis longus* were mostly easily recognised due to the fact that this tendon appears very hypoechoic when compared with other tendons (Fig. 21). This hypoechogenicity is brought about as a result of the transverse course this tendon takes in this area before joining the tendon of *M. flexor digitorum longus*. This displaces the fibres from an orientation perpendicular to the ultrasound beam, resulting in this unavoidable hypoechoic artifact just before the highly echogenic line representing the tarsometatarsus. Plantar longitudinal scans revealed tendons that lie within the longitudinal scanning plane; such tendons include those of *Mm. flexor perforans et perforatus digiti III*, *flexor perforatus digiti III* and *flexor hallucis longus*. These three have a typical fibrillar ultrasonographic echotexture in that they appear as highly hyperechoic structures within which are multiple closely-aligned, highly echogenic parallel lines. The peritendinous sheath appears as a highly echogenic line surrounding each tendon. The tendons of *Mm. flexor digitorum longus* and *flexor perforatus digiti IV* are not demonstrated in the presented longitudinal scan. However, shifting the position of the scanning head medially and then laterally from the central plantar position reveals that these structures have the same ultrasonographic appearance as the other tendons.

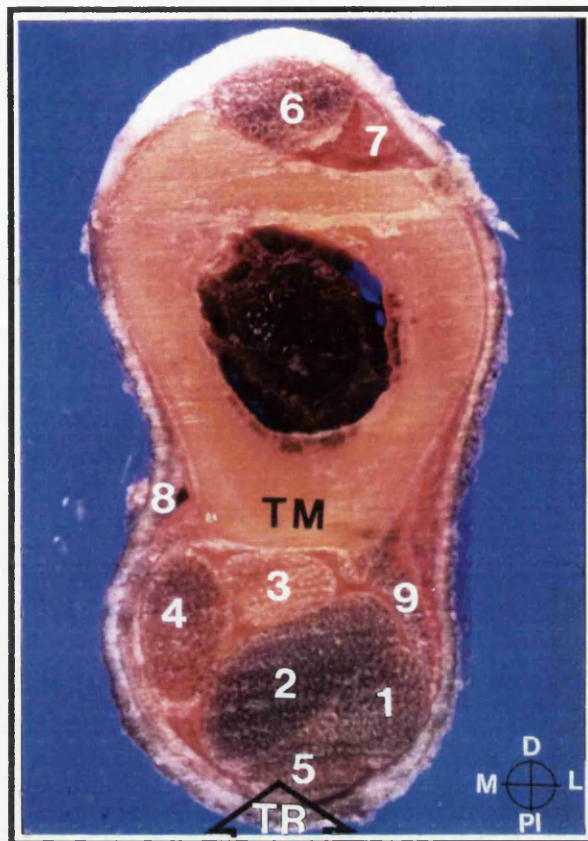


**Figure 20.** Frozen transverse section of the distal pelvic limb of *Struthio camelus* corresponding to Level 4 in Fig. 2

1. Tendon of M. flexor perforans et perforatus digiti III
2. Tendon of M. flexor perforatus digiti III
3. Tendon of M. flexor hallucis longus
4. Tendon of M. flexor digitorum longus
5. Tendon of M. flexor perforatus digiti IV
6. Tendon of M. extensor digitorum longus
7. M. extensor proprius digiti III
8. Medial metatarsal vein
9. Flexor sheath

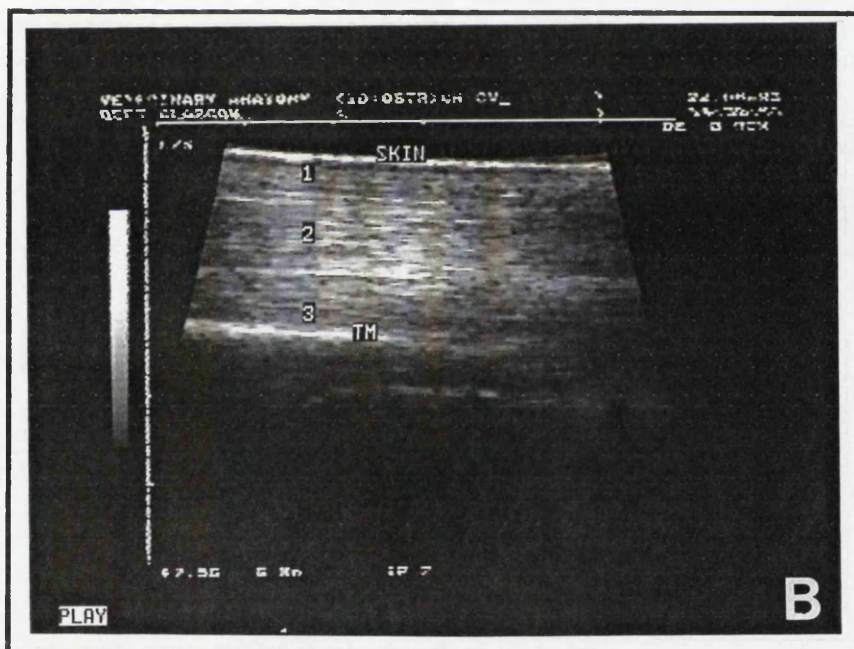
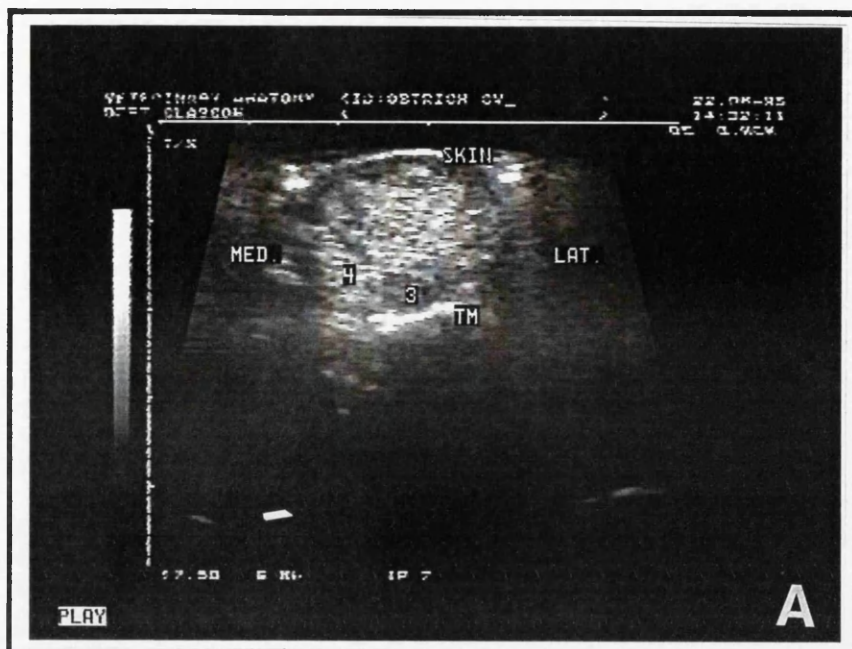
TM =Tarsometatarsus

TR =Transducer position

**Figure 21.** Transverse (A) and longitudinal (B) ultrasound scans of the distal pelvic limb of *Struthio camelus* corresponding to Level 4 in Fig. 2.

Note the hypoechogenic artifactual appearance of the tendon of *M. flexor hallucis longus* in a transverse scan.

1. Tendon of *M. flexor perforans et perforatus digiti III*
  2. Tendon of *M. flexor perforatus digiti III*
  3. Tendon of *M. flexor hallucis longus*
  4. Tendon of *M. flexor digitorum longus*
- TM = Tarsometatarsus



## Level 5

**Cross-sectional anatomy** (Fig. 22). As the flexor tendon bundle approaches the metatarsophalangeal joint, there is an increase in the space between the tendon bundle and the tarsometatarsus. This space is occupied by metatarsal blood vessels and nerves supplying the foot. The tendons of *Mm. flexor hallucis longus* and *flexor digitorum longus* join to form a single tendon. This conjoined tendon is seen to lie on a deeper level to the tendons of *Mm. flexor perforans et perforatus digiti III*, *flexor perforatus digiti IV*, and *flexor perforatus digiti III*, and all the tendons are tightly bound together by a surrounding flexor sheath with minimal amounts of separating connective tissue between individual tendons. A tiny muscle belly representing part of the origin of *M. adductor digiti IV* can be seen lying on the plantolateral aspect of the distal tarsometatarsus. Dorsally, the large tendon of *M. extensor digitorum longus* and the smaller tendon of *M. extensor proprius digiti III* can be seen running close to one another. The overall sizes of all these tendons do not vary significantly from level 4.

**Ultrasonographic appearance.** Both transverse (Fig. 23A) and longitudinal (Fig. 23B) ultrasound scans were taken. In the transverse images the flexor tendon bundle appeared homogenous and highly echogenic. Due to the tight binding of the flexor sheath and the presence of minimal amounts of connective tissue separating the tendons in the bundle, individual tendon boundary visualization (resolution) was poor. Deep to the flexor tendon bundle lay an anechoic area representing the region occupied by blood vessels, nerves and a small muscle belly of *M. adductor digiti IV*. The deepest linear hyperechoic line represents an echo from the tarsometatarsus.

Central longitudinal ultrasound scans clearly showed the two tendons of *Mm. flexor perforatus digiti III* (after joining with the tendon of *M. fibularis longus*) and *flexor digitorum longus* (after joining with the tendon of *M. flexor hallucis longus*), the latter seen lying at a deeper level to the former. These appeared as hyperechoic structures with internal, closely-aligned, echogenic parallel lines. The peritendinous sheath appeared as a highly echogenic line bordering each tendon. Other tendons were out of the central axial view and could only be brought into view after shifting the transducer laterally and medially.

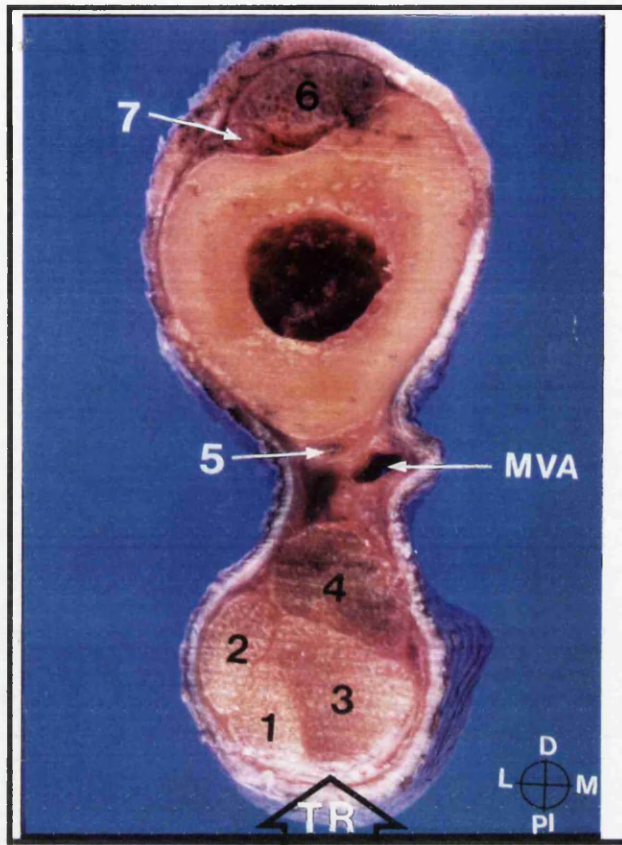


**Figure 22.** Frozen transverse section of the distal pelvic limb of *Struthio camelus* corresponding to Level 5 in Fig. 2. Note the tight binding of these tendons, with very little connective tissue between them.

1. Tendon of M. flexor perforans et perforatus digiti III
2. Tendon of M. flexor perforatus digiti IV
3. Tendon of M. flexor perforatus digiti III
4. Tendon of M. flexor digitorum longus
5. M. adductor digiti IV
6. Tendon of M. extensor digitorum longus
7. M. extensor proprius digiti III

MVA = Medial metatarsal vein and artery

TR = Transducer position

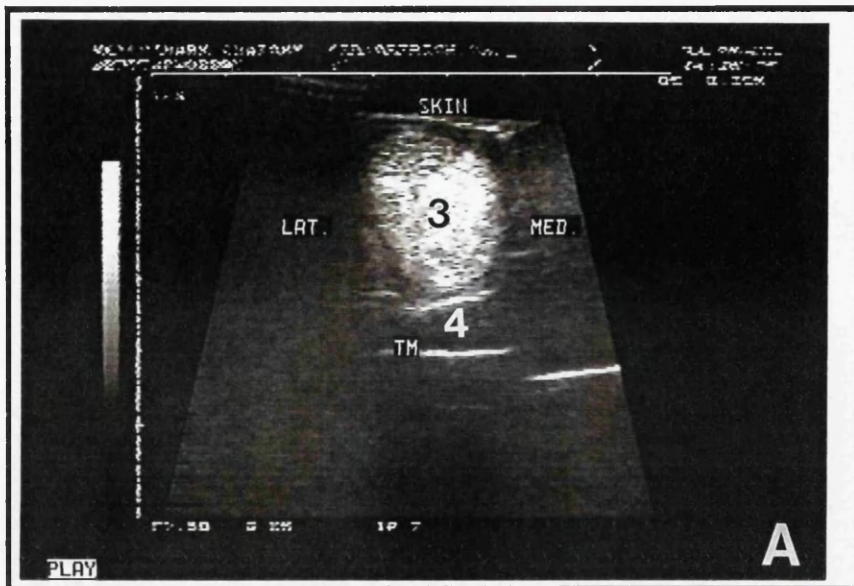


**Figure 23.** Transverse (A) and longitudinal (B) ultrasound scans of the distal pelvic limb of *Struthio camelus* corresponding to Level 5 in Fig. 2

- |  |                    |
|--|--------------------|
| 1. Tendon of M. flexor perforatus digiti III   | TM = Tarsometarsus |
| 2. Tendon of flexor digitorum longus           |                    |
| 3. Flexor tendon bundle                        |                    |
| 4. Anechoic area with blood vessels and nerves |                    |

## Level 6

**Cross-sectional anatomy** (Fig. 24A). There are a number of noticeable anatomic changes that take place in this zone. Generally, there is an increase in the size and shape of all the tendons which now take their new courses to their respective digits for insertion. The thick crescent-shaped fibrocartilagenous plantar ligaments across the two metatarsophalangeal joints also appear in this zone. Due to the enormous disparity in the size of the two digits, it is not surprising that the plantar ligament across the metatarsophalangeal joint for digit III is better developed compared to its counterpart associated with digit IV. Lateral and medial collateral ligaments associated with this joint are also seen fused with abaxial and axial extensions of the plantar ligaments on both digits. The tendon of *M. flexor digitorum longus* splits into two branches, one to each of the digits. The branch to digit III is ovoid and lies deep to the tendons of *Mm. flexor perforatus digiti III* and *flexor perforans et perforatus digiti III*, while the smaller round branch to the fourth digit lies deep to the tendon of *M. flexor perforatus digiti IV*. The tendon of *M. flexor perforatus digiti IV* has increased in size and changed shape to a round tendon. Like other tendons in this zone, the three flexor tendons of the third digit i.e. the tendons of *Mm. flexor digitorum longus* (deep), *flexor perforans et perforatus digiti III* (intermediate) and *flexor perforatus digiti III* (superficial) increase in size and run through a deep sulcus in the plantar ligament while being ensheathed by a strong fibrous flexor sheath, the *Vaginae fibrosae* which is an extension of the plantar ligament. The tendons of *Mm. flexor perforans et perforatus digiti III* and *flexor perforatus digiti III* are comma-shaped, whilst the tendon of *M. flexor digitorum longus* is oval in shape. Traces of muscle fibres of small *M. extensor brevis digiti IV* are seen inserting on the axial aspect of the proximal phalanx of the fourth digit.

**Ultrasonographic appearance** (Fig. 24B) Only transverse ultrasound scans could be carried out at this level. Longitudinal scans were successful for two main reasons. Firstly, the flexor tendons send branches to their respective digits, resulting in a considerable space between the two bundles of tendons and making it practically impossible to have one central longitudinal scanning plane. Secondly, the concave curvature of the foot surface at this level made it impossible to obtain adequate contact between the foot surface and the microconvex linear transducer. This leaves a transverse scan as the only ideal way of imaging this area, and even with transverse scans it is difficult to direct the beam at 90 degrees to most tendons at one time. This occasionally results in false hypoechogenicity in some tendons. Due to the foregoing reasons, there is poor resolution between the anatomic structures of the fourth digit.

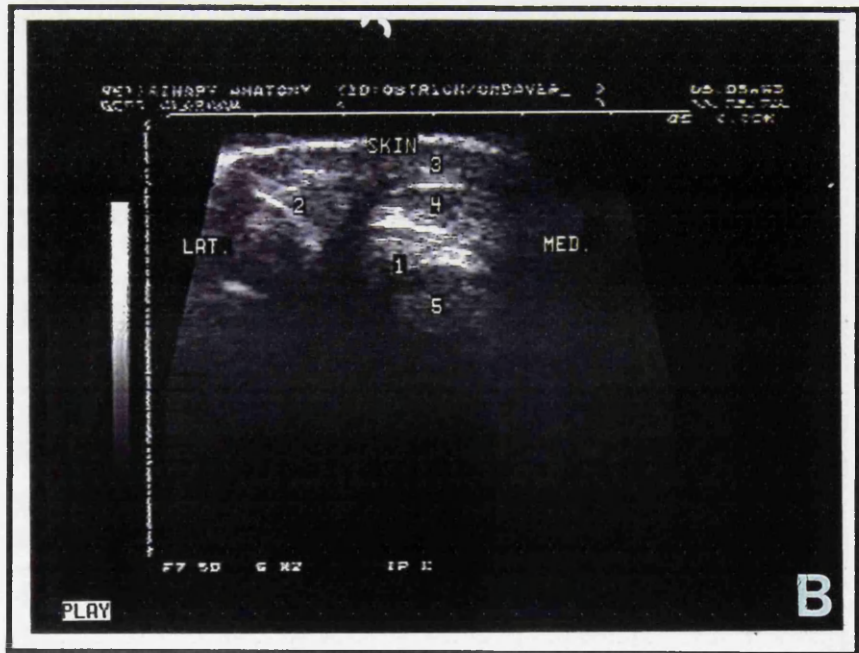
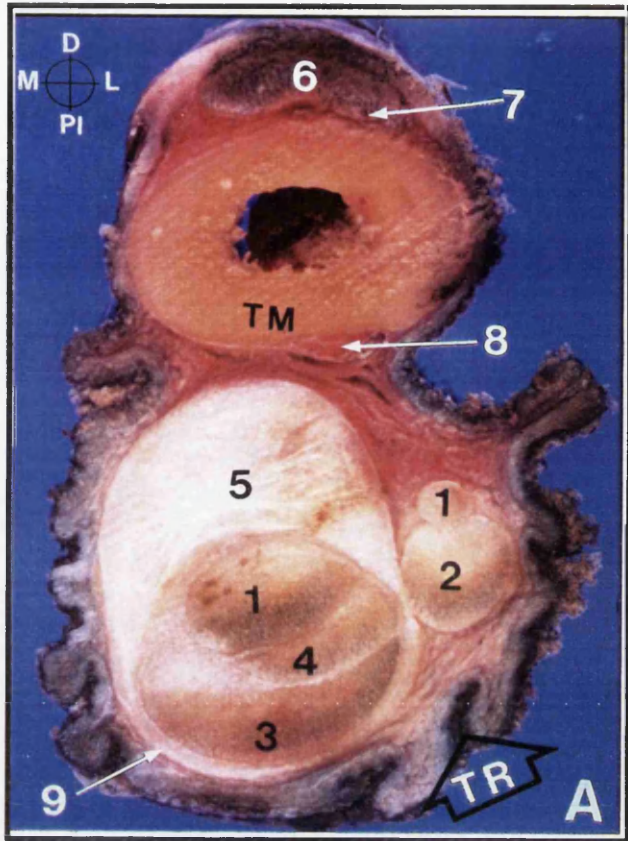
Tendons that were clearly imaged on the third digit include the tendons of *Mm. flexor perforatus digiti III*, *flexor perforans et perforatus digiti III* and *flexor digitorum longus*. They appeared as half-moon shaped, closely opposed, echogenic structures with highly echogenic margins and relatively lower internal echogenicity. Due to its deep location, the plantar ligament appears as a relatively less echogenic structure deep to the tendons. The tendon of *M. flexor perforatus digiti IV* was seen as a hyperechoic structure, whilst the tendon of *M. flexor digitorum longus* to the fourth digit turned out to be too small to be imaged and distinguished separately.

**Figure 24.** Frozen transverse section (A) and a corresponding transverse ultrasound scan (B) of the distal pelvic limb of *Struthio camelus*. The point corresponds to Level 6 of Fig. 2

1. Tendon of M. flexor digitorum longus
2. Tendon of M. flexor perforatus digiti IV
3. Tendon of M. flexor perforatus digiti III
4. Tendon of M. flexor perforans et perforatus digiti III
5. Plantar ligament of metatarsophalangeal joint
6. Tendon of M. extensor digitorum longus
7. Tendon of M. extensor proprius digiti III
8. M. adductor digiti IV
9. Vaginae fibrosae

TM= Tarsometatarsus

TR =Transducer position



## Level 7

**Cross-sectional anatomy** (Fig. 25A). On the third digit the tendon of *M. flexor perforatus digiti III* can be seen to split into its axial and abaxial branches ready to insert on the abaxioplantar and axioplantar surfaces of the first interphalangeal plantar ligament, whilst the tendons of *Mm. flexor perforans et perforatus digiti III* and *flexor digitorum longus* continue with their distal phalangeal course. These latter two tendons are crescent-shaped with that of *M. flexor digitorum longus* lying deeper to the tendon of *M. flexor perforans et perforatus digiti III*. Dorsal metatarsal vein and artery lie between the two trochleae. Tendons of *Mm. flexor perforatus digiti IV* and *flexor digitorum longus* (the latter, tiny) are the main structures observed on the plantar aspect of digit IV.

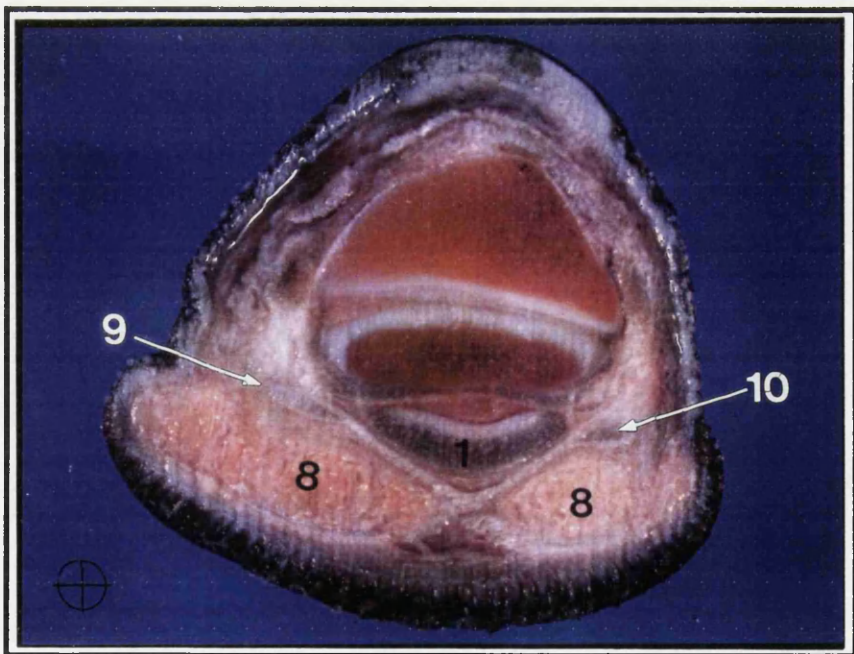
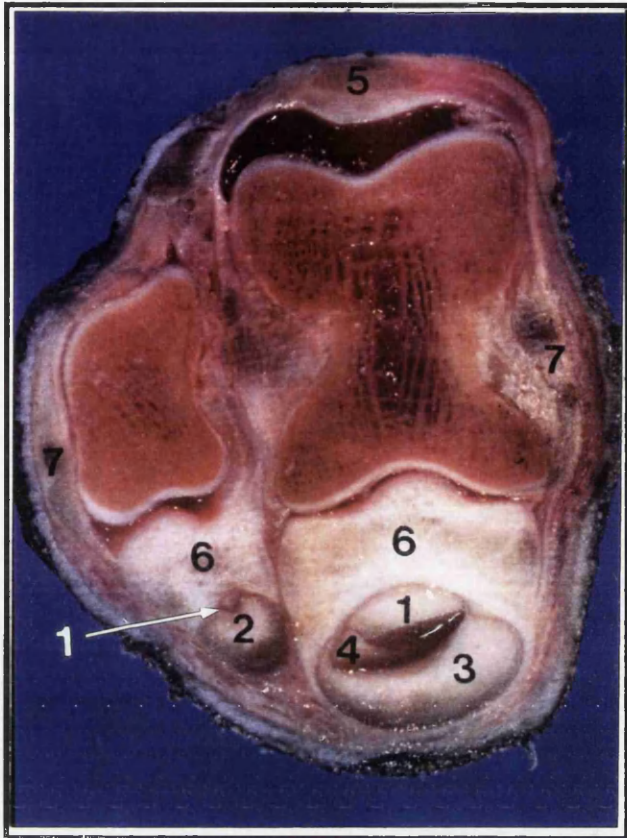
## Level 8

**Cross-sectional anatomy** (Fig. 25B). Some of the main features seen here include the bilobed digital cushion and the abaxial and axial digital ligaments of this digit which are seen above the digital cushion. The tendon of *M. flexor perforans et perforatus digiti III* divides into its axial and abaxial branches before inserting onto the axial and abaxial aspects of the second interphalangeal joint. The tendon of *M. flexor digitorum longus* continues with its distal phalangeal course.

Similar structures in the fourth digit are too small to be readily visualised in such a gross cross-sectional study.

**Figure 25.** Frozen transverse sections of the distal pelvic limb (digits) of *Struthio camelus*. (A) represents Level 7 whilst (B) represents Level 8 in Fig.2

1. Tendon of M. flexor digitorum longus
2. Tendon of M. flexor perforatus digiti IV
3. Tendon of M. flexor perforatus digiti III
4. Tendon of M. flexor perforans et perforatus digiti III
5. Tendon of M. extensor digitorum longus
6. Plantar ligament of metatarsophalangeal joint
7. Ligamentum collaterale and joint capsule
8. Digital cushion
9. Ligamentum abaxiale digiti III
10. Ligamentum axiale digiti III



## 4.5 PATHOLOGICAL STUDY RESULTS

The seven pairs of deformed limbs were divided into two groups; the immature (young birds) birds and the mature birds (aged 2 years and above). The common findings were categorised according to the groups. In both groups, a clear pattern of lateral rolling or curling of the third digit, with the claw pointing medially, emerged in all specimens with rolled toes.

**Immature group.** These had slight oedema in the subcutaneous tissues of the distal pelvic limb with the larger muscle groups (extensor and flexor muscles) appearing reddish, although there was no evidence of inflammation, regeneration or repair. Gross abnormalities in tendons and ligaments were confined to the foot, being seen only in areas around and distal to the metatarsophalangeal joints; no gross lesions were observed proximal to the metatarsophalangeal joints. The most frequent findings were of stretched and partially or completely ruptured flexor tendons, and of laxity of the collateral ligaments of the interphalangeal joints resulting, in most specimens, in the subluxation and loss of congruency of these joints. Conversely, the articular cartilage and plantar ligaments associated with these joints were still intact with no signs of either erosion or degeneration. The bony components (tibiotarsus, tarsometatarsus and phalanges) as well as the intertarsal and metatarsophalangeal joints, were normal.

*Radiological findings* (Fig. 26). The radiographic appearance of the intertarsal joint required careful consideration. In young or immature ratites, the radiographs gave an impression of osseous epiphyses contrary to the normal cartilaginous epiphyses usually seen in the long bones in all birds. What appear to be osseous epiphyses are, in fact, the proximal row of tarsal bones fusing with the tibia and the distal row fusing with the

metatarsus.

Dorsoplantar radiographs showed no significant abnormal findings but the lateral radiographs revealed a lateral rotation of the phalanges about the long axis of the digit, with the first interphalangeal joint acting as the major centre of rotation. Such a rotation usually involves the third digit; the fourth digit is similarly affected, but follows prior involvement of the third digit. This rotation changes the orientation of individual phalanges in relation to one another and is observed radiographically as a loss of symmetry in each one of these phalanges when compared with those of the normal limbs. There were no significant differences in bone opacity between normal and abnormal limbs. The metatarsophalangeal joints remained stable in these immature cases.



**Figure 26.** Lateral radiograph of the distal left pelvic limbs of 48 day-old ostrich chicks. Rolled(A) and normal third digit (B). The rotation in A is seen as a loss of symmetry of the phalanges. Arrow heads indicate tarsal bones fusing to the tibia and metatarsus.

**Mature group.** As in the case of the immature group, no significant abnormal changes were seen in tendons and ligaments in the area proximal to the metatarsophalangeal joint however. Signs of degeneration of soft tissues were invariably observed around the metatarsophalangeal joint. Here, the flexor sheath had ruptured and degenerated in a few places (Fig. 27). As a result of this, the flexor sheath was unable to restrain the bundle of flexor tendons. The topographical relationships of these tendons were seen to present a disrupted appearance (compare Figs. 22 and 27). The area between the flexor tendon bundle and the distal tarsometatarsus initially occupied by blood vessels (Fig. 27) was now occupied by a mass of fibrous tissue that compressed and pushed the blood vessels medially. Other pathological changes included the loss of congruency between the deep surfaces of the plantar ligaments and their corresponding grooves on the trochleae due to the massive deposition of fibrous connective tissue in this area. This served to remove the sockets of reception for the heads of the trochleae, leading to very restricted movements of the metatarsophalangeal joints. Although generally thickened, the joint capsule showed areas of degeneration and had ruptured in several places, allowing the leakage of synovial fluid into the surrounding tissues. Lateral collateral ligaments across the metatarsophalangeal joints had avulsed from their proximal (trochlea) attachments and partially degenerated. While running through the flexor groove of the plantar ligaments, the flexor tendons regained their normal topographical relationships, although their individual strength appeared to be reduced due to some fibre rupture and degeneration within them. Both extensor tendons increased in size and underwent ossification close to their points of osteophytic attachment (Fig. 28). Osteophytes or abnormal bony outgrowths were commonly observed at the sites of ligamentous or tendinous attachments. Regardless of all the pathological changes in this area, the metatarsophalangeal joint remained reasonably stabilised by the remaining plantar ligaments.

Osteophytes or bony spurs were also observed growing between the trochleae. They are produced by the resulting abnormal tendinous or ligamentous traction.

Within the digits, there was a widespread degeneration of flexor tendons, plantar and collateral ligaments, and joints, accompanied by massive fibrous tissue deposition in the areas of digital pressure (Fig. 28), resulting from the shift in the pressure surface from the normal plantar surface (with digital cushion pads) to the lateral surface in line with phalangeal rotation. The degeneration of the major joint restraints resulted in subluxation and loss of joint congruity in all the interphalangeal joints. The articular surfaces of these joints became grossly disrupted, with subsequent cartilage loss and abnormal surface contouring. Marginal osteophytes were formed at points of tendon attachments on the dorsal, axial and abaxial sides of the phalanges, remodelling the tuberculum extensorium into exhibiting sharp, cranially-projecting tuberculum extensorium. No osteophytes were observed at the plantar (flexor) tendon attachments on the phalanges.

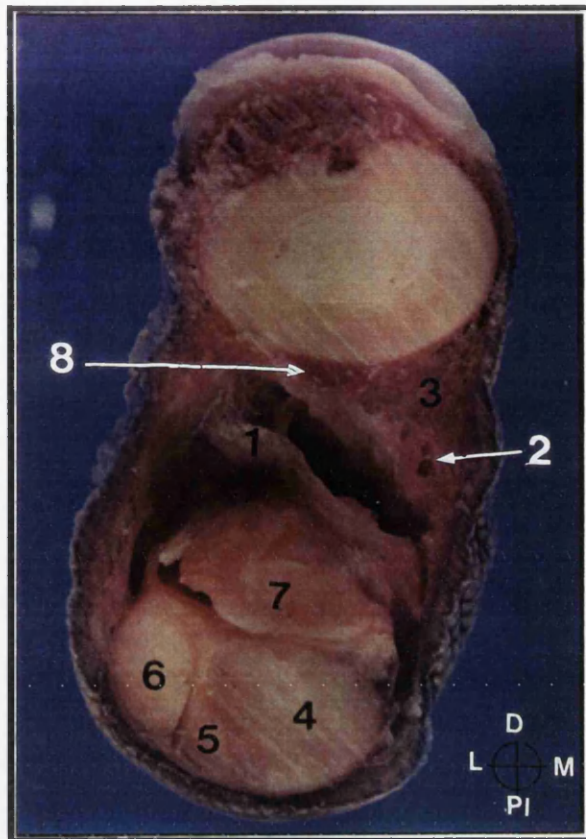


**Figure 27.** Frozen transverse section of the distal pelvic limb of an adult *Struthio camelus* with a rotated toe, corresponding to Level 5 in Fig. 2.

1. Ruptured flexor sheath
2. Medial metatarsal vein and artery
3. Aggregated fibrous tissue
4. Tendon of M. flexor perforatus digiti III
5. Tendon of M. flexor perforatus digiti IV
6. Tendon of M. flexor perforans et perforatus digiti III
7. Tendon of M. flexor digitorum longus
8. M. adductor digiti IV

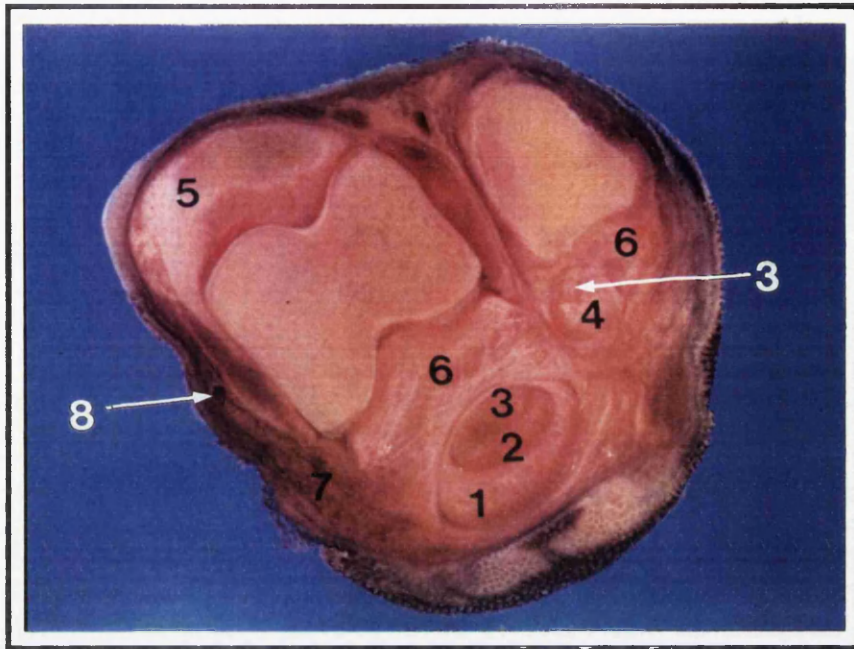


**Figure 28.** Frozen transverse section of the distal pelvic limb of an adult *Struthio camelus* with a rotated toe, taken at Level 7 in Fig. 2 (compare with Fig. 25A)

1. Tendon of M. flexor perforatus digiti III
2. Tendon of M. flexor perforans et perforatus digiti III
3. Tendon of M. flexor digitorum longus
4. Tendon of M. flexor perforatus digiti IV
5. Ossified tendon of M. extensor digitorum longus
6. Plantar ligament of metatarsophalangeal joint
7. Aggregated fibrous tissue
8. Digital blood vessels

Note the displacement of the plantar ligament of the metatarsophalangeal joint of digit IV

*Radiological findings* : The abaxio-axial view showed an increase in radiopacity on the distal axial and abaxial aspects of the phalanges, indicating the locations of the marginal osteophytes. The *tuberculum extensorium* of the phalanges were remodelled and appeared as sharp cranially-pointing spurs (Fig. 29). Dorsoplantar views revealed a general increase in the joint spaces, a slight loss of congruity in the metatarsophalangeal joints, and a luxation of the interphalangeal joints coupled with a lateral rotation of the toes, with the first, and most severely affected, interphalangeal joint acting as the centre of rotation (Fig. 31). There were no significant differences in bone opacity between the normal and abnormal specimens.

Preliminary estimates of bone torsion in both the tarsometatarsus and first phalanx were made by comparing the angle of deviation between the transverse axis of the proximal articular surface (taken as the standard reference point) with that of the distal articular surface. These revealed a common abaxial rotation in each of the two bones (Fig. 30). The most severely rotated tarsometatarsus had a distal abaxial rotation of approximately 30 degrees (as measured with a protractor), whilst the first phalanx of digit III was the most severely rotated with an abaxial rotation of approximately 35 degrees.

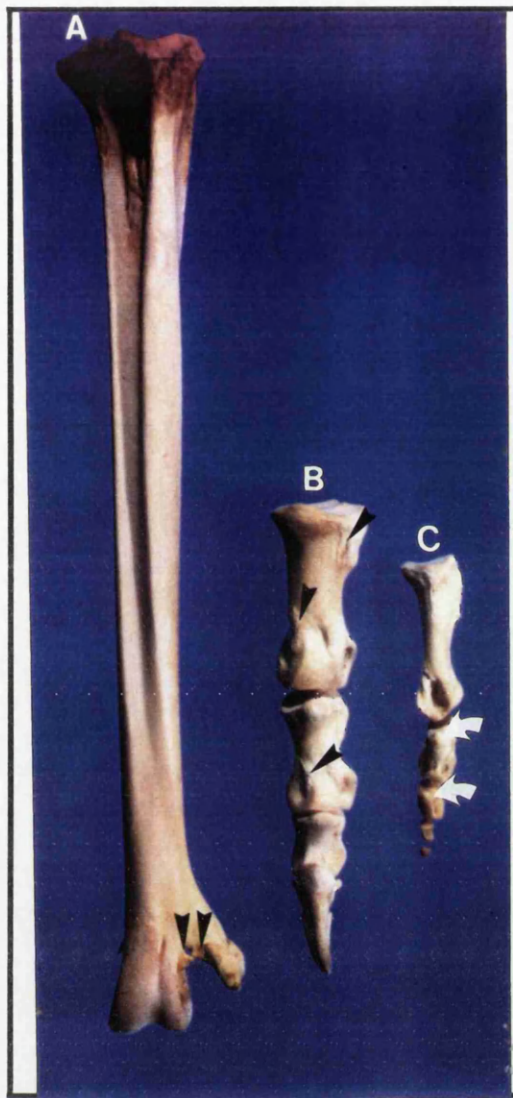


**Figure 29.** Tarsometatarsus and phalanges from an adult ostrich with a rotated tarsometatarsus and rolled toes. Arrow heads show areas of osteophyte formation. Note the abaxial rotation of the distal tarsometatarsus (A) and the first phalanx of digit III (B), and the remodelling of the tuberculum extensorium into sharp spurs (curved arrows).

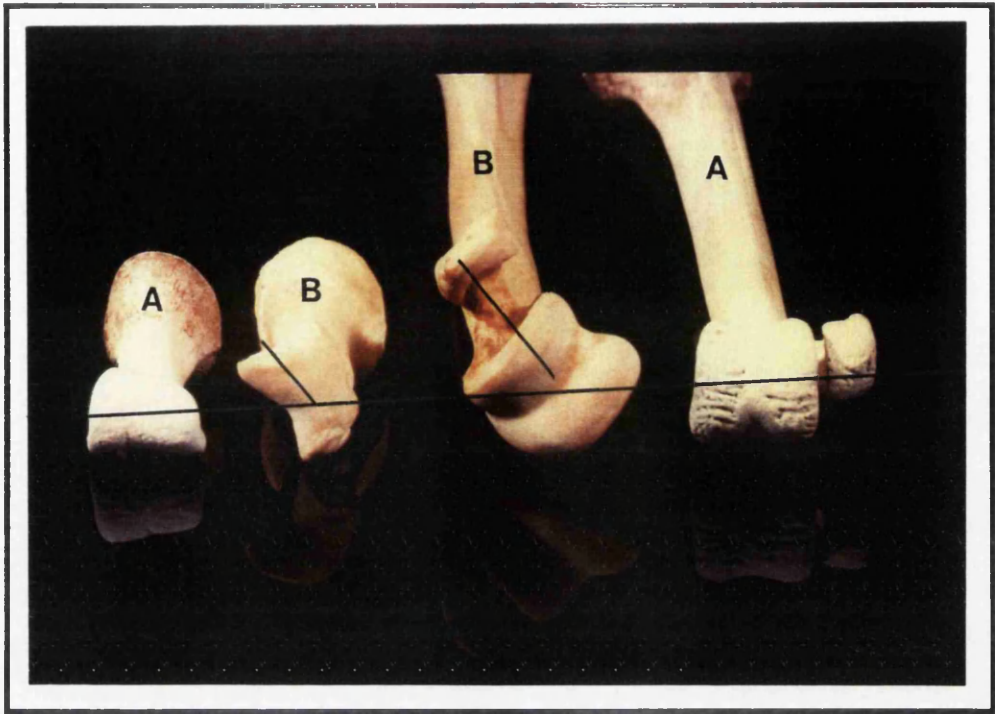


**Figure 30.** Normal (A) and rotated (B) tarsometatarsus and first phalanx of an adult ostrich. Note the angle of abaxial rotation of the distal parts of the bones from an affected limb.



**Figure 31.** Dorsoplantar radiograph of rotated (A) and normal (B) toes of two different adult ostriches. Note the increase in the joint spaces (arrows) and the lateral rotation of the toe, centred on the first interphalangeal joint, in the affected bird. The metatarsophalangeal joint remains stable, whilst the first phalanx is seen to have rotated abaxially. (arrow heads).

# CHAPTER 5

## DISCUSSION

### 5.1 OSTEOLOGY

**Phylogenetic aspects of distal pelvic limb osteology in the ostrich.** A number of the osteological features of the pelvic limb of the Ostrich described in this study confirm those described by Cracraft (1974), who considered them to represent both a major morphological advancement over more primitive ratites [such as the extant tinamous (*Tinamidae*) and kiwis (*Apterygidae*)] and a strong argument for the monophyletic origin of the super family *Struthionoidea*. Such features include the greatly enlarged *Crista cnemialis medialis* of the tibiotarsus, the development of the *Epicondylus medialis tibialis*, the deepening and lengthening of the cranial tarsometatarsal groove, and the development of the centrally located hypotarsus with its plantar surface being marked by the *Fossae parahypotarsalis lateralis* and *medialis*. In addition, certain osteological features noted in this study are, as Cracraft (1974) suggested, indicative of the closer lineal relationship within the *Struthionoidea*, between the ostriches (*Struthionidae*) and rheas (*Rheidae*) rather than between these families and the emus (*Dromaiidae*) and cassowaries (*Casuariidae*). Such features include the flattened and caudally-prominent raised lateral condyle of the tibiotarsus, the very pronounced lateromedial constriction of the cnemial crest bases, the very marked cranial and very slightly proximal projection of the *Crista cnemialis medialis*, the great reduction to a knob like process of the *Crista cnemialis lateralis*; the incomplete ossification (in the ostrich) of the supratendinal bridge (it is still present, but very poorly developed in rheas), and the lateral displacement of a single large, long hypotarsal ridge, with the concomitant loss of the intercotylar prominence.

**Cnemial crests.** The characteristically enlarged *Crista cnemialis medialis* and the smaller knob-like *Crista cnemialis lateralis* represent a functional osteological feature peculiar to the ostrich. The former provides *Mm. gastrocnemius pars interna, tibialis cranialis, fibularis longus* and *extensor digitorum longus* with a much wider area of origin, thereby increasing the forces generated on flexing the intertarsal joint. This unique development of the crests is possibly related to the ostrich's propensity for fast running and strong forward kicking ability. Diving birds such as auks and cormorants have a similar adaptation of the cnemial crests in the tibiotarsus, although in these cases both crests are enlarged for the attachment of similar muscles which provide for a powerful underwater forward stroke during swimming (Raikow, 1970; Owre, 1967; Wilcox, 1952).

**Pons supratendineus (supratendinal bridge).** This bridge, which appears to represent another important functional osteological feature, is located at the cranial distal extremity of the tibiotarsus and does not ossify completely in the ostrich. In other avian species such a bridge is primarily a tendinous structure in young birds but ossifies in the adult to form a complete bony bridge (Baumel, 1979). As noted in the results, in the ostrich it has tendinous and osseous components even in mature birds. The slight flexibility exhibited by the more extensive tendinous component would appear to be a design that allows for a slight extension of the bridge whenever subjected to the tensile forces exerted by the substantial tendon of *M. cranialis tibialis*, the latter passing under this bridge before its insertion on the proximal dorsal surface of the tarsometatarsus. It is reasonable to assume a similar construction of this bridge in diving birds, which have been observed to have some similar adaptations with the ostrich in the hind limb, although this does not yet appear to have been studied.

**Phalanges.** Phalanges are relatively small bony structures in the ostrich but serve a very important role as final points of insertion for tendons of

muscles of the distal pelvic limb transmitting muscle forces down the limb. In order to fulfil this role, individual phalanges in the ostrich have developed lateral extensions, *Tuberculae medialis* and *lateralis* on their distal proximities, to provide wider and more stable areas of insertion for the tendons onto the phalanges. Although digit III is composed of four phalanges, this study has clearly shown the presence of a terminal (fifth) phalanx within digit IV contrary to an earlier report by Fowler (1991) who noted only four phalanges in this digit. This fifth phalanx is poorly developed and seen as a minute round bone, easily overlooked during routine dissections. Careful examination, either by dissection or by radiography, however, would confirm its presence, an important point to be observed as it is in danger of being widely considered that the ostrich is the only bird to possess a fourth digit composed of four phalanges only (Fowler, 1991)

## 5.2 DISTAL PELVIC LIMB MUSCULATURE

Generally the muscles, tendons and ligaments in this part of the pelvic limb are well developed, as might be expected given that the ostrich depends heavily on the pelvic limb for survival and to support body weights of as much as 160 kg (Sanft, 1972; Mallet, 1994). Indeed, Alexander *et al.* (1979) have noted that the principal muscles of the crural region in the ostrich are some three times the mass (assessed as a percentage of body weight) of the corresponding muscles of the antelope, although the comparatively longer individual muscle fibres in the ostrich exert slightly less force than in the antelope. A total of fifteen muscles were identified in this study while the following muscles, generally found in birds (Getty, 1975; Van Berge, 1979), were absent; *M. plantaris*, *M. extensor hallucis longus*, *M. extensor hallucis brevis*, *M. flexor hallucis brevis*, *M. abductor digit II*, *M. flexor phalangis secundi digiti III*, *M. abductor digiti IV* and *M.*

*fibularis brevis*. This reduction in the total number of muscles is basically due to the absence of digits I and II in the ostrich.

**M. cranialis tibialis.** Like most muscles of the pelvic limb in the ostrich, this muscle is well developed. Its stout tendon of insertion appears to differ morphologically from that in other avian species in that it increases in size substantially as it crosses the cranial aspect of the intertarsal joint before splitting into two short tendons at its point of insertion on the tarsometatarsus. The small *M. extensor proprius digiti III* originates between these two tendons. It appears reasonable to assume that these two insertion points give this muscle, a major flexor of the intertarsal joint, a broader and more stable insertion point, while the enlarged segment of the tendon across the intertarsal joint helps to stabilise this joint cranially.

**M. flexor hallucis longus.** It is surprising to note the presence of this muscle despite the absence of the hallux (digit I) in the ostrich. The relationship between the tendon of this muscle and that of *M. flexor digitorum longus*, the tendons of the two muscles joining in the proximal tarsometatarsal region, was noted in birds by Gadow (1896), who described and listed eight different configurations or groups for these conjoined tendons. Berger (1960) greatly extended these observations into other avian species and also described the existence of the eight groups of conjoined tendons in birds. These groups are customarily known as the Gadow tendon distribution pattern types. In this study however, it has been shown that the ostrich does not fit into any of the established Gadow patterns, due to the absence of the hallux. It is now necessary, therefore, to include an additional ninth pattern to represent this species. This pattern would show complete fusion of these two tendons with the resultant conjoined flexor tendon inserting only onto the present third and fourth digits.

**M. fibularis brevis.** The present study failed to confirm the presence of *M. fibularis brevis* in the ostrich leg, and therefore could not support the

assertions of Pavaux and Lignereux (1995) concerning the presence of this muscle. Although the present study demonstrated a very small, relatively insubstantial ligamentous structure laterally transversing the intertarsal joint and occupying the site at which *M. fibularis brevis* would be expected to be found, no evidence for the presence of muscle tissue in this structure could be seen on gross examination. It therefore seemed apparent that this structure was incapable of undertaking any type of muscular activity and it must surely be dubious to list it as *M. fibularis brevis*, a functional muscle, as Pavaux and Lignereux appear to have done. On the other hand, Berger (1960) reported the absence of *M. fibularis brevis* in ratites generally, except for *Apteryx*, and made no mention of the remnant of this muscle in the ostrich. The author's views about this ligamentous structure is that it is, based on its position and orientation, probably a functionless remnant of *M. fibularis brevis*.

### **5.3 FUNCTIONAL MORPHOLOGY**

The ostrich limbs would be very inadequate and ineffectual structures for withstanding gravitational forces if their ability to sustain, balance and transmit the stresses of the body weight was not supplied by their various components (bones, cartilage, ligaments and tendons).

#### **5.3.1 Joint stability**

In birds such as ostriches with long legs, a reduced number of toes (decreased area of the foot surface) and relatively short toes, the tibiotarsus and tarsometatarsus must be nearly equal in length in order for the centre of gravity to remain over the toes while the bird is settling on the ground or getting up (Storer, 1960). In addition to this, the pelvic limb joints must be fairly stable. The stability created by these joints will ensure the provision of a strong support and good platform by the leg and feet respectively. The stability of these joints depends on the various structures

that make up each joint, as well as the associated muscular mechanisms, coupled with forces such as stresses of body weight. Any failure in any of the joint architectural components, normal muscle mechanisms or inability to stabilise the stresses of body weight on the feet (base) is likely to result in a malformation or instability of these joints e.g. rolled toes in young birds. Contraction of extensor and flexor muscles to tighten their tendons and binding of the joints by ligaments and joint capsules all contribute towards normal stable joints.

**Stabilizing features of the intertarsal joint.** The medial deviation of each intertarsal joint ("knocked-kneed" design) results in the unequal distribution of gravitational and locomotory forces over this joint. In order to counteract these forces, a number of specialised features were observed, including the more substantial development of *Ligamentum collaterale mediale* (*pars longa* and *brevis*). This is located on the longer, medial, and convex curvature of this joint and could therefore be expected to receive more tensile stresses compared with the less developed *Ligamentum collaterale laterale* located on the shorter, lateral concave curvature. The lateral aspect of this joint, however, could be expected to receive a higher compressional force compared with the medial aspect; the presence of the single observed lateral meniscus could therefore act to absorb these compressional forces (and thus prevent excessive wear) between the two opposing joint surfaces. In addition to these primary joint restraints, the stability of this joint may be assisted on its plantar aspect by *Cartilago tibialis* together with the flexor tendon bundle in a very organised manner so as to offer maximum functional stability to this joint. This is achieved by means of the strength of the observed fibrous connection between *Cartilago tibialis* and the overlying tendon of *M. gastrocnemius*. The resultant integrated arrangement of these structures achieves a united stabilising functional unit on the plantar aspect of this joint such that, in ostriches, cases of "slipped gastrocnemius" tendon (pers. obs.) involve all

the above mentioned structures being displaced from the plantar aspect of this joint as a unit, and not just the gastrocnemius tendon itself, as seen in other avian species, especially domestic fowl.

**Stabilizing features of the metatarsophalangeal and interphalangeal joint.** During walking or running, the metatarsophalangeal joint is raised on and off the ground. Alexander (1985), in his investigation of stresses acting in the ostrich leg, found that with a minimum duty factor (the fraction of the duration of the stride for which the feet are on the ground ) of 0.29, a peak force of 2.7 times body weight acted on the foot of the ostrich. Most of this force is transmitted through the metatarsophalangeal joint down the digits to act vertically half way along the principal toe. Given the role played by these joints in the distribution of such vertical forces, it follows that any change in the stability of the joints could be expected to alter the load distribution on the foot as a whole and therefore a number of strong anatomical features are needed to contribute to the much-needed stability of these joints. Two strong collateral ligaments on either side of each joint and a joint capsule reinforced on the plantar aspect by a thick fibrocartilaginous *Ligamentum plantaris* carefully check common modes of joint displacement such as distal distention, adduction-abduction and axial rotation.

### **5.3.2 Tendons and ligaments as functional units**

Tendons form a link between the muscles generating tensile force and their points of attachment to the skeleton, and may stabilize one or more joints in their course. In order to make efficient structures that transfer muscle forces, tendons need to act as a functional unit and also need to store elastic energy. In order for tendons to function as a unit, they are tightly bound together by strong sheaths and retinacula that keep them close to the skeletal plane so that they maintain a relatively constant moment arm rather than bow stringing across the joints. This is clearly

demonstrated when observing the arrangement and disposition of the digital flexor tendon bundles in the ostrich in the present study. Alexander (1985) showed that there were substantial savings of elastic energy by stretched tendons in a running ostrich. In the ostrich there is a decrease in postural stability as a result of a reduction in the surface area in contact with the ground as expressed in the number and length of toes, with only the large toe carrying most of the body's weight (Marshall, 1960). In order to fulfil the mechanical requirements of a supporting base the ostrich hind limb has a non-yielding resistance to the downward force of gravity. This is represented by the hardness or solidity of supporting structures which combine the properties of non-compressibility and cohesion (ligaments, tendons and bones). Therefore the function of weight-bearing in the hind limb ligaments or tendons cannot be disassociated from that of its bones; they are cohesive elements of the segmented hind limb framework.

**Storage of elastic energy.** The solidity of bone tissue for transmission of invisible mechanical force and the high tensile strength and elasticity of the foot ligaments and tendons (especially those of the flexor muscles) represent specialised qualities. The elasticity of tendons in the legs and feet of many terrestrial animals provides an important mechanism for saving substantial quantities of muscular energy during locomotion (Shadwick, 1990; Alexander, 1984.). Ostriches resemble cursorial mammals in relation to the maximum stresses normally imposed on the component tissues of their legs and the importance of tendon elasticity for running (Alexander, 1985 ). The body is decelerated as the foot lands on the ground, causing kinetic and potential energy to be stored transiently as strain energy in tendons and muscles that are stretched by the impact forces (Shadwick, 1990 ). Elastic recoil, primarily by the tendons, converts most of the stored energy back to kinetic and potential energy as the foot leaves the ground (Alexander, 1983 ). The kinetic and potential energies of a biped fluctuate as it runs, and have minimum values in each step as the

centre of mass passes over the supporting foot. The elasticity of tendons reduces the energy costs of running by storing elastic strain energy during the minima, so that less energy is lost and has to be replaced by muscular work (Alexander *et al.*, 1979).

**Ligamentum plantaris.** The *Ligamentum plantaris* across the tarsometatarsophalangeal joint is the thickest and, as well as inserting on the proximal base of the first phalanx, also sends two strong ligamentous bands to the base of the distal end of the same phalanx. These ligamentous extensions of the *Ligamentum plantaris* as observed in this study do not appear to have been described in any bird before. Nordin and Frankel (1981), however, have reported the presence of similar plantar plate extensions, which they referred to as the checkrein ligaments, in the human finger. In the ostrich some of the likely functions of the *Ligamentum plantaris* are to limit hyperextension of the metatarsophalangeal joint and hold in place the flexor tendon bundle. Although some authors have reported the presence of *Ligamentum plantaris* in different species of birds such as the domestic pigeon, (*Columba livia*), (Cracraft, 1971) and American coot (*Fulica americana*), (Rosser *et al.*, 1982); it does not appear to have been noted in the ostrich before.

**Digital check apparatus.** The specialised group of ligaments found on the plantar aspect of the ostrich's foot in the present study, referred to as the digital check apparatus, does not appear to have been described in birds previously. The ligaments comprising this check apparatus, that is *Ligamenta abaxiale* and *axiale digiti III*, *Ligamenta abaxiale* and *axiale digiti IV* and *Ligamentum interdigitale digiti III et IV*, all have the same origin from the *Pulvinus metatarsalis*. The position in each digit of *Ligamenta abaxiale* and *axiale* suggest that they are involved in the stabilisation of the joints over which they run, whilst the *Ligamentum interdigitale digiti III et IV* would seem to be ideally situated to prevent hyper-abduction (separation) of digits III and IV in relation to one another. In all other birds the *Pulvinus*

*metatarsalis*, located at the distal end of the tarsometatarsus and the bases of the digits, only serves as a pad to withstand compression (Cane and Spearman, 1967; Baumel, 1979). It also appears to play an additional role in the ostrich, being a strong point of origin for the ligaments that form this digital check apparatus. This check apparatus seen in the ostrich appears to be functionally comparable to the interdigital ligaments found in the bovine foot (Getty, 1975; Dyce *et al.*, 1987)

#### **5.4 ULTRASONOGRAPHY IN THE EXAMINATION OF THE OSTRICH LIMB.**

Ultrasound has been used in humans and other animals such as horses to examine and diagnose a wide range of musculoskeletal disorders, including tendons and ligaments damage (Rantanen, 1982; Fornage, 1989; Fornage and Rifkin, 1988; Crass *et al.*, 1988; Denoix, 1994). It has the prime advantage of being non-invasive when compared to other imaging modalities and it is relatively inexpensive when compared to magnetic resonance imaging.

However, the technique does possess a number of drawbacks of which the operator must be aware and these have already been reviewed in the opening chapter of this thesis. In the present study the boundaries between normal tendons, especially in transverse scans, could not be consistently visualised. This was probably due to the tight binding of the tendons by the flexor sheath that surrounds them, the very limited amounts of connective tissue separating them creating inter-tendinous spaces too small to be visualised. The use of a higher frequency transducer, such as a 10 MHz, could possibly facilitate individual visualisation of the tendon boundaries by improving the resolution. Nevertheless, by correlating obtained ultrasonograms with the topographical information derived from the cross-

sectional anatomy of the limbs at predetermined levels, it was possible to recognize and characterize the ultrasonographic appearance of the tendons in the distal region of the pelvic limb.

In all the limbs that were scanned, the normal flexor tendons appeared similar to those visualised in other animals such as horses and humans in being homogenous and echogenic (Rantanen, 1982; Fornage; 1989, Fornage and Rifkin, 1988; Crass *et al.*, 1988; Kaplan *et al.*, 1990). The tendons were most echogenic when they were at 90 degrees to the transducer interface. When the ultrasound beam was oriented obliquely to the tendons a false hypoechogenicity was visualised, as was the case with the tendon of insertion of *M. flexor hallucis longus* at level 4. Directing the beam at 90 degrees to all the tendons at one time was difficult, particularly at level 6 where the tendons had branched to their respective digits, giving a wide area between the two tendon bundles. This resulted in one group of tendons being more echogenic than the other at any one given scanning position. In young birds with smaller tendons there was absolutely no resolution obtained in either transverse and longitudinal scans. As a result, in these birds normal tendons appeared as one hyperechoic bundle with no individual tendon separations.

Ultrasonography of the distal pelvic limb in the ostrich may prove to be a useful clinical application to non-invasively evaluate potential limb disorders. Used in conjunction with radiography, ultrasound can provide additional information in examining the ostrich hind limb.

## **5.5 GROSS PATHOLOGICAL OBSERVATIONS ON ROLLED TOES IN THE OSTRICH**

In a cursorial bird like the ostrich, the legs are required to carry a large total body weight (adult males weighing upto 160 Kgs), the centre of gravity of

the bird falling between the two hind limbs. The stresses imposed upon the legs, therefore, could, in both posture and locomotion terms, be expected to play a significant role in the modelling of the component bones and joints of each limb. Indeed, studies done in humans revealed that body weight and body mass index were directly related to bone and joint problems (Anderson and Felson, 1988). It is not unexpected, therefore, to find that limb problems are relatively common in growing and adult ostriches (Flieg, 1973; Gandini *et al.*, 1986; Guittin, 1986). Such limb problems have been known and documented for many years in domestic poultry (Riddell, 1975; Duff and Thorp, 1985; Duff and Thorp, 1985), having first been described in turkey poults (Laursen-Jones, 1968)

**Causes of leg problems in the ostrich.** The aetiology of musculoskeletal disorders in ostriches seems to be multifactorial. Although not documented, a strong genetic predisposition was suspected following a review of records from large American ostrich farms (producing more than 100 chicks annually) in which leg deformities such as tibiotarsal and/or tarsometatarsal rotation, and curled or rolled toes, were traced back to one or two hens (Hicks-Allredge, 1995). The inherited component of the musculoskeletal disorders in ostriches is still not clear and is an important area for further investigation especially as such a relationship has been established in some mammalian species such as the horse (Owen, 1975). However, improper incubation temperature (Hallam, 1992; Jensen *et al.*, 1992; Anon, 1993), excessive incubator humidity (Anon, 1993), allowing chicks too much room to move around after hatching (Hallam, 1992; Anon, 1993), improper nutrition and housing (Wallach, 1970; Flieg, 1973; Guittin, 1986), and very high protein diets (Gandini *et al.*, 1986) have all been suggested as contributing variables to the disease process.

In the latter case, Gandini *et al.*, (1986) studied the effect of different diets

on the growth of 8-10-day-old ostrich chicks over a period of eight weeks. The diets were isocaloric (2,700 kcal/kg), but contained 14,16,18 or 20% protein. Data on average body weight per chick, weight gain, and feed/gain are presented in Appendix 2. Their results indicated that leg problems were highest in chicks that were on 20% protein. This study indicated that increases in the protein content in excess of 16% in ostrich chick rations is not only expensive but increases the chances of exacerbating leg deformities.

Calcium and phosphorus levels also appear to play a role in such disorders. After Van Heerden *et al.*, (1985) and Levy *et al.*, (1989) established normal serum-phosphorus and calcium levels for ostriches of various ages and under varying management systems, Benzuidenhout *et al.* (1994) established that although the serum phosphorus and calcium levels of both affected and normal birds were within the normal range, bone calcium and phosphorus in chicks with leg deformities was significantly ( $p < 0.05$ ) lower. This was not unexpected as blood calcium and phosphorus levels are inevitably maintained at the cost of other tissues. Gandini *et al.*, (1986) also found that pathological conditions such as rolled toes and rotation of the tibiotarsus and tarsometatarsus, produced in young ostrich chicks at 6-7 weeks of age by dietary control experiments, could be improved after the administration of calcium borogluconate. All these results indicate that dietary, and not serum calcium and phosphorus levels, cause the majority of limb abnormalities in ostriches. Further investigation into those factors responsible for producing poor calcium and phosphorus incorporation into bone (mineralization) in affected birds would be of great benefit. To date, these factors remain unknown.

#### **The rolled toe condition.**

Rolled toes are common among ostrich chicks. It is a condition unlikely to

be related to riboflavin deficiency, which produces the similar curly toe paralysis in chicken flocks (Nairin and Watson, 1972), as in ostriches rolled toes are usually a problem associated with individual birds rather than the flock (Austic and Scott, 1991). As the ostrich chick grows, the malalignment of the toe will induce a lateral or medial vector force in the entire leg and, if not corrected in time results in other abnormalities such as tibiotarsal and/or tarsometatarsal rotation or slipped gastrocnemius tendon (Hicks-Allredge, 1995). In the latter case, the gastrocnemius tendon does not completely slip off its position across the plantar surface of the intertarsal joint, as it does in other avian species such as broiler chickens (Craig, 1967), but involves simply a combined rotation of the fixed gastrocnemius tendon and tibial cartilage about their fixed distal tarsometatarsal attachment.

**Effect on joints.** In this study, gross examination of rolled toe specimens examined grossly revealed a complete breakdown of the first interphalangeal joint with subsequent medial deviation and degeneration of the other interphalangeal joints. The metatarsophalangeal joint remained relatively stable in all the specimens examined, giving a clear image of the high level of susceptibility to deformity of the interphalangeal joints compared to the metatarsophalangeal joint. Part of the explanation for this disparity in joint reaction and subsequent breakdown may lie in the study done by Alexander *et al.*, (1979) into the running mechanics of the ostrich. They found that, in order to maintain vertical stability during locomotion, a maximum force of 2.7 times body weight, is applied in the middle of the contact period of the foot with the ground, as the centre of mass of the bird passes over the foot. The vertical force imposed at this time was estimated as  $nmg/4B$ , where  $mg$  is the weight of the bird and  $B$  is the duty factor (duty factor is the fraction of the duration of the stride for which each foot is on the ground). They also estimated the point of application of this force on the foot using Muybridge's (1957) photographs

of an ostrich running, the latter indicating that the metatarsophalangeal joint is raised off the ground during the contact period but the first interphalangeal joint and the part of the toe distal to it remain on the ground (Alexander *et al.*, 1979) during running. The applied force was found to be centred in the middle of the area of ground contact, falling more towards the first rather than the second interphalangeal joint of the third digit. The force acting through the smaller fourth digit was regarded as negligible considering the great difference in size and ground contact each toe makes with the ground. It appears, therefore, that the two interphalangeal joints of the third digit are subjected to the majority of this highly tensile vertical force and its resultant stresses, which could therefore be expected to make them more susceptible to deformation.

The observed breakdown of these joints in all the long-standing cases of rolled toes were characterised by degenerative joint disease-like changes. These included degeneration, subluxation or luxation, and instability or joint incongruence accompanied by marginal (periarticular) osteophyte formation at or near the junctional zone where the articular cartilage, periosteum, ligaments or tendons of insertions and the joint capsule merge. Following the stretching or tearing of the insertions of either the joint capsule or the ligaments or tendons, osteophytes may develop as the damaged fibrous tissue undergoes chondrification and endochondral ossification (Marshall, 1969; Doige, 1988; Resnick and Niwayama, 1983; Resnick and Niwayama, 1988). When mature, such osteophytes are composed of dense trabecular bone that is continuous with the underlying bone. Their growth is not continuous, but once formed osteophytes persist as multiple periarticular spurs of bone that may cause joint enlargement (Doige, 1988). In the present study, in long-standing cases of rolled toes in ostrich, bony spurs or osteophytes could have resulted from abnormal ligamentous and tendinous traction at points of insertion (Rodan and Rodan, 1983; Doige, 1988 ). It was interesting to note, therefore, that the

undamaged extensor tendons did, as ought to be expected, result in osteophyte formation.

Degeneration of joints is seen by some workers as a disorder of mechanical origin that may be caused by overuse or incorrect use of the joint and by repeated failure of the force attenuating mechanisms (Olsson, 1978; Peyron, 1986; Jayo, *et al.*, 1987). Various syndromes of degenerative joint disease occur in other mammals and some are given specific names. In horses, *ring-bone* refers to degenerative joint disease of the interphalangeal joints. *Bone spavin* refers to degenerative joint disease of the intertarsal or tarsometatarsal joints (McIlwraith, 1982). In all these syndromes, the formation of periarticular osteophytes is prominent and frequently leads to bony ankylosis of the affected joint.

Joint laxity of the interphalangeal joints was a common feature observed in all the early stage (young) specimens, although without accompanying degenerative changes at this time. Joint laxity (often self correcting) is also common in new-born foals and is attributed to the laxity of the collateral ligaments of major joints of the limb (Doige, 1988). In calves with osteogenesis imperfecta, joint laxity is associated with defective synthesis of collagen and with hypoplasia of tendons and ligaments (Termine *et al.*, 1984). Many different theories regarding its aetiopathogenesis have been advanced over the years but most of them agree that it is a biomechanical disease in which there is an imbalance between muscle mass and tendon growth and strength leading to joint laxity (instability) and eventually, to degenerative joint disease (Riser, 1975; Brandt, 1981). In the ostrich, where there is concentration of the applied vertical forces on the reduced foot/surface contact area due to the decrease in the number of toes, joint instability could be excessively exacerbated, often leading to the development of rolled toe.

**Effects on tendons.** Tendons like other biological materials exhibit viscoelastic behaviour when loaded continuously or intermittently. Under

constant load, the tendon will elongate immediately (elastic response) and continue to creep or elongate slowly (Goldstein *et al.*, 1987). It has been hypothesised that under dynamically varying forces creep could occur and cumulative strain could develop in the tendon. If this cumulative strain exceeds a given threshold, then an inflammatory response may develop (Goldstein, 1981). Abrahams (1967) observed permanent deformation in horse flexor tendon when strained beyond 2-3%. In the ostrich this has yet to be determined.

When the force magnitude or load intensity on the hind limb is no longer stable, as in the case of rolled toes in ostrich, the tendons will be the first to fail in their roles as force transmitters before other musculoskeletal components fail or remodel to suit their new functions. A failure to adapt to dynamically varying forces (excessive bodyweight) may give four possible results. There may be permanent deformation as a result of mechanical microfailure, the tendon or ligament may fray due to mechanical wear, there may be shearing and/or rupture of the synovium, or the nutrition and innervation of the tendon may be greatly compromised (Goldstein, 1981).

The reasons for this failure can be partially explained in terms of origin, composition and load-induced changes in collagen fibril populations in tendons. Tendons originate from mesenchymal cells that condense and differentiate into fibroblasts, which produce collagen, ground substance and enzymes characteristic of this tissue (Kastelic, and Baer, 1978). The metabolic activity of tendon fibroblasts, along with the composition and morphology of the tendon, have been shown to vary considerably with age and location in response to alterations in force application (Fitton-Jackson, 1956; Parry and Craig, 1977; Curwin *et al.*, 1988). Studies done in White Leghorn chickens (Curwin *et al.*, 1994) indicated that tendon length increases fast in young birds but that there is a mismatch in the growth rates of tendon and muscle at 4-8 weeks of age, with tendon growth lagging behind muscle growth. Although tendons develop autonomously

(Kieny and Chevallier, 1979), they also respond to increased loading by changing size and composition (Amiel and Kleiner, 1988). Muscle growth, which increases force production, may also stimulate subsequent tendon growth as long as the growth rate difference between the two structures is not too large. Such growth rates may differ in the early critical periods, although both might appear similar over larger time periods (Curwin *et al.*, 1994). In ostrich chicks such an early period of disproportionate muscle and tendon growth may be critical because it could result in an increase in the stress (force per unit area) on the young tendon, and thus make the tendons mechanically vulnerable to failure. If such a situation were to arise, the tendons (especially the weight-bearing flexor tendons) would remain stretched (resulting in a rolled toe) while slowly re-establishing the hydroxypyridinium cross-links which are directly related to the strength of a tendon (Amiel and Kleiner, 1988). These biomechanical characteristics of young tendons partially explain an important observation made in ostrich chicks by Deeming (pers. comm., 1995) in which he indicated that, out of those ostrich chicks that suffer from rolled toes early in their lives, below the age of 4 weeks, most will resolve this condition themselves, although approximately a third will then experience a recurrence at 6-8 weeks of age. The recurrence may be due to failure by some of the chicks to re-establish adequate hydroxypyridinium cross-links to sustain the increasing body weight forces.

All examined specimens of rolled toes in both immature and mature birds showed marked tendon stretching, rupture and/or degeneration, mainly confined to the distal extremities of the foot with little or no pathological tendon lesions being observed proximal to the metatarsophalangeal joint. Part of the possible explanation for these observations may lie in the work of Viidik (1979) and Curwin *et al.*, (1994). The former showed that in mammalian tendons, the density of collagen in tendon, as represented by hydroxyproline concentration, directly related to tendon strength, increased

with age (Viidik, 1979) while Curwin *et al.*, (1994) further investigated this parameter in chickens by studying the concentration of hydroxyproline in different regions of the tendon. They found out that the distal digital regions of avian tendons tend to have lower hydroxyproline concentrations in growing birds, making them weaker and therefore more vulnerable to mechanical failures. It could be inferred, therefore, that the tendons of young growing ostrich chicks may contain lower hydroxyproline concentrations in their distal extremities, leading to the observed pathologies in the present study. This area would therefore be worthy of future investigation.

**Tendon ossification.** Extensor tendon ossification was observed in two adult birds exhibiting rolled toes. Previous studies have indicated a relationship between such tendon ossification and the vascular supply to the tendon (Rothman and Parke, 1965; Rothman and Rubin, 1967), observations supported by the work of Johnson (1960) who demonstrated that tendon calcification in the turkey started at sites of maximal tension, at points midway between the longitudinal vessels supplying the tendon, and concluded that it was areas of relative hypovascularity that would be predisposed to calcification. Rothman and Parke (1965) have provided strong statistical evidence supporting just such a relationship between hypovascularised areas and tendon ossification by means of degenerative calcification, events which appear to be initiated as a result of localised ischaemia, subsequently leading to cellular damage and release of lysozymes, thus altering the matrix of the tendons in such a way as to render them liable to calcification (Rothman and Rubin, 1967). As already noted (Johnson, 1960) such degenerative ossification of hypovascularised tendons only occur in tendons subjected to significant tensile stress. An investigation into the vascular supply to the tendons of the distal pelvic limb of the ostrich would significantly contribute to an understanding of the extensor tendon ossification seen in the present study.

**Effects on bones.** Most hind limb abnormalities in ostrich chicks almost always start with an initial abnormality of the toe. As the chick grows, the misalignment of the toe will induce a lateral or medial vector force in the entire leg which, if not corrected in time, will result in other abnormalities such as tibiotarsal and/or tarsometatarsal rotation (observed in this study), or "slipped gastrocnemius" tendon. In young and growing birds bone is continually remodelled to maintain a form appropriate to its biomechanical function. While most work in animals has focused on the hormonal and biochemical factors that influence skeletal growth, mechanical factors also play an important role in growth and modelling of bone. (Bertram and Biewener, 1988). Frequently referred to as "functional adaptation", the remodelling response of bone to changes in physical usage has had a long history, initiated by Wolff (1892) who noted that the maintenance and transformation of skeletal form is greatly influenced by the mechanical forces acting on a bone during its use. It is now accepted that bone growth remodelling reflects a complex interplay of not only genetic, hormonal and biochemical factors (Raisz and Bingham, 1972; Hall, 1982; Rodan and Rodan, 1983), but mechanical factors as well. In the present study, adult specimens of rolled toes demonstrated the remodelling and functional adaptation of the distal tarsometatarsus and first phalanx of digit III. This could have been initiated by the laxity of the interphalangeal joints, resulting in rolled toe and a subsequent change in the direction of mechanical forces exerted by the flexor tendon bundle onto the bones, resulting, with time, in a functional remodelling of these bones as seen in the present study.

**Vascular involvement.** Vascular involvement or entrapment following a rolled toe cannot be ruled out. In rolled toes, blood vessels were frequently found to be compressed by the accumulated fibrous tissue which acts as a pad to the usually abaxially-rolled toe. This could be expected to exert significant compression force on the entrapped segment of the blood

vessels during walking, and their lumina may be partially or intermittently occluded. Such obliteration of blood vessels at this level would probably lead to hypovascularity of the digital flexor tendons resulting in ischaemia and subsequent cellular damage, release of lysozymes, and tendon degeneration. Such flexor tendon degeneration was a common feature in adult cases of rolled toes in the current study. It is therefore essential that the condition be corrected as early as possible, prior to significant vascular damage. There is, however, need for more study on such vascular involvement associated with rolled toes in ostriches.

**Treatment of rolled toes.** Treatment of rolled toes should be initiated soon after recognition of the problem. The younger the bird, the faster the response to therapy, because stretched tendons become less responsive with time. Two categories of treatment modalities have been reported but one has to wait until the bird is at least two weeks old before attempting to correct these rolled toes by the conservative non-invasive treatment of splinting, younger birds being too susceptible to stress to attempt such a remedy (Kocan and Crawford, 1994). Out of newly-hatched ostrich chicks noted with rolled toes, a third will show a reappearance of signs at about 6-8 weeks of age (Deeming, pers. comm., 1995). In this latter group correction by taping or splinting is now difficult due to the greater forces required for the realignment of the toes. As a result a second method of treatment, developed in Australia, utilizes a hinged external fixation device involving invasive surgery (Poulton and De Garis, 1994).

## **5.6 FUTURE WORK AND CONCLUSION.**

Clinical evaluation and treatment of abnormal distal pelvic limb conditions affecting the ostrich requires detailed knowledge of the morphological characteristics of this region. Indeed, this investigation of the normal anatomy of the distal pelvic limb of the ostrich was designed to be used as

a baseline for future comparison studies of abnormal conditions affecting the lower limb. Although the use of diagnostic ultrasound imaging techniques in the examination of mammalian soft tissue structures is well established, their use in the field of avian studies is still in its infancy. The results of this study indicate that ultrasound can be used to image the normal ostrich flexor tendons. The ultrasonographic appearance of the normal ostrich flexor tendons had similarities to those previously reported in other animals. Such techniques, with their ability to distinguish anatomical textures and dimensions as a result of characteristic differences in acoustic impedance at tissue interfaces, have an extremely useful role to play in ostrich anatomical, pathological and clinical studies by helping to elucidate soft tissue structures and relationships in a non-invasive manner. Used in conjunction with conventional radiography, it would allow a more complete assessment of lower limb abnormalities to be made, any change in texture, size or spatial orientation being readily determined. Future work in this area should be done to study the usefulness of ultrasound in diagnosing various hind limb abnormalities, and muscle and tendon defects.

To date, relatively little information is available on the causal factors of musculoskeletal disorders in the ostrich, such as that of rolled toes examined in the present study. The real causes of these disorders are complex and multifactorial, and need further investigation. One area for future research could be the establishment of normal mineral values in serum, bone, and other tissues (e.g. liver) in ostriches at various ages and stages of growth, in order to accumulate baseline values for those areas where ostrich farming is undertaken. Other fields that may benefit from investigation are the effect of age, sex, breeding season and genetics on the absorption and metabolism of the various minerals involved in bone formation. Values for optimal body weights in birds of selected

predetermined age groups would also be of value in trying to prevent excessive weight problems leading to musculoskeletal abnormalities such as rolled toes seen in this study. There is also a need for study on the normal vasculature and innervation of the ostrich hind limb in order to ascertain their role in both normal and abnormal situations, in the development or exacerbation of hind limb disorders.

## **APPENDICES**

	<b>Pork</b>	<b>Lamb</b>	<b>Beef</b>	<b>Turkey</b>	<b>Chicken</b>	<b>Ostrich</b>
<b>Calories</b>	275	205	240	135	140	96.9
<b>Protein gm</b>	24	22	21	25	27	22
<b>Fat gm</b>	19	13	15	3	3	2
<b>Sat Fat gm</b>	7	5.6	6.4	0.9	0.9	0
<b>Mon-U gm</b>	8.8	4.9	6.9	0.5	1.1	0
<b>Pol-U gm</b>	2.2	0.8	0.6	0.7	0.7	0
<b>Chlstrl gm</b>	84	78	77	59	73	53
<b>Carboh gm</b>	0	0	0	0	0	2.1
<b>Calc mg</b>	3	8	9	16	13	5.2

**Appendix 1.** Ostrich meat comparison based on a 3 oz serving.

From "Nutritive Value of Foods" U.S.D.A., Home and Garden Bulletin number 72 and AMSI Quality Testing Laboratory report, 1989.

<b>CP, %</b>	<b>B/Weights, g</b>	<b>W/Gain, g</b>	<b>F/intake, g</b>	<b>Feed/gain</b>
14	6,350	5,438	11,912	2.19
16	9,400	8,440	14,563	1.72
18	9,580	8,754	14,468	1.65
20	10,010	9,134	15,453	1.69

**Appendix 2.** Performance of ostrich chicks on diets containing four levels of protein for eight weeks.

## LIST OF REFERENCES

- Abrahams, M.** (1967). Mechanical Behaviour of Horse Tendon in *Vitro*. *Medical and Biological Engineering*, **5**, 433-445.
- Alexander, R. M.** (1983). *Animal Mechanics*, Second Edition. Blackwell Scientific, Oxford, pp. 5-31.
- Alexander, R. M.** (1984). Elastic Energy Stores in Running Vertebrates. *American Zoologist*, **24**, 85-94.
- Alexander, R. M.** (1985). The Legs of Ostriches (*Struthio camelus*) and Moas (*Pachyornis*). *Acta Biotheoretica*, **34**, 165-174.
- Alexander, R.M., Maloiy, G.M.O., Njau, R. and Jayes, A.S.** (1979). Mechanics of Running Ostrich (*Struthio camelus*). *Journal of Zoology*, **187**, 169-178.
- Amiel, D. and Kleiner, J.B.** (1988). Biochemistry of Ligament and Tendon. *In: Collagen, Volume Three*, (Ed. M.E. Nimni). Biotechnology, CRC Press, pp. 223-251.
- Anderson, J.J. and Felson, D.T.** (1988). Factors Associated with Osteoarthritis of the Knee in the first National Health and Nutrition Examination Survey: Evidence for an Association with Overweight, Race and Physical Demands of Work. *American Journal of Epidemiology*, **128**, 179-189.
- Anon, J.** (1993). Programme Booklet of the American Ostrich Association 1993 Convention and Annual Meeting, p. 58.
- Athey, P.A. and McClendon, J.** (1983). *Diagnostic Ultrasound for Radiographers*. Multi-Media Publishing Incorporation, Denver, U.S.A.
- Austic, R.E. and Scott, M.L.** (1991). Nutritional Diseases. *In: Diseases of Poultry*, Ninth Edition, (Ed. B.W. Calnek). Wolf Publishing Limited, London, pp. 45-71.
- Ballantine, H.T., Bolt, R.H., Heuter, T.F. and Ludwig, G.D.** (1950). The Detection of Intracranial Pathology by Ultrasound. *Science*, **112**, 525-

**Bartrum, R.H.J. and Crow, H.C.** (1983). *Real-Time Ultrasound for Physicians and Technical Personnel*. W.B. Saunders, Philadelphia, U.S.A.

**Baumel, J.J.** (1979). *Nomina Anatomica Avium, An Annotated Anatomical Dictionary of Birds*. Academic Press, London.

**Becker, E.L. and Landau, S.I.** (1986). *International Dictionary of Medicine and Biology*. Wiley, New York, U.S.A.

**Beddard, F.E.** (1898). *Structure and Classification of Birds*. Green and Company, Longman, London.

**Berger, A.J.** (1960). The musculature. *In: Biology and Comparative Physiology of Birds*. Volume One, (Ed. A.J. Marshall), Academic Press, London, pp. 301-344.

**Betram, J.E.A. and Biewener, A.A.** (1988). Bone Curvature: Sacrificing Strength for Load Predictability? *Journal of Theoretical Biology*, **131**, 75-92.

**Bezuidenhout, A. and Burger, W.P.** (1993). The Incidence of Tibiotarsal Rotation in the Ostrich (*Struthio camelus*). *Journal of South African Veterinary Association*, **64** (4), 159-161.

**Bezuidenhout, A.J., Burger, W., Piers, F. and Soley, J.T.** (1994). Serum and Bone-Mineral Status of Ostriches with Tibiotarsal Rotation. *Onderstepoort Journal of Veterinary Research*, **61**, 203-206 .

**Brandt, K.D.** (1981). The Biology of Osteoarthritis. *Current Theriogeological Research*, **30**, 25-30.

**Brown, T.G.** (1960). Direct Contact Ultrasonic Scanning Techniques for Direct Visualisation of Abdominal Masses; Medical Electronics. Proceedings of Second International Conference on Medical Electronics. (Ed. C.H. Smyth). Illife and Sons Limited, London, pp. 358-366.

**Butler, D.L., Grood, E.S. and Noyes, F.R.** (1978). Biomechanics of Ligaments and Tendons. *Exercise and Sports Science Review*, **6**, 125-181

**Cameron, J.R. and Skofronick, J.G.** (1979). *Medical Physics*. John Wiley and Sons, New York, pp. 253-293.

**Cane, A.K. and Spearman, R.I.C.** (1967). A Histochemical Study of Keratinization in the Domestic fowl (*Gallus gallus*). *Journal of Zoology*, **153**, 337-352.

**Cartee, R.E.** (1980). Ultrasonography: A New Diagnostic Technique for Veterinary Medicine. *Veterinary Medicine*, **75**, 1524-1533.

**Cho, P., Brown, R. and Anderson, M.** (1984). Comparative Anatomy of Ratites. *Zoo Biology*, **33**, 133-144.

**Clouston, W.M. and Lloyd, H.M.** (1987). Immobilization-induced Hypercalcemia and Regional Osteoporosis. *Clinical Orthopaedics*, **216**, 247-252.

**Cracraft, J.** (1971). The Functional Morphology of the Hind limb of the Domestic Pigeon, (*Columba livia*). *Bulletin of American Museum of Natural History*, **144**, 171-268.

**Cracraft, J.** (1974). Phylogeny and Evolution of Ratite Birds. *Ibis*, **116**, (4), 494-521.

**Craig, F.** (1967). Traumatic Hock Disorder in Poultry. *Proceedings of the 16th West Poultry Diseases Conference*, pp. 11-12.

**Crass, R.J., Van De Vegte, G.L. and Harkary, L.A.** (1988). Tendon Echogenicity: Ex.Vivo Study. *Radiology*, **167**, 499-501.

**Cuesta, I., Riber, C., Pinedo, M., Gata, J., and Castejon, F.** (1994). Ultrasonographic Measurement of Palmar Metacarpal Tendon and Ligament Structures in the Horse. *Veterinary Radiology and Ultrasound*, **36** (2), 131-136.

**Curwin, S.L., Vallas, A.C., and Wood, J.** (1988). Immature Tendon Adaptation to Strenuous Exercise. *Journal of Applied Physiology*, **67**, 2297-2301.

- Curwin, S.L., Roy, R.R., and Vailas, A.C. (1994).** Regional and Age Variations in Growing Tendon. *Journal of Morphology*, **221**, 309-320.
- Deeming, D.C. (1994).** An Ostrich Opportunity with Hangland Farm Ostriches, September, 1994, p. 5.
- Deeming, D.C. and Ayres, L. (1994).** Factors Affecting the Rate of Growth of Ostrich (*Struthio camelus*) Chicks in Captivity. *The Veterinary Record*, **135**, 617-622.
- Deeming, D.C., Ayres, L. and Ayres, F.J. (1993).** Observations on the Commercial Production of the Ostrich (*Struthio camelus*) in the United Kingdom: Incubation. *The Veterinary Record*, **132**, 602-607.
- Denoix, J. (1994).** Functional Anatomy of Tendons and Ligaments in the Distal Limbs of the Horse (manus and pes). *Veterinary Clinics of North America: Equine Practise*, **10** (2), 273-320.
- Doige, C. (1988).** Skeletal System. *In: Special Veterinary Pathology*, (Ed. R.G. Thomsom). B.C. Decker Incorporation, Philadelphia, pp 467-507.
- Donald, I. and Brown, T.G. (1961).** Demonstration of Tissue Interfaces Within the Body by Ultrasonic Echo Sounding. *British Journal of Radiology*, **34**, 539-546.
- Duff, S.R.I. and Thorp, B.H. (1985).** Abnormal Angulation/Torsion of the Pelvic Appendicular Skeleton in Broiler Fowl: Morphological and Radiological Findings. *Research in Veterinary Science*, **39**, 313-319.
- Duff, S.R.I. and Thorp, B.H. (1985).** Patterns of Physiological Bone Tortion in the Pelvic Appendicular Skeletons of Domestic Fowl. *Research in Veterinary Science*, **39**, 307-312.
- Dyce, K.M., Sack, W.O., and Wensing, C.J.G. (1987).** Textbook of Veterinary Anatomy. W.B. Saunders Company, Philadelphia, pp. 13-19.
- Dyson, S. (1994).** Tendon and Ligament Injuries. *The Veterinary Clinics of North America*, **10** (2), 66-70.
- Edler, I. (1955).** The Diagnostic Use of Ultrasound in Heart Disease. *Acta*

*Medica Scandinavica*, supplement, **308**, 32-36.

**Elliot, D.H.** (1965). Structure and Function of Mammalian Tendon. *Biological Reviews of Cambridge Philosophical Society*, **40**, 392-421

**Evans, J.H. and Barbenel, J.C.** (1975). Structural and Mechanical Properties of Tendon Related to Function. *Equine Veterinary Journal*, **7**, 1-8

**Fitton-Jackson, S.** (1956). Morphogenesis of Avian Tendon. *Proceedings of Royal Society of London*, **B144**, 556-572.

**Flieg, G.M.** (1973). Nutritional Problems in Young Ratites. *International Zoo Yearbook*, **13**, 158-163.

**Foggin, C.M. and Honywill, J.** (1992). Observations on the Artificial Incubation of Ostrich Eggs with Special Reference to Water Loss. *Zimbabwe Veterinary Journal*, **23** (2), 81-89.

**Fornage, B.D.** (1986). Achilles Tendon: US Examination. *Radiology*, **159**, 759-764.

**Fornage, B.D.** (1987). The Hypoechoic Normal Tendon: A Pitfall. *Journal of Ultrasound Medicine*, **6**, 19-22.

**Fornage, B.D.** (1989). Ultrasonography of Muscles and Tendons. Examination Technique and Atlas of the Normal Anatomy of the Extremities. Spring-Verlag, New York.

**Fornage, B.D. and Rifkin, M.D.** (1988). Ultrasound Examination of Tendons. *Radiologic Clinics of North America* **26** (1), 87-107.

**Fowler, M.E.** (1991). Comparative Clinical Anatomy of Ratites. *Journal of Zoo and Wildlife Medicine*, **22**, (2), 204-227.

**Fuss, F.K. and Gasser, C.R.** (1992). Cruciate Ligaments of the Avian Knee: Insight into a Complex System. *Journal of Morphology*, **214**, 139-151.

**Fyke, F.E., Greenleaf, J.F. and Johnson, S.A.** (1979). Continuous

Wave Measurements of Acoustic Attenuation in an Oil/Polymer Mixture. *Ultrasound in Medical Biology*, **5**, 87-90.

**Gadow, H.** (1896). A Dictionary of Birds, Newton Edition. Black, London.

**Gandini, G.C.M., Burroughs, R.E.J., and Ebedes, H.** (1986). Preliminary Investigation into the Nutrition of Ostrich Chicks (*Struthio camelus*) Under Intensive Conditions. *Journal of the South African Veterinary Association*, **57**, 39-42.

**Getty, G.** (1975). Sisson and Grossman's The Anatomy of the Domestic Animals, Fifth Edition. W.B. Saunders Company, Philadelphia, U.S.A.

**Goddard, P.J.** (1995). Veterinary Ultrasonography. C.A.B. International, Wallingford, UK.

**Goldstein, S. A.** (1981). Biomechanical Aspects of Cumulative Trauma of Tendons and Tendon Sheaths. PhD. Thesis, University of Michigan.

**Goldstein, S. A., Armstrong, T.J., Chaffin, D.B. and Matthews, L.S.** (1987). Analysis of Cumulative Strains in Tendons and Tendon Sheaths. *Journal of Biomechanics*, **20**, (1), 1-6.

**Guittin, P.** (1986). Bowleg Syndrome in Ratite Birds. *Avicultural Magazine*, **92**, 70-79.

**Hall, B.K.** (1982). The Role of Tissue Interactions in the Growth of Bone. In: Factors and Mechanisms Influencing Bone Growth, (Ed. D.A.Dixon and B. Sarnat). Alan, R. Liss, New York.

**Hallam, M.G.** (1992). THE Topaz Introduction to Practical Ostrich Farming. Harare, Zimbabwe, pp. 149.

**Harcke, H.T., Grissom, L.E. and Finkelstein, M.S.** (1985). Evaluation of the Musculoskeletal System with Sonography. *American Journal of Research*, **150**, 1253-1261.

**Haughton, S. and Norman, A.** (1865). Notes on Animal Mechanics III, on the Muscular Mechanism of the Leg of the Ostrich. *Proceedings of the Royal Irish Academy*, **9**, 50-61.

- Hauser, M.L. and Rantanen, N.W.** (1983). Ultrasound Appearance of the Palmar Metacarpal Soft Tissues of the Horse. *Journal of Equine Veterinary Science*, **3**, 19-22.
- Herring, D.S. and Bjornton, G.** (1989). Physics Facts and Artifacts of Diagnostic Ultrasound. *Seminars in Veterinary Medicine and Surgery (Small Animal)*, **4**,(1), 2-12.
- Hick-Aldredge, K.** (1995). Ostrich Management. In: Current Veterinary Therapy XII, Small Animal Practice, (Ed .J.D. Bonagura). Philadelphia, W.B Saunders Company, pp. 1307-1321.
- Howry, D.H.** (1958). Development of an Ultrasonic Diagnostic Instrument. *American Journal of Physics in Medicine*, **37**, 234.
- Jayo, M., Leipold, H.W., Dennis, S.M. and Eldridge, F.E.** (1987). Brachygnathia Superior and Degenerative Joint Disease: A New Lethal Syndrome in Angus Calves. *Veterinary Pathology*, **24**, 148-155.
- Jensen, J.M., Johnson, J.H. and Weiner, S.T.** (1992). Husbandry and Medical Management of Ostriches, Emus and Rheas. Wildlife and Exotic Animal TeleConsultants, Texas, USA.
- Johnson, L.C.** (1960). Mineralization of the Turkey Leg Tendon. I. Histology and Histochemistry of Mineralization. In: Calcification in Biological Systems, (Ed. R.F. Sognaes). W.B. Saunders Company, Philadelphia, U.S.A., pp 163-165.
- Kaplan, P.A, Matamoros, A. and Anderson, J.C.** (1990). Sonography of the Musculoskeletal System. *American Journal of Research* **155**, 237-245.
- Kastelic, J. and Baer, E.** (1978). The Multicomposite Structure of Tendon. *Connective Tissue Research*, **6**, 11-23.
- Kieny, M. and Chevallier, A.** (1979). Autonomy of Tendon Development in the Embryonic Chick Wing. *Journal of Embryology and Experimental Morphology*, **49**, 153-165.

- King, A.S. and McLelland, J. (1984).** Birds: Their Structure and Function. Academic Press Incorporation, London.
- Kirberger, R.M. (1995).** Imaging Artifacts in Diagnostic Ultrasound; A Review. *Veterinary Radiology and Ultrasound*, **36** (4), 297-306.
- Kremkau, F.W. and Taylor, K.J.W. (1986).** Artifacts in Ultrasound Imaging. *Journal of Ultrasound Medicine*, **5**, 227-237.
- Kocan, A.A. and Crawford, J.A. (1994).** An Ostrich Farmer's Handbook. The ostrich News Incorporation, Cache, Oklahoma, U.S.A.
- Laursen-Jones, A.P. (1968).** Leg Abnormalities in Turkey Poults. *The Veterinary Record*, December, 597.
- Levy, A., Perelman, B., Waner, T., Van Grevenbrok, M., Van Creveld, C., and Yagil, R. (1989).** Reference Blood Chemical Values in Ostriches (*Struthio camelus*). *American Journal of Veterinary Research*, **50**, 1548-1550.
- Ludwig, G.D. and Struthers, F.W. (1949).** Consideration Underlying the Use of Ultrasound to Detect Gall-stones and Foreign Bodies in the Tissue. *US Navy Medical Research Institute Report*, **4**, 1-27.
- MacAlister, A. (1864).** On the Anatomy of the Ostrich (*Struthio camelus*). Proceedings of Royal Institute of Anatomy, London, pp. 531-561.
- McIlwraith, C.W. (1982).** Current Concepts in Equine Degenerative Joint Disease. *Journal of American Veterinary Medical Association*, **180**, 239-250.
- McKittrick, M.C. (1991).** Phylogenic Analysis of Avian Hindlimb Musculature. University of Michigan Zoology publications, **179**.
- McLelland, J.J. (1990).** A Colour Atlas of Avian Anatomy. Holfe, London.
- Mallet, F.D. (1994).** A Note on the Musculature of the Proximal Part of the Pelvic Limb of the Ostrich (*Struthio camelus*). *Journal of South African Veterinary Association*, **64**, (1), 5-9.

- Marshall, A.J.** (1960). *Biology and Comparative Physiology of Birds*, Volume One. Academic Press, New York, U.S.A.
- Marshall, J.L.** (1969). Periarticular Osteophytes. Initiation and Formation in the Knee of the Dog. *Clinical Orthopaedics*, **62**, 37-47.
- Miles, K.G.** (1989). Basic Principles and Clinical Applications of Diagnostic Ultrasonography. *Compendium on Continuing Education for Practicing Veterinarians*, **11**, (5), 609-622.
- Miyagima, G., Wagai, T., Uchid, R. and Hagiwara, Y.** (1952). Diagnosis of Intracranial Disease by Ultrasound. *Tokyo Medical Journal*, **70**, 632.
- Muybridge, E.** (1957). *Animals in Motion*, Second Edition. New York, U.S.A.
- Nairin, M.E. and Watson, A.R.A.** (1972). Leg Weakness of Poultry-a Clinical and Pathological Characterisation. *Australian Veterinary Journal*, **48**, 645-655.
- Nicoll, R.G., Wood, A.K. and Martin, I.C.A.** (1993). Ultrasonographic Observations of the Flexor Tendons and Ligaments of the Metacarpal Region of Horses. *American Journal of Veterinary Research*, **54**, 502-506.
- Nordin, M. and Frankel, V.H.** (1981). *Basic Biomechanics of the Musculoskeletal System*, Second Edition. Lea and Febiger, Philadelphia, U.S.A. p. 283.
- Nyland, T.G. and Mattoon, J.S.** (1995). *Veterinary Diagnostic Ultrasound*, First Edition. Saunders, Philadelphia, U.S.A.
- Odle, B.** (1994). Facts About Ratites. *Journal of American Veterinary Medical Association*, **205** (12), 1661-1662.
- Olsson, S.E.** (1978). Osteochondritis in Domestic Animals. *Acta Radiologica , Supplement*, **358**.
- Owen, J.M.** (1975). Abnormal Flexion of the Corono-pedal Joint or "Contracted Tendons" in Unweaned Foals. *Equine Veterinary Journal*, **7**,

40-43.

**Owre, O.T.** (1967). Adaptation for Locomotion and Feeding in the Anhinga and the Double-crested Cormorant. *Ornithological Monologia*, **6**, 1-138.

**Park, R.D., Nyland, T.G., Lattimer, J.C., Miller, C.W. and Lebel, J.L.** (1981). B-mode Gray-scale Ultrasound: Imaging Artifacts and Interpretation Principles. *Veterinary Radiology*, **22**, (5), 204-210.

**Pharr, J.W. and Nyland, T.G.** (1984). Sonography of the Equine Palmar Metacarpal Soft Tissues. *Veterinary Radiology*, **25**, (6), 265-273.

**Parry, D.A.D. and Craig, A.S.** (1977). Quantitative Electron Microscope Observations of the Collagen Fibrils in Rat-tail Tendon. *Biopolymers*, **16**, 1015-1031.

**Pavaux, C. and Lignereux, Y.** (1995). A Myological Dissection of the Shank and Foot in an Ostrich (*Struthio camelus*). *Anatomia, Histologia, Embrologia*, **24**, 127-131.

**Peyron, J.C.** (1986). Osteoarthritis. The Epidemiologic Viewpoint. *Clinical Orthopaedics*, **213**, 13-19.

**Poulton, P.J. and De Garis, P.** (1994). Treatment of Rotated Toe in Ostrich Chicks. Proceedings Of Ostrich Odyssey **94**, September 1994, Canberra, Australia, pp. 74-76.

**Powis, R.L. and Powis, W.J.** (1984). A Thinker's Guide to Ultrasonic Imaging. Urban and Schwarzenberg, Munich.

**Raikow, R.J.** (1970). Evolution of Diving Adaptations in the Stifftail Ducks. *University of California Publications of Zoology*, **94**, 1-52.

**Raisz, L.G. and Bingham, P.J.** (1972). Effect of Hormones on Bone Development. *Annual Reviews of Pharmacology*, **12**, 337-352.

**Rantanen, N.W.** (1982). The Use of Diagnostic Ultrasound in Limb Disorders of the Horse: A Preliminary Report. *Journal of Equine Veterinary Science*, **2**, 62-64.

**Rantanen, N.W. and Ewing, R.L. (1981).** Principles of Ultrasound Application in Animals. *Veterinary Radiology*, **22**, (5), 196-203.

**Rantanen, N.W. and Gaines, R. (1983).** The Use of Diagnostic Ultrasound to Detect Structural Damage to the Soft Tissues of the Extremities of the Horse. *Journal of Equine Veterinary Science*, **3**, 134-135.

**Reece, R.L. and Butler, R. (1984).** Some Observations on the Development of the Long Bones of Ratite Birds. *Australian Veterinary Journal*, **61**, (12), 403-405.

**Resnick, D. and Niwayama, G. (1983).** Radiology: Entheses and Enthesopathy. *Radiology* **146**, 1-9.

**Resnick, D. and Niwayama, G. (1988).** Supporting Structures, Syndesmoses and Entheses. *In: Diagnosis of Bone and Joint Disorders, Second Edition, Volume Five.* W.B Saunders, Philadelphia, U.S.A., pp. 2974-2977.

**Riddell, C. (1975).** Selection of Broiler Chickens for a High and Low Incidence of Tibial Dyschondroplasia with Observations on Spondylolisthesis and Twisted Legs (Perosis). *Poultry Science*, **55**, 145-151.

**Riddell, C. (1983).** Pathology of the Skeleton and Tendons of Broiler Chickens Reared to Roaster Weights. I. Crippled Chickens. *Avian Diseases*, **27**, 950-962.

**Riser, W.H. (1975).** The Dog as a Model for Study of Hip Dysplasia. *Veterinary Pathology*, **12**, 235-334.

**Rodan, G.A. and Rodan, S.B. (1983).** Expression of the Osteoblastic Phenotypes. *In: Bone and Mineral Research Annual 2*, (Ed. W.A. Peck). Elsevier, Boston, U.S.A., pp. 224-285.

**Rosser, B.W.C., Secoy, D.M. and Riegert, P.W. (1982).** The Leg Muscles of the American Coot (*Fulica americana*). *Canadian Journal of Zoology*, **60**, 1236-1256.

**Rothman, R.H. and Parke, W.W.** (1965). The Vascular Anatomy of the Rotator Cuff Tendon. *Clinical Orthopaedics*, **41**, 176.

**Rothman, R.H. and Rubin, M.L.** (1967). Tendon Calcification and Vascularity. *Surgery Gynaecology and Obstetrics*, **125**, (3), 577-580.

**Sanft, K.** (1972). Ratites. *In: Grzimek's Animal Life Encyclopaedia*, Volume Seven. Van Nostrand Reinhold, New York, pp. 89-109.

**Shadwick, R.E.** (1990 ). Elastic Energy Storage in Tendons: Mechanical Differences Related to Function and Age. *Journal of Applied Physiology*, **68**, (3), 1033-1040.

**Shirley, I.M., Blackwell, R.J., Cusick, G., Farman, D.J. and Vicary, F.R.** (1978). User's Guide to Diagnostic Ultrasound. Pitman Medical, Tunbridge, U.K., pp. 1-15.

**Smit, D.J.V.Z.** (1963). Ostrich Farming in the Little Karoo , Bulletin,358, Republic Of South Africa, Department of Agricultural Technical Services.

**Sommer, F.G. and Taylor, K.J.W.** (1983). Differentiation of Acoustic Shadowing due to Calculi and Gas Collections. *Radiology*, **135**, 399-403.

**Spaulding, K.,** (1984). Ultrasonic Anatomy of the Tendons and Ligaments in the Distal Metacarpal-Metatarsal Region of the Equine Limb. *Veterinary Radiology*, **25**, (4), 155-166.

**Storer, R.W.** (1960). Adaptive Radiation in Birds. *In: Biology and Comparative Physiology of Birds*, Volume One, (Ed. A.J. Marshall). Academic Press, London, pp. 60-74.

**Termine, J.D., Robey, P.G. and Fisher, L.W.** (1984). Osteonectin, Bone Proteoglycan, and Phosphophoryn Defects in a Form of Bovine Osteogenesis Imperfecta. *Proceedings of National Academy of Science*, U.S.A., **81**, 2213-2217.

**Thaler, I. and Manor, D.** (1990). Transvaginal Imaging: Applied Physical Principles and Terms. *Journal of Clinical Ultrasound*, **18**, 235-238.

**Vanden Berge, J.C.** (1979). Myologia. *In: Nomina Anatomica Avium*. An Annotated Anatomical Dictionary of Birds, (Ed. J.J. Baumel, A.S. King, A.M. Lucas, J.E. Breazile, H.E. Evans). Academic Press, London, pp. 175-205.

**Van Heerden, J., Dauth, J., Jarvis, M.J.F., Keffen, R.H., Denny, J.E.F.M., Dreyer, M.J. and Kriek, N.P.J.** (1983). Blood Chemical and Electrolyte Concentrations in Ostrich (*Struthio camelus*). *Journal of South African Veterinary Association*, **56**, 75-79.

**Viidik, A.** (1979). Connective Tissues: Possible Implications of the Temporal Changes for the Aging Process. *Mechanisms of Ageing Development*, **9**, 267-285.

**Vogel, K.G. and Heinegard, D.** (1985). Characterisation of Proteoglycans from Adult Bovine Tendon. *Journal of Biological Chemistry*, **260**, 9298-9306.

**Voster, B.J.** (1984). Nutritional Muscular Dystrophy in a Clutch of Ostrich Chicks. *Journal of the South African Veterinary Association*, **55**, (1), 39-40.

**Wallach, J.D.** (1970). Nutritional Diseases of Exotic Animals. *Journal of American Veterinary Medical Association*, **157**, (5), 583-599.

**Webb, J.E., Wallwork, J.A. and Elgood, J.H.** (1979). Guide to Living Birds. The Macmillan Press, London.

**Wells, P.N.T.** (1969). The Physical Principles of Ultrasonic Diagnosis. Academic Press, London.

**Wilcox, H.H.** (1952). The Pelvic Musculature of the Loon (*Gavia immer*). *American Midl.ands Naturalist*, **48**, 513-573.

**Wild, J.J., French, A.C. and Neal, D.** (1950). Detection of Cerebral Tumours by Ultrasonic Pulses. *Cancer*, **4**, 708.

**Winsberg, F. and Cooperberg, P.G.** (1982). Real-Time Ultrasonography. Churchill Livingstone, New York.

**Wolff, J.** (1892). *In: The Law of Bone Remodelling* (Translated by P.

Maquet, and R. Furlong, 1986). Springer-Verlag, Berlin.

**Wortman, J.A. and Rantanen, N.W.** (1986). Alternate imaging. *In*: Textbook of Diagnostic Radiology (Ed. D.E. Thrall). Philadelphia, W.B. Saunders Co., 541-548.

**Ziskin, M.C.** (1975). Basic Principles. *In*: Diagnostic Uses of Ultrasound. Grune and Stratton Incorporation, New York, U.S.A., pp. 1-30

**Zwiebel, W. J.** (1983). Review of Basic Terms Used in Diagnostic Ultrasound. *Seminars in Ultrasound*, 4, (1), 60-62.

